# Msb2, a mucin-like membrane protein functioning in signalling and pathogenesis of *Fusarium oxysporum*

Elena Pérez Nadales

PhD Thesis

University of Córdoba

March 2010

TITULO: *Msb2, a mucin-like membrane protein functioning in signalling and pathogenesis of Fusarium oxysporum*

AUTOR: *Elena Pérez Nadales*

---


Campus de Rabanales
Ctra. Nacional IV, Km. 396
14071 Córdoba

www.uco.es/publicaciones
publicaciones@uco.es

---

ISBN-13: 978-84-693-2987-0

UNIVERSIDAD D CÓRDOBA

**Facultad de Ciencias**

**Departamento de Genética**

# Msb2, a mucin-like membrane protein functioning in signalling and pathogenesis of *Fusarium oxysporum*

Trabajo realizado en el Departamento de Genética de la Universidad de Córdoba para optar al grado de Doctora en Biología por la Licenciada:

**Elena Pérez Nadales**

**D. Antonio Di Pietro**, Profesor Titular del Departamento de Genética de la Universidad de Córdoba

Informa:

Que el trabajo titulado "**Msb2, a mucin-like membrane protein functioning in signalling and pathogenesis of *Fusarium oxysporum***" realizado por Dña. Elena Pérez Nadales bajo su dirección, puede ser presentado para su exposición y defensa como Tesis Doctoral en la Universidad de Córdoba.

Y para que así conste, expido el siguiente informe

Córdoba, 24 de Febrero de 2010

*Dr. Antonio Di Pietro*
Profesor Titular
Departamento de Genética
Universidad de Córdoba

**Dña. Ángeles Alonso Moraga**, Directora del Departamento de Genética de la Universidad de Córdoba

Informa:

Que el trabajo titulado "**Msb2, a mucin-like membrane protein functioning in signalling and pathogenesis of *Fusarium oxysporum***" realizado por Dña. Elena Pérez Nadales bajo la dirección de D. Antonio Di Pietro puede ser presentado para su exposición y defensa como Tesis Doctoral en el Departamento de Genética de la Universidad de Córdoba.

Y para que así conste, expido el siguiente informe

Córdoba, 24 de Febrero de 2010

*Drª. Ángeles Alonso Moraga*
Directora
Departamento de Genética
Universidad de Córdoba

Este trabajo ha sido realizado en el Departamento de Genética de la Universidad de Córdoba, financiado por SIGNALPATH Marie Curie Research Training Network.

*This work has been conducted in the Department of Genetics of the University of Córdoba and financially supported by the SIGNALPATH Marie Curie Research Training Network.*

# Acknowledgements

First and foremost, I am deeply grateful to my supervisor, Prof. Antonio Di Pietro, for his support, availability and flexibility throughout these years, which has made it really easy to work and communicate with him. I deeply appreciate the opportunity he has given me to develop this work within the Fusarium Group and within the *SIGNALPATH Marie Curie Research Training Network*. It has been a privilege to learn with him and enjoy his wonderful sense of humour. Secondly, I would like to thank Prof. Maria Isabel González Roncero (Reyes) for her valuable support for the development of our work and for my own professional development. Thanks also to all the other members of the Fusarium Group, especially Esther Martinez for valuable technical assistance. I am also grateful to my colleagues at the Departments of Genetics, Cellular Biology and Microbiology of the University of Cordoba for valuable help with materials and methodology throughout this work, including biostatistical analysis, sequence analysis software, protein analysis procedures, yeast work and administrative and technical support. My gratitude goes to Prof. Maria del Mar Malagón and Prof. Emilo Fernández for their help in key moments of my professional career. Thanks to Prof. Tore Samuelsson (University of Goteborg, Sweden) for kindly providing the PTSpred algorithm. Thanks to Dr. Paul Cullen (University of Buffalo, USA) and Dr. George Sprague (University of Oregon, USA) for kindly providing plasmids and yeast strains, and for their valuable advice. Thanks also to Prof. Hauro Saito (University of Tokio, Japan) for kind comments on our work. Special thanks to the State Russian Museum (Saint-Petersburg, Russia) for giving permission to

reproduce a work by Kasimir Malevich from the State Russian Museum collections. Thanks to all member of the PhD defence board for kindly accepting our invitation to participate in the assessment of this work.

Thanks to all my friends in the laboratory, especially Rafa, Manu, Esther, Lola, Tere, Maribel M, Yolanda, David, Maribel P, Mada, Ana Pi and Gemo, who have been directly involved in helping me with different aspects of this work. It is a privilege to count on your support every day and to share worries and happiness with you. My deepest thanks go to my tutors and professors at the Universities of Cordoba and Westminster. Thanks to the Marie Curie Actions and the *SIGNALPATH Marie Curie Research Training Network,* firstly to the PIs for organising great courses and meetings and for insightful discussions and advice along these meetings. Secondly, thanks to all the other Signalpath students for wonderful moments shared throughout these years. Warm thanks to Prof. Neil Gow (University of Aberdeen, UK) for his support and for providing us with moments of great fun with his amazing storytelling skills.

Thanks to Dr. Alison Lloyd (MRC Laboratory for Molecular Cell Biology and Cell Biology Unit at University College London, UK) for the opportunity she gave me within her group and for her support. It was great to work with her and she has definitely been the person that has most greatly influenced my approach to Science. I cannot be grateful enough to Dr. Trevor Martin and Saira Cawthraw (Veterinary Laboratories Agency, Weybridge, UK) for taking me into their group and teaching me so much and for helping me find the financial support to complete my University studies. Thanks to all the other exceptional people that this profession brought to me in UK, who have then become great friends. Saira, Verity, Mark, Mavis, Toria, Susie, thank you for your genuine friendship. I owe you all my love for your country and your identity. I miss you.

Thanks to my friends Ana and Perico who know me and care for me and who I love so much. Thanks to my friends, Maria Jesús, Neda, Saira, Pili and Amalia for loving me and filling my life with great people and moments. Thanks to all my other great friends in Cordoba and elsewhere for their generosity, support and encouragement.

Thanks most of all to my family. To my father, who instilled in me the commitment and perseverance to reach my aims. Thanks to my three sisters for their love. To my uncle Antonio, thanks for always being present, for instilling in me the curiosity for small things, for bringing magic

and imagination to my life. Thanks to my mother and grandparents because their love has been fundamental in my life. And last but not least, I want to thank Jose for being by my side throughout these years, for knowing me and understanding me and for helping me so much these last two months. I love you.

*To my family*

# Agradecimientos

Quisiera agradecer en primer lugar a mi director de tesis, Prof. Antonio Di Pietro, su ayuda a lo largo de estos años. Trabajar con él ha sido un privilegio y ha resultado muy fácil por su completa disponibilidad, su flexibilidad, su confianza y su fantástico sentido del humor, que tanto valoro. Aprecio la oportunidad que me ha dado de desarrollar este trabajo en el Grupo de Fusarium y dentro de la Red Signalpath. Gracias en segundo lugar a la Prof.ª M. Isabel González Roncero (Reyes) por su apoyo a nuestro trabajo y al Grupo así como por su valiosa aportación a mi formación a lo largo de estos años. Gracias a Esther Martínez por su invaluable ayuda técnica. Gracias a todas y cada una de las demás personas del grupo de Fusarium así como a los demás compañeros y compañeras de los Departamentos de Genética, Biología Celular y al grupo de *D. hansenii* del Departamento de Microbiología de la UCO por su valiosísima ayuda y apoyo con materiales y métodos requeridos para este estudio que incluyen software para análisis de secuencias, análisis bioestadístico, análisis de proteínas, manejo de la levadura y apoyo técnico y administrativo. Me siento muy agradecida a la Prof.ª Angeles Alonso por su ayuda con la parte administrativa de mi tesis. Mi agradecimiento a la Prof.ª Maria del Mar Malagón y al Prof. Emilio Fernández por su ayuda en momentos claves de mi trayectoria profesional. Gracias también al Prof. Tore Samuelsson (Universidad de Goteborg, Suecia) por proporcionarnos el algoritmo PTSpred. Gracias al Dr. Paul Cullen (Universidad de Buffalo, EEUU) y al Dr. George Sprague (Universidad de Oregon, EEUU) por enviarnos plásmidos y cepas de *S. cerevisiae* y por sus valiosos consejos. Gracias al Prof. Hauro Saito (Universidad de Tokio, Japón) por comentarios a

cerca de nuestro trabajo. Gracias de forma especial al State Russian Museum (San Petersburgo, Rusia) por dar permiso para la reproducción de uno de los trabajos de Kasimir Malevich. Gracias a los miembros del tribunal por aceptar nuestra invitación a participar en la evaluación de este trabajo.

Gracias a todos mis amigos y amigas del laboratorio, especialmente a Rafa, Manu, Esther, Lola, Tere, Maribel M, Yolanda, David, Maribel P, Mada, Ana Pi y Gemo que han participado de forma directa en algún aspecto de este trabajo. Es un lujo poder contar con vosotros para compartir preocupaciones y alegrías. Gracias por vuestro arropo, vuestro cariño y vuestra amistad. Mi más sincero agradecimiento a los profesores de la Universidades de Córdoba y Westminster. Gracias a Marie Curie Actions y a la Red *SIGNALPATH* en primer lugar a los Investigadores Principales por la organización de cursos, reuniones y congresos y por sus valiosas aportaciones a nuestro trabajo durante dichas reuniones. En segundo lugar, gracias a los demás estudiantes de la Red por momentos estupendos. Mi agradecimiento más cálido para el Prof. Neil Gow (Universidad de Aberdeen, Reino Unido) por su interés por nuestro trabajo, por su apoyo y por proporcionarnos momentos muy divertidos con su increible habilidad para contar historias.

Gracias a la Dr[a]. Alison Lloyd (MRC Laboratory for Molecular and Cell Biology, University College London, Reino Unido) por la oportunidad que me brindó en su grupo, por su confianza y porque ha sido sin duda la persona que mas ha influido en mi forma de acercarme a la Ciencia. Mi más sincero y profundo agradecimiento al Dr. Trevor Martin y a Saira Cawthraw (Veterinary Laboratories Agency, Weybridge, Reino Unido) por acogerme en su grupo, por enseñarme tanto y buscar la financiación necesaria para completar mis estuidos en el Reino Unido. Gracias a todas las demás personas excepcionales que me trajo esta profesión en Inglaterra y que hoy son grandes amigos. Saira, Verity, Mark, Mavis, Toria, Susie, gracias por vuestra amistad. A vosotros os debo mi amor por vuestro país y por vuestra identidad.

Gracias a mi amiga Ana y mi amigo Perico por todo lo que me dan, sin pedirme nunca nada a cambio, por recordarme quien soy y quererme. Gracias a mi amigas Maria Jesús, Neda, Pili, Amalia y Saira por elegirme y quererme y llenar mi vida de personas maravillosas. Gracias a todos los demás amigos y amigas excepcionales, Roberto, Pilar, Norberto, Patricia, Jean, Christine, que me habéis abierto vuestros brazos en Córdoba y en cada parte del mundo.

Gracias por último y sobre todo a toda mi familia, incluida mi familia por parte de Jose. Gracias a mi padre, que siempre me inculcó la constancia y el compromiso que me han ayudado a llegar hasta aquí. A mis hermanas, María, Rocío y Ana, por quererme y por entenderme. A mi tito Antonio, gracias por estar siempre presente, por traer a mi vida la curiosidad por las cosas pequeñas, la magia y la imaginación. Gracias a mi madre y a mis abuelos y abuelas porque su amor ha sido fundamental en mi vida. Y gracias por último a Jose, que me conoce y me comprende, por toda su ayuda para completar mi tesis en estos últimos dos meses, por estar a mi lado, por hacerlo todo fácil. Te quiero.

*A mi familia*

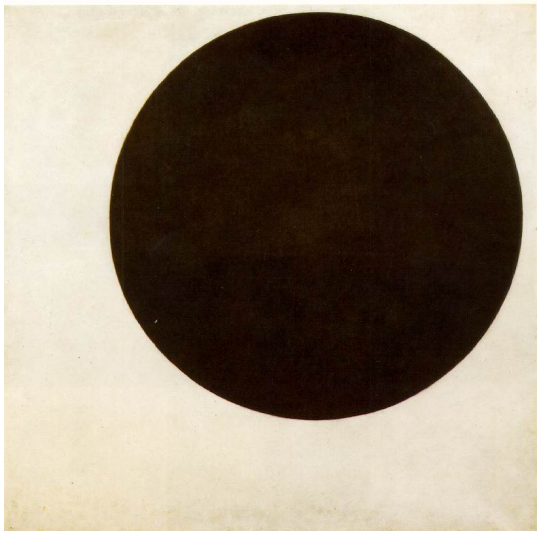

“Black circle” by Kasimir Malevich. © 2010, State Russian Museum

"Caught up in the concept of practical realism, Man wishes to shape all of nature according to his ideal design. But this entire objective, scientifically underpinned practical realism and the entire culture it has brought forth are an idea that will never be realised, because there is nothing that is ideal in nature, unless it is in non-objectiveness. In non-objectiveness, however, every notion of an ideal, of usefulness, of perfection disappears" (Malevich, 1926).

# Curriculum vitae

## Personal information


| | |
|---|---|
| | Pérez-Nadales, Elena |
| Address | Departamento de Genética. Facultad de Ciencias. |
| | Campus de Rabanales, s/n. Ed-C5, 1 planta. 14071 Córdoba. Spain |
| Telephone | + 34 957 21 89 81 |
| E-mail | ge2penae@uco.es/epereznadales@hotmail.com |
| Nationality | Spanish |
| D.O.B. | 15th July 1976 |


## Education

*June 2007*: MSc in Genetics, Molecular and Cellular Biology, University of Cordoba.

*June 2001*: BSc. Applied Biology with First Class Honours, University of Westminster, London. Final year project: Development of a TaqMan PCR assay for genotyping of the sheep prion protein gene.

*June 1998*: Certificate of Proficiency in English, Cambridge University.

## Professional experience

*December 2005 – present*

PhD student. Department of Genetics. Faculty of Science. Rabanales University Campus, University of Cordoba, Spain.

*September 2002 – April 2004*

Research assistant. MRC Laboratory for Molecular and Cell Biology at University College London, University College London, Gower Street, London WC1E 6BT, UK.

*February 2002 – September 2002*

Research assistant. Department of Physiology, Royal Free and University College Medical School, University College London, Rowland Hill Street, London NW3 2PF, UK.

*January 1999 – February 2002*

Assistant Scientific Officer. Transmissible Spongiform Encephalopathies and Molecular Biology (TMB) Department, Veterinary Laboratories Agency, Woodham Lane, New Haw, Addlestone, Surrey KT15 3NB.

## Publications

Rispail, N.; Soanes, D; Ant, C.; Czajkowsky, R.; Grünler, A.; Huguet, R.; Pérez-Nadales, E.; Poli, A.; Sartorel, E.; Valiante, V.; Yang, M.; Beffa, R.; Brakhage, A.; Gow, N.; Kahmann, R.; Lebrun, M.-H.; Lenasi, H.; Perez-Martin, J.; Talbot, N; Wendland, J.; Di Pietro, A. (2009). Comparative genomics of MAP kinase and calcium-calcineurin signalling components in plant and human pathogenic fungi. *Fungal Genetics and Biology, 46*, 287-298.

González-Roncero, M. I.; De la Hera, C.; Di Pietro, A.; Ruiz-Roldán, M. C.; Rispail, N.; Martínez-Rocha, A.; Córdoba, L.; Martín-Urdiroz, M.; Prados, R. C.; Martínez-Aguilera, E.; Pareja, Y.; Sánchez López-Berges, M.; Pérez-Nadales, E.; De Miguel, C.; López-Fernández, L. (2009). Book Chapter 9: Análisis molecular de la patogénesis en *Fusarium oxysporum*. *Biotecnología,* 36-38.

Harrisingh, M. C.; Pérez-Nadales, E.; Parkinson, D. B.; Malcolm, D. S.; Mudge, A. W.; Lloyd, A. C. (2004). The Ras/Raf/ERK signalling pathway drives Schwann cell dedifferentiation. *EMBO Journal, 23*, 3061-3071.

Pérez-Nadales, E. and Lloyd, A. C. (2004). Essential function for ErbB3 in breast cancer proliferation. *Breast Cancer Research, 6*, 137-139.

Mitchell, P. J.; Pérez-Nadales, E.; Malcolm, D.S. and Lloyd, A.C. (2003). Dissecting the contribution of p16(INK4A) and the Rb family to the Ras transformed phenotype. *Molecular and Cellular Biology, 23*, 2530-2542.

## Contributions to scientific meetings

Pérez-Nadales, E., Di Pietro, A. Conference presentation. MAPK Signalling during Fungal Pathogenesis, European Conference on Fungal Genetics (ECFG10). Amsterdam, The Netherlands, 2010.

Pérez-Nadales, E., Di Pietro, A. The membrane mucin Msb2 controls invasive growth and plant infection in *Fusarium oxysporum*. Conference presentation. MAPK Signalling during Fungal Pathogenesis, SIGNALPATH Final International Meeting. Berlin, October 2009.

Pérez-Nadales, E. Msb2: a putative membrane mucin functioning in signalling and pathogenesis of *Fusarium oxysporum.* Talks given at the scientific meetings of the SIGNALPATH Marie Curie Research Training Network:
Aberdeen, April 2009.
Copenhagen, September 2008.
Ljubljana, May 2008.
Jena, December 2007.
Lyon, May 2007.
Exeter, September 2006.

Pérez-Nadales, E., Di Pietro, A. Msb2: a putative membrane mucin functioning in signalling and pathogenesis of *Fusarium oxysporum*. Conference presentation. European Conference on Fungal Genetics (ECFG9). Edinburgh, UK, 2008.

Pérez-Nadales, E., Di Pietro, A. Msb2, una proteína de membrana de tipo mucina implicada en señalización y patogénesis de *Fusarium oxysporum*. Poster presentation. Congreso Nacional de Micología, Córdoba, September 2008

Rispail, N.; González-Roncero, M. I.; Ruiz-Roldán, M. C.; De la Hera, C.; Di Pietro, A.; Martínez-Rocha, A.; Córdoba, L.; Martín-Urdiroz, M.; Prados, R. C.; Martínez-Aguilera, E.; Pareja, Y.; Sánchez López-Berges, M.; Pérez-Nadales, E**.** Ingeniería genética en hongos. Jornadas de divulgación de la investigación en biología molecular, celular, genética y biotecnología. Abstract contribution. III Jornadas de divulgación de la investigación en biología molecular, celular, genética y biotecnología. Córdoba 2007.

Pérez-Nadales, E., Di Pietro, A. Msb2, una proteína de membrana de tipo mucina implicada en señalización y patogénesis de *Fusarium oxysporum*. Conference presentation. Micelio: Red Temática Española de Hongos Filamentoso. San Sebastián, July 2008.

Pérez-Nadales, E.; Harrisingh, M. C.; Lloyd, A.C. The role of Ras/Raf signalling in primary Schwann cells. Oral presentation. Centro Nacional de Investigaciones Oncológicas (CNIO). Madrid, December 2003.

Pérez-Nadales, E.; Cawthraw, S., Martin, T.C. Development of a TaqMan PCR assay for genotyping of the sheep prion protein gene. Conference presentation. Young Scientist Meeting, Veterinary Laboratories Agency, Surrey, September 2000.

## Participation in Networks and Committees

EU Signalpath Marie Curie Research Training Network. November 2005 – October 2009.

# Index

# List of figures

# List of tables

# Abbreviations

| | |
|---|---|
| aa | aminoacid |
| Af | *Aspergillus fumigatus* |
| Ag | *Ashbya gossypii* |
| atm | atmospheres |
| bp | base pairs |
| Ca | *Candida albicans* |
| CFW | Calcofluor white |
| cm | centimeters |
| CR | Congo red |
| CT | cytoplasmic tail |
| DNA | deoxyribonucleic acid |
| ER | endoplasmic reticulum |
| Fg | *Fusarium graminearum* |
| Fo | *Fusarium oxysporum* |
| g | grams |
| GPI | glycosyl-phosphatidyl-inositol |
| h | hours |
| HA | human influenza hemagglutinin epitope tag |
| Kb | kilobases |
| kb | kilobases |
| kDa | kiloDalton |
| l | liter |
| M | molar |
| MAPK | Mitogen-activated protein (MAP) kinase |
| Mg | *Magnaporthe grisea* |
| mg | miligrams |
| MHD | mucin homology domain |
| min | minutes |
| ml | mililitres |
| mM | milimolar |
| MM | Puhalla's minimal medium |
| Nc | *Neurospora crassa* |
| nm | nanometer |
| nm | nanometers |
| ºC | centrigrade degrees |
| ORF | Open Reading Frame |
| PBS | Phosphate Buffer Saline |
| PCR | Polymerase Chain Reaction |

| | |
|---|---|
| PDA | Potato Dextrose Agar |
| PDB | Potato Dextrose Broth |
| PGA | Polygalacturonic acid medium |
| PRD | Positive regulatory domain |
| qPCR | real time quantitative PCR |
| RNA | ribonucleic acid |
| rpm | revolutions per minute |
| RPT | internal repeat |
| Sc | *Sacharomyces cerevisiae* |
| SH3 | SRC Homology 3 Domain |
| SM | Synthetic Defined Medium |
| SS | N-terminal signal sequence |
| STR | Ser/Thr/Pro-rich |
| TM | transmembrane domain |
| Tm | melting temperature |
| U | units |
| Um | *Ustilago maydis* |
| w/v | weight per volume |
| v/v | volume per volume |
| YPG | Yeast extract Peptone Glucose |
| α | anti- |
| Δ | deletion |
| μ | micro |
| μg | microgram |
| μl | microliter |
| μm | micrometer |
| μM | micromole |

### Aminoacid list

| | |
|---|---|
| alanine | Ala (A) |
| arginine | Ala (R) |
| asparagine | Asn (N) |
| aspartic acid | Asp (D) |
| cysteine | Asp (C) |
| glutamic acid | Glu (E) |
| glutamine | Gln (Q) |
| glycine | Gly (G) |
| histidine | His (H) |
| isoleucine | Ile (I) |
| leucine | Leu (L) |
| lysine | Lys (K) |
| methionine | Met (M) |
| phenylalanine | Phe (F) |
| proline | Pro (P) |
| serine | Ser (S) |
| threonine | Thr (T) |
| tryptophan | Trp (W) |
| tyrosine | Tyr (Y) |
| valine | Val (V) |

# Summary

Fungal pathogenicity on plants requires a conserved mitogen-activated protein kinase (MAPK) cascade homologous to the yeast filamentous growth pathway. How this signalling cascade is activated during infection remains poorly understood. In the soilborne vascular wilt fungus *Fusarium oxysporum,* the orthologous MAPK Fmk1 is essential for pathogenicity on tomato plants. Here we investigated the role of the mucin-type transmembrane protein Msb2 in activation of Fmk1 and in control of invasive growth and virulence. *F. oxysporum* strains lacking *msb2* had reduced phosphorylation levels of Fmk1 and shared characteristic phenotypes with Δ*fmk1* mutants, including defects in hyphal growth under nutrient-limited conditions, invasion of the underlying substrate and colonization of living plant tissue. Similar growth and virulence phenotypes were observed in deletion mutants lacking the tetraspan membrane protein Sho1. Interestingly, loss of Msb2 or Sho1 also caused hypersensitivity to cell wall targeting compounds which was exacerbated in a Δ*msb2*Δ*fmk1* double mutant, suggesting that Msb2 contributes to cell wall integrity via a pathway independent of Fmk1. While individual deletion of Msb2 or Sho1 caused a partial reduction of virulence on tomato plants, loss of both proteins abolished virulence, equivalent to loss of Fmk1. Our results indicate that Msb2 and Sho1 have partially redundant functions upstream of Fmk1 in promoting invasive growth and virulence of *F. oxysporum,* revealing a novel role of transmembrane mucins in fungal pathogenicity on plants.

# Resumen

La patogénesis fúngica en plantas requiere la participación de una cascada de proteína quinasas activadas por mitógenos (MAPK) altamente conservada, ortóloga a la ruta MAPK que regula el crecimiento filamentoso en levadura. Actualmente se desconocen los componentes que activan esta ruta durante la infección. En el hongo patógeno del suelo *F. oxysporum,* causante de la marchitez vascular, la MAPK ortóloga Fmk1 es esencial para la patógenesis en plantas de tomate. En el presente estudio se ha investigado el papel de la proteína transmembrana de tipo mucina Msb2 en la activación de Fmk1, así como su función en la regulación del crecimiento invasivo y la virulencia. Mutantes de *F. oxysporum* en el gen *msb2* mostraron niveles reducidos de fosforilación de Fmk1 y compartían características fenotípicas con los mutantes Δ*fmk1*, tales como defectos en el crecimiento de las hifas en condiciones de limitación de nutrientes, en la invasión del medio subyacente o en la colonización del tejido vivo de la planta. Mutantes en el gen *sho1* que cifra una proteína de cuatro dominios transmembrana mostraron fenotipos similares con defectos en crecimiento y virulencia. La pérdida individual de Msb2 o Sho1 confirió un fenotipo de sensibilidad a compuestos que afectan la pared celular, mientras que el mutante doble Δ*msb2*Δ*fmk1* mostró una sensibilidad aún mayor. Ello sugiere que Msb2 contribuye al mantenimiento de la integridad celular a través de una ruta

independiente de Fmk1. La pérdida de Msb2 o Sho1 resultó en una reducción parcial de la virulencia en plantas de tomate, sin embargo, la ausencia de ambas proteínas en el doble mutante produjo la pérdida total de virulencia hasta el nivel observado en el mutante Δ*fmk1*. Los resultados indican que Msb2 y Sho1 tienen funciones parcialmente redundantes aguas arriba de la MAPK Fmk1 en el crecimiento invasivo y la virulencia de *F. oxysporum,* revelando un nuevo papel de las mucinas transmembrana en la patogénesis fúngica sobre plantas.

# Introduction

## *1. Fusarium oxysporum*

*Fusarium* species are ubiquitous in soil, plant debris, and other organic substrates (Booth, 1971). The widespread distribution of the genus relies on its ability to grow on a wide range of substrates and on its efficient mechanisms for dispersal (Burgess, 1981). *F. oxysporum* is the causal agent of vascular wilt disease in a wide variety of economically important crops, although the species also includes non-pathogenic and saprophytic isolates as well parasites of other organisms. Vascular wilt disease is a major limiting factor in the production of many agricultural and horticultural crops, including tomato (*Lycopersicon spp.*), banana (*Musa spp.*), cabbage (*Brassica spp.*), onion (*Allium spp.*), cotton (*Gossypium spp*), flax (*Linum spp.*), muskmelon (Cucumis spp.), pea (*Pisum spp.)*, watermelon (*Citrullus spp.*), carnation (*Dianthus spp.)*, chrysanthemum (*Chrysanthemum spp.),* gladiolus (*Gladiolus spp.*) and tulip (*Tulipa spp.*) (Armstrong and Armstrong, 1981).

Besides its well-studied activity as a plant pathogen, *F. oxysporum* is also known as a serious emerging pathogen of humans, causing a broad spectrum of infections ranging from superficial to locally invasive or disseminated. The latter affect exclusively

immunocompromised patients and frequently have lethal outcomes (Nucci and Anaissie, 2002; Ortoneda *et al.*, 2004). *F. oxysporum*, together with *F. solani* and *F. verticillioides*, are responsible for practically all of the cases of invasive fusariosis in humans (Guarro and Gene, 1995; Nucci and Anaissie, 2007). Several Fusarium species are used for biological disease control, for the production of secondary metabolites with biological and commercial interest such as cyclosporin or giberellins (Desjardins *et al.*, 1993), and for production of fungal biomass (Quorn) for food production (Wiebe, 2002).

Research on fundamental aspects of fungal pathogenesis requires the development of suitable experimental models. Species such as *Magnaporthe grisea* or *Ustilago maydis* that infect rice and maize, respectively, have been established as models for aerial plant pathogens. On the other hand, *F. oxysporum* provides an excellent model for soilborne plant pathogens and has recently been proposed as a model for the study of fungal trans-kingdom pathogenicity on plants and mammals (Ortoneda *et al.*, 2004).

## 1.1. Taxonomy

Based on the structures bearing conidiogenous hyphae, *Fusarium spp.* are classified under the subclass Hyphomycetidae within the Deuteromycetes. *F. oxysporum*, as decribed by Snyder & Hansen (Snyder and Hansen, 1940), comprises all the species, varieties and forms recognised by Wollenweber & Reinking (Wollenweber and Reinking, 1935) within a grouping called section *elegans*. Morphological characterization of *F. oxysporum* is based on the shape of macroconidia, the structure of microconidiophores, and the formation and disposition of chlamydospores (Beckman, 1987). Due to shortcomings of morphological characters for delineating species and subgeneric groupings of the genus *Fusarium,* research focus has shifted to molecular tools for identification and determination of evolutionary relationships among species. These molecular tools include sequencing, Restriction Fragment Length Polymorphism (RFLP) and Random Amplified Polymorphic DNA (RAPD).

Plant pathogenic isolates of *F. oxysporum* have been traditionally classified into formae speciales based on the host plant species (Armstrong and Armstrong, 1981). Over 120 formae speciales have been described (Hawksworth *et al.*, 1995). Each forma specialis consists of isolates with the ability to cause wilt on a given host or a narrow range of host species. Further subdivisions of formae speciales into physiological races are based on their capacity to cause disease on different host cultivars (Correll, 1991). The genetic basis of host specificity (*formae speciales*) and cultivar specificity (races) in *F. oxysporum* is currently the subject of intense studies (Takken and Rep, 2010). Determining formae speciales in *F. oxysporum* mostly relies on the time-consuming procedure of testing the fungus for pathogenicity on various plant species (Fravel *et al.*, 2003), although a recent study identified genes specific for the forma specialis *lycopersici* pathogenic on tomato (Michielse and Rep, 2009).

*F. oxysporum* lacks a known sexual cycle. Vegetative hyphal fusion and heterokaryon formation between individuals has been suggested as a way of horizontal gene transfer between isolates, but is generally restricted to compatible strains with similar genotypes (Kistler, 1997). These exclusive networks of strains capable of heterokaryon formation are designated as vegetative compatible groups (VCGs) (Puhalla, 1985).

## 1.2. Biology and epidemiology

Culture conditions affect growth rate, shape, size and abundance of conidia as well as number of septa and pigmentation (Booth, 1971). *F. oxysporum* is able to change its morphology and colour depending on the environmental conditions. In general, aerial mycelium appears first in a white colour and then turns to a variety of colours, ranging from pink to dark purple, depending on the isolate and environmental conditions.

Asexual reproduction in *F. oxysporum* is accomplished by asexual conidia (Gordon and Martyn, 1997). The species produces three types of asexual spores: microconidia, macroconidia and chlamydospores (Figure 1) (Agrios, 1997). Microconidia are one or two-cell dispersal structures that are abundantly produced under most conditions. This type of

spore is most roduced within the xylem vessels of infected plants. Macroconidia contain three to five cells and are gradually pointed and curved toward the ends. Macroconidia are commonly found on the surface of dead plants killed by the pathogen. Chlamydospores are round, thick-walled spores produced either terminally or intercalary on older mycelium. These spores contain either one or two cells (Agrios, 1997). They are produced in axenic cultures as well as in the host during the final stages of disease and their biological function is primarily long-term survival in soil.

In short distances, *F. oxysporum* propagates mainly through water irrigation or contaminated equipment. The fungus can also travel long distances within infected plants, soil or by wind in the form of microconidia. Although it can infect fruit tissue and contaminate seeds, propagation rarely happens by way of the seed (Agrios, 1997).


**Figure 1. Fusarium conidia.**
(**A**) Macroconidia. (**B**) Microconidia. (**C**) Clamydospores

## 1.3. Life Cycle

*F. oxysporum* is a saprophytic fungus that can survive for long time periods in infected plant debris in the soil as mycelium or conidia, but most commonly as chlamydospores (Agrios, 1997). Chlamydospores remain dormant until stimulated to germinate by nutrients released from roots. Root invasion is followed by the penetration of the cortex, colonization of the vascular tissue and development of systemic vascular wilt disease (Agrios, 1997). While the plant is alive, fungal growth is restricted to the xylem tissues and a few adjacent cells. Only when the plant dies the fungus grows out of the vascular

system into adjacent parenchyma cells producing large amounts of conidia and chlamydospores (Agrios, 1997).

### 1.3.1. Formation and germination of spores

Chlamydospore formation in pathogenic *Fusarium* species commonly takes place in hyphae in the infected and decaying host tissue (Nash *et al*. 1961, Christou & Snyder 1962) and from macroconidia that originate from sporodochia within lesions at the soil level (Nash *et al*. 1961, Christou & Snyder 1962). It has been suggested that chlamydospore formation depends on the nutrient status of the environment (Schippers and Van Eck, 1981). Conidia are subjected to much lower nutrient levels under field conditions than on the exprerimental conditions of a rich agar media plate. Once carbohydrates are released from decaying plant tissue or from roots, chlamydospore germination is stimulated (Schippers and Van Eck, 1981) (Figure 2D)

### 1.3.2. Infection

After germination, infection hyphae adhere to host roots (Bishop and Cooper, 1983b; Di Pietro *et al.*, 2001) and penetrate them directly (Rodriguez-Galvez and Mendgen, 1995) (Figure 2A). Penetration of the root is likely to be controlled by a combination of factors including plant and fungal compounds that function as activators or inhibitors of germination and infection tube formation, and possibly by structural cues on the plant surface (Mendgen *et al.*, 1996). The most common sites of direct penetration are located at or near the tip of both taproots and lateral roots (Lucas, 1998). The pathogen enters the apical region of the root where the endodermis is not yet fully differentiated (Agrios, 1997) (Figure 2B). During colonisation, the mycelium advances inter- and intra-cellularly through the root cortex until it reaches the xylem vessels and extends through the vessels via the pits (Bishop and Cooper, 1983b). The fungus remains exclusively within the xylem vessels, using them as avenues to colonize the host (Figure 2C). Colonization of the vascular system is rapid, and frequently facilitated by the formation of microconidia within the xylem vessels (Beckman *et al.*, 1961), that are detached and carried upward in the

sap stream (Bishop and Cooper, 1983b). Once the perforation plates stop the microconidia, they germinate and germ tubes penetrate the perforation plates, forming new hyphae and subsequently conidiophores and microconidia (Beckman and Halmos, 1962; Beckman *et al.*, 1961).

### 1.3.3. Development of vascular wilt disease

Vascular wilt is most likely caused by a combination of pathogen activities and plant defense responses. The former include accumulation of fungal mycelium in the xylem vessels and phytotoxin production, while the latter include production of vascular gels, gums and tyloses, and vessel crushing by proliferation of adjacent parenchyma cells (Beckman, 1987). Ultimately, wilt symptoms are caused by severe water stress mainly due to vessel occlusion. Symptoms are variable, but include combinations of vein clearing, leaf epinasty, wilting, chlorosis, necrosis, and abscission. Severely infected plants wilt and die, while plants affected to a lesser degree become stunted and lose productivity. The most prominent internal symptom is vascular browning (Beckman, 1987)

## 1.4. Management of Fusariosis

Management of Fusarium wilt is achieved through chemical soil fumigation or resistant cultivars. However, the broad-spectrum biocides used to fumigate soil before planting, particularly methyl bromide, are environmentally damaging and are now banned in most countries. By large, the most cost effective and environmentally safe method of control is the use of resistant plant cultivars, when available (Fravel *et al.*, 2003). Resistant tomato and melon cultivars are highly successful in conferring resistance to certain races of *F. oxysporum* f.sp. *lycopersici* and *F. oxysporum* f.sp. *melonis*, respectively (Joobeur *et al.*, 2004; Ori *et al.*, 1997). In cases where there is no resistance against Fusarium wilt, the disease can only be controlled by preventing the introduction of the pathogen, the destruction of diseased plants, or the isolation of susceptible plants from infected sites.

Studies on biological control of Fusariosis under greenhouse and field conditions have been focused on the application of selected strains of antagonistic bacteria or non-pathogenic strains of *F. oxysporum*. Several mechanisms contribute to the biocontrol capacity of these biocontrol agents, including competition for nutrients in the soil affecting the rate of chlamydospore germination, antibiosis, competition for infection sites on the root and triggering of plant defence reactions, inducing systemic resistance (Khan *et al.*, 2006; Larena *et al.*, 2002; Larkin and Fravel, 2002).

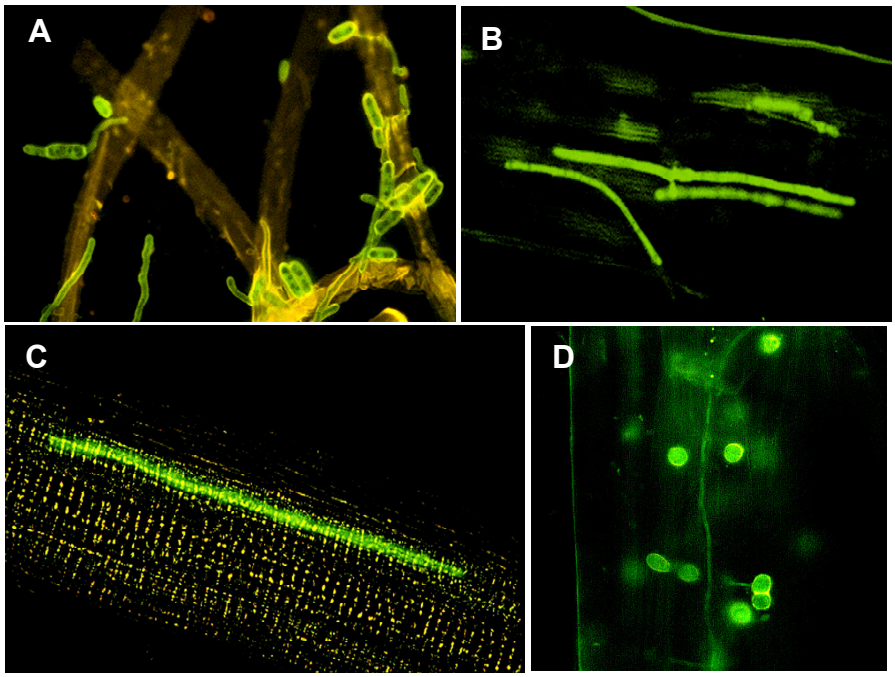


**Figure 2. Sequence of events during vascular infection of tomato by *F. oxysporum* f. sp. *lycopersici*.**
(A) Germinated microconidia and penetration hyphae of wild-type strain 4287 attaching to the surface of tomato roots 24 h after inoculation. B. and C. Infection hyphae of wild-type strain 4287 growing in the root cortex, 5 days after inoculation (B); and in a root xylem vessel, 7 days after inoculation (C). D. Chlamydospores of *F. oxysporum* produced on dying plant tissue. From (Di Pietro *et al.*, 2001).

## 2. Plant-pathogen interactions

### 2.1. Virulence mechanisms

Pathogenic fungi have developed strategies to invade and grow within plant hosts. Contrary to bacteria and viruses, multicellular fungi are able to actively penetrate plant surfaces. The cuticle is the first barrier encountered by aerial plant pathogens. Many plant pathogenic fungi secrete cutinases for enzymatic degradation of the cuticle, as is the case in *F. solani* f. sp. *pisi* on pea (Maiti and Kolattukudy, 1979). Some pathogens are able to penetrate by way of infection hyphae, whereas others elaborate specialized infection structures called appressoria, that are able to generate turgor pressure (Hamer and Talbot, 1998; Sweigard *et al.*, 1992). Penetration through the roots, which lacks a cuticle, does not require cutinases, but relies on secretion of other cell wall-degrading enzymes such as cellulases and pectinases, as in the case for *F. oxysporum* (Di Pietro *et al.*, 2009).

Penetration is followed by colonisation of the living plant tissue. At this stage, the fungus often secretes toxins or plant hormone-like compounds that manipulate the plants' physiology to the benefit of the pathogen (Knogge, 1996). Recent evidence has shown that fungal pathogens are also able to produce effector molecules that suppress the plant defence response (De Wit *et al.*, 2009). Some phytopathogenic fungi secrete enzymes for detoxification of plant antifungal compounds. One such enzyme is tomatinase, which degrades the plant saponin α-tomatine and has been extensively characterised in *F. oxysporum* (Pareja-Jaime *et al.*, 2008; Roldan-Arjona *et al.*, 1999). Interestingly, *F. oxysporum* is able to use the degradation product of this hydrolysis to suppress induced plant defence responses by interfering with fundamental signal transduction processes (Bouarab *et al.*, 2002).

### 2.2. Plant defence mechanisms

Although plants lack a classical immune system, they have evolved efficient mechanisms to protect themselves against pathogens. Indeed, plants are resistant to most pathogens

in their environment, either because they are not host plants for a particular pathogen or because they are host plants but have resistance genes that allow them to specifically recognize distinct pathogen races (Scheel, 1998). Two types of plant resistance response can be distinguished: nonhost and host or race/cultivar specific resistance response. In both cases, the biochemical processes involved in pathogen resistance are similar (Somssich and Hahlbrock, 1998).

Resistance in plants is characterised by the inability of the pathogen to grow and spread and often takes the form of a hypersensitive reaction (Agrios, 1997). The hypersensitive response is characterized by localised cell death at the site of infection. As a result, the pathogen is confined to necrotic lesions near the site of infection (Van Loon, 1997). Tissues surrounding necrotic lesions undergo localized acquired resistance (Baker *et al.*, 1997; Fritig *et al.*, 1998; Hammond-Kosack and Jones, 1996). These local responses often lead to nonspecific resistance throughout the plant, known as systemic acquired resistance, providing long-term protection against challenge infection by a broad range of pathogens (Fritig *et al.*, 1998; Ryals *et al.*, 1996; Sticher *et al.*, 1997; Van Loon, 1997). The metabolic alterations in localized acquired resistance include: cell wall reinforcement by deposition and crosslinking of polysaccharides, proteins, glycoproteins and insoluble phenolics; stimulation of secondary metabolic pathways, some of which yield small compounds with antibiotic activity (the phytoallexins) but also defense regulators such as salicylic acid, ethylene and lipid-derived metabolites; accumulation of broad range of defense-related proteins and peptides (Fritig *et al.*, 1998; Hahn, 1996).

## 2.3. Plant-pathogen recognition

Plant-pathogen interaction is a complex process with several stages and levels of recognition that determine either success or failure of the infection process (Callow, 1987). Pathogen detection is the first step for activation of plant defence mechanisms if invasion is to be stopped. Plants respond to attacks by pathogens at two levels (Jones and Dangl, 2006). At level one, the plant is able to recognise molecules commonly produced by all microbes, called pathogen-associated molecular patterns (PAMPS),

including polysaccharides and gycoproteins present in fungal cell walls. As a consequence, plants are generally non-hosts for most pathogens and therefore can be considered resistant.

Successful pathogens have evolved mechanisms to overcome this first layer of defense, either by evading detection or by suppressing the defense response by the means of secreted effectors. In this case, the plant becomes a host for a given pathogen species, establishing a compatible interaction. During evolution, plants have acquired a second level, of defense, based on the capacity to recognise these specific virulence factors called effectors, and mounting a hypersensitive response (Jones and Dangl, 2006).

In the 50´s, Flor proposed the gene-for-gene hypothesis (Flor, 1947, 1971), establishing that for every avirulence gene (*avr*) from the pathogen there is a corresponding host resistance gene (*R*). Loss or mutation of an *avr* gene would lead to a loss of resistance mediated by the corresponding R gene (Farman *et al.*, 2002). The *F. oxysporum* f. sp. *lycopersici*-tomato interaction was recently shown to fulfil the gene-for-gene model. In this forma specialis, there are three known races, named in order of discovery race 1, race 2, and race 3 (Table 1). These are defined by their capacity to produce vascular wilt on tomato cultivars carrying different resistance genes. Genes *I-1*, *I-2* and *I-3* confer resistance against race 1, race 2 and race 3, respectively (Beckman, 1987). The tomato *I-2* resistance gene as well as several avirulence genes from *F. oxysporum* have been cloned, providing molecular support for the gene-for-gene hypothesis in this pathogen-host interaction (Takken and Rep, 2010).

**Table 1. Races and resistance genes described in the *F. oxysporum f. sp. lycopersici* – tomato interaction.**
From (Takken and Rep, 2010).

| Race | Resistance genes in tomato cultivars | | |
|---|---|---|---|
| | I-1 | I-2 | I-3 |
| Race 1 | Avirulent | Virulent/Avirulent | Virulent/Avirulent |
| Race 2 | Virulent | Avirulent | Virulent/Avirulent |
| Race 3 | Virulent | Virulent | Avirulent |

One of these avirulence proteins is Six1 which is secreted during colonisation of the xylem and mediates recognition by resistance gene *I-3*. Strains defective in *six1* are virulent on *I-3* plants, while those expressing the gene are not. However, loss of Six1 comes at a cost for the pathogen, causing a global reduction of virulence (Rep *et al.*, 2004).

## 2.4. Fungal genes required for pathogenicity on plants

The current increase in the number of pathogenic isolates resistant to fungicides respresents a threat for agriculture and human health, underscoring the need for developement of new active principles. Cross-resistance makes it necessary to develop antifungals with new modes of action. The information provided by the sequencing of fungal genomes is aiding the identification of new genes and proteins that could be useful for the design of targeted drugs (Isaacson, 2002). However, a deeper understanding of the molecular basis of infection is required to focus the development of novel strategies for disease control.

In *F. oxysporum* and in other fungal pathogens, two main strategies have been used for identification of pathogenicity genes. The first is reverse genetics, involving targeted deletion of candidate genes whose products may be involved in known biological functions relevant for infection (Di Pietro *et al.*, 2003). This strategy has been facilitated recently through the sequencing of the genome of *F. oxysporum* f. sp. *lycopersici* (Ma *et al.*, 2010). A second strategy known as forward genetics involves generation of pathogenicity mutants by random insertional mutagenesis followed by identification of the genes affected in these mutants (Madrid *et al.*, 2003). Methods used for random insertional mutagenesis include the use of small transposable elements (Li Destri Nicosia *et al.*, 2001; Lopez-Berges *et al.*, 2009), *Agrobacterium tumefaciens* (ATMT)-mediated transformation (de Groot *et al.*, 1998; Michielse *et al.*, 2009a) and restriction enzyme-mediated integration (REMI) mutagenesis (Imazaki *et al.*, 2007; Namiki *et al.*, 2001).

Genes that have a significant effect on pathogenicity are often found to regulate expression of many other genes. Among these regulatory genes are those encoding signalling components and transcription factors (Table 2).

**Table 2. *F. oxysporum* genes with an effect in pathogenesis.**
Adapted from (Michielse and Rep, 2009)

| Gene | Product/function | Effect of gene inactivation/deletion | Reference |
|---|---|---|---|
| *arg1* | Argininosuccinate lyase | Strongly reduced virulence, arginine auxotrophy | (Namiki *et al.*, 2001) |
| *chs2* | Class II chitin synthase | Reduced virulence | (Martin-Urdiroz *et al.*, 2008) |
| *chs7* | Chaperone-like protein | Reduced virulence | (Martin-Urdiroz *et al.*, 2008) |
| *chsV* | Class V chitin synthase | Strongly reduced virulence, hypersensitive to α-tomatine and $H_2O_2$ | (Madrid *et al.*, 2003) |
| *chsVb* | Class VII chitin synthase | Non-pathogenic, hypersensitive to Congo red and Calcofluor white | (Martin-Urdiroz *et al.*, 2008) |
| *cmle1* | Carboxy- cis, cis-muconate cyclase | Non-pathogenic, reduced growth on phenolic compounds | (L. Reijnen and C. B. Michielse, unpublished results) |
| *clc1* | Chloride channel | Reduced virulence, deficient in laccase activity, increased sensitivity to oxidative stress | (Canero and Roncero, 2008) |
| *con7* | Transcription factor | Non-pathogenic | (Pareja-Jaime *et al.*, unpublished results) |
| *cti6* | Transcription factor | Reduced virulence | (Michielse *et al.*, 2009a) |
| *dcw1* | Cell wall protein | Reduced virulence | (Michielse *et al.*, 2009a) |
| *fbp1* | F-box protein | Reduced virulence, impaired in root attachment and invasive growth | (De Miguel & Hera, unpublished results) |
| *fga1* | G-protein α-subunit | Markedly reduced virulence, decreased conidiation | (Jain *et al.*, 2002) |
| *fga2* | G-protein α-subunit | Non-pathogenic, increased resistance to heat | (Jain *et al.*, 2005) |

| | | | |
|---|---|---|---|
| *fgb1* | G-protein β-subunit | Markedly reduced virulence, decreased conidiation | (Delgado-Jarana *et al.*, 2005; Jain *et al.*, 2003) |
| *fmk1* | Mitogen-activated protein kinase | Non-pathogenic, impaired in root attachment and invasive growth | (Di Pietro *et al.*, 2001) |
| *fnr1* | Transcription factor | Markedly reduced virulence, reduced ability to use secondary nitrogen sources | (Divon *et al.*, 2006) |
| *fow1* | Mitochondrial carrier | Strongly reduced virulence, impaired in plant colonization | (Inoue *et al.*, 2002) |
| *fow2* | Transcription factor | Non-pathogenic, impaired in invasive growth, not in root attachment | (Imazaki *et al.*, 2007) |
| *FOXG_09487* | Hypothetical protein | Reduced virulence | (Michielse *et al.*, 2009a) |
| *fpd1* | Similar to chloride conductance regulatory protein | Markedly reduced virulence | (Kawabe *et al.*, 2004) |
| *frp1* | F-box protein | Non-pathogenic, impaired in root colonization and penetration, impaired growth on various carbon sources | (Duyvesteijn *et al.*, 2005; Jonkers *et al.*, 2009) |
| *ftf1* | Transcription factor | Reduced virulence (RNAi silencing) | (Ramos *et al.*, 2007); J. M. Diaz-Minguez (University of Salamanca, personal communication) |
| *gas1* | β-1,3-Glucanosyltransferase | Markedly reduced virulence, reduced growth on solid medium | (Caracuel *et al.*, 2005) |
| *msb2* | Transmembrane mucin-like protein | Markedly reduced virulence, reduced growth on solid media, increased sensitivity to cell wall stress. | (Pérez-Nadales and Di Pietro, this work) |
| *pacC* | Transcription factor | Increased virulence and transcription of acid-expressed genes | (Caracuel *et al.*, 2003) |
| *pex12* | Peroxin | Reduced virulence, impaired in growth on fatty acids | (Michielse *et al.*, 2009a) |

| | | | |
|---|---|---|---|
| *pex26* | Peroxin | Reduced virulence, impaired in growth on fatty acids | (Michielse *et al.*, 2009a) |
| *rho1* | Monomeric G protein | Markedly reduced virulence, reduced growth on solid media | (Martinez-Rocha *et al.*, 2008) |
| *sge1* | Transcription factor | Non-pathogenic, reduced conidiation | (Michielse *et al.*, 2009b) |
| *sho1* | Tetraspan transmembrane protein | Markedly reduced virulence, reduced growth on solid media, increased sensitivity to cell wall stress. | (Pérez-Nadales and Di Pietro, this work) |
| *six1* | Small secreted protein | Reduced virulence, effect more pronounced on 4- to 5-week-old plants | (Rep *et al.*, 2005) |
| *snf1* | Protein kinase involved in carbon catabolite repression | Markedly reduced virulence, reduced growth on complex carbon sources | (Ospina-Giraldo *et al.*, 2003) |
| *ste12* | Transcription factor | Markedly reduced virulence, impaired in invasive growth | (Asuncion Garcia-Sanchez *et al.*, 2009; Rispail and Di Pietro, 2009) |
| *tom1* | Tomatinase enzyme | Reduced virulence, reduced tomatinase activity, increased sensitivity to $\alpha$-tomatine | (Pareja-Jaime *et al.*, 2008) |
| *veA* | Regulatory protein | Reduced virulence, altered development and reduced secondary metabolism | (López-Berges *et al.*, unpublished results) |
| *velB* | Regulatory protein | Reduced virulence, altered development and reduced secondary metabolism | (Lopez-Berges *et al.*, 2009) |

## 2.5. *F. oxysporum* as an opportunistic pathogen of mammals

Besides causing vascular wilt disease in a great number of plant species, *F. oxysporum* is also considered an emergent pathogen of humans (Boutati and Anaissie, 1997), together with other oppotunisitc fungal species such as *Aspergillus fumigatus*, *A. flavus*, *A. terreus*,

*Penicillium marneffei*, *Coccidioides immitis*, *Sporothix schenckii* and certain serotypes of *Cryptoccocus neoformans* and *Candida albicans*. Human infections caused by *Fusarium,* mainly *F. solani* and *F. oxysporum* (O'Donnell *et al.*, 2004), represent nowadays the second most frequent cause of fungal systemic infections with fatal outcomes in immunocompromised patients (Nucci and Anaissie, 2002; Zhang *et al.*, 2006). Immunosupression is generally associated with therapies related to cancer treatment or organ and tissue transplants (Zhang *et al.*, 2006).

Due to the ability of *F. oxysporum* to infect plants as well as humans, this species has been postulated as a model for the genetic disecction of fungal virulence in both systems (Ortoneda *et al.*, 2004). This work established that the 4287 strain from *F. oxysporum* f. sp. *lycopersici*, which is pathogenic in tomato plants, is able to kill immunodepressed mice. Analysis of *F. oxysporum* mutants derived from this strain revealed that the same virulence factors that are essential for plant infection may not be essential for infection of mammals and viceversa (Table 3). Recently, however, it has been shown that the simultaneous deletion of two factors that are individually not essential for pathogenesis can result in avirulence in mice. Such is the case of the double Δ*fmk1*Δ*fgb1*, which is unable to kill immunodepressed mice (Prados-Rosales *et al.*, 2006).

**Table 3. *F. oxysporum* genes studied both in plant and animal models.**

| Mutant | Phenotype in Plant | Phenotype in Mouse | Referencia |
|---|---|---|---|
| Δ*fgb1* | Avirulent | Virulent | (Delgado-Jarana *et al.*, 2005) |
| Δ*fmk1* | Avirulent | Virulent | (Di Pietro *et al.*, 2001; Ortoneda *et al.*, 2004) |
| Δ*fmk1*Δ*fgb1* | Avirulent | Avirulent | (Prados-Rosales *et al.*, 2006) |
| Δ*chsV* | Avirulent | Virulent | (Madrid *et al.*, 2003) |
| Δ*pacC* | Virulent | Avirulent | (Caracuel *et al.*, 2003; Ortoneda *et al.*, 2004) |
| Δ*fpr1* | Virulent | Avirulent | Prados-Rosales and Di Pietro, unpublished |
| Δ*rho1* | Avirulent | Virulent | (Martinez-Rocha *et al.*, 2008) |
| Δ*wc1* | Virulent | Avirulent | Ruíz-Roldán *et al* (unpublished) |

## 3. Mitogen-activated protein kinase signal transduction pathways

Like all living organisms, fungi are able to sense and respond to changes in the environment. Signal transduction pathways play a central role in perception of such changes and in activation of the intracellular molecular machinery leading to adaptive cell responses. Typically, transduction of a signal involves binding of a given ligand to a cognate receptor, leading to conformational changes in the receptor and subsequent activation of one or several downstream components. Eventually, this will produce changes the expression profile of genes within the responding cells and alter cellular behaviour.

In eukaryotic cells, a conserved family of serine/threonine protein kinases known as mitogen-activated protein (MAP) kinases (MAPKs) functions in transduction of a variety of extracelular signals and in regulation of several developmental processes (Widmann *et al.*, 1999). MAP Kinase pathways comprise a conserved module of three kinases: the MAP kinase (MAPK), the MAP kinase kinase (MAPKK or MEK) and the MAP kinase kinase kinase (MAPKKK or MEKK) that sequentially activate each other by phosphorylation (Figure 3). The upstream signals are sensed by specific receptors that trigger the central module directly or through intermediate signalling components. MAPKs phosphorylate a diverse set of substrates, including transcription factors, translational regulators, MAPK-activated protein kinases, phosphatases, and other classes of proteins, thereby regulating metabolism, cellular morphology, cell cycle progression, and gene expression in response to a variety of extracellular stresses and molecular signals.

### 3.1. MAP kinase pathways in *S. cerevisiae*

Our current understanding of MAPK pathways is largely based on research in the model organism *Saccharomyces cerevisiae*. Four MAPKs regulate cell growth and morphogenesis in response to different environmental stimuli in yeast (Figure 3): Fus3 controls the response to mating pheromones, Kss1 regulates a morhogenetic switch in response to nutrient conditions, Hog1 is required for adaptation to hyperosmotic stress

and Mpk1/Stl2 controls cell surface remodelling under hypo-osmotic stress (Qi and Elion, 2005). In addition, MAPK-mediated regulation of the cell cycle has been well documented in the case of Fus3 (Elion, 2000; Peter *et al.*, 1993) and Hog1 (Clotet and Posas, 2007; Escote *et al.*, 2004; Yaakov *et al.*, 2009). A fifth MAPK, Smk1 specifically regulates sporulation (Gustin *et al.*, 1998). It lacks upstream MEK or MEKK and has no homologue in other fungi, except for certain ascomycetous yeasts such as *Ashbya gossypii* and *Kluyveromyces lactis* (Zhao *et al.*, 2007). Several recent reviews provide excellent overviews of the yeast MAPK signalling networks leading from signals to transcriptional targets (Chen and Thorner, 2007).

### 3.1.1. Different MAPK cascades share common upstream components

Three of the five yeast MAPK pathways (Fus3, Kss1 and Hog1) are activated by a common upstream module composed of the cytosolic protein Ste20, a member of the p21-activated protein kinase (PAK) family of protein kinases, the small GTPase protein Cdc42, a global establisher of cell polarity, and the MAPKK Ste11 (Figure 3). Additionally, the Fus3 and Kss1 pathways share the MAPKK Ste7, and signalling through Kss1 and Hog1 pathways also requires two shared membrane components, Msb2, a member of the membrane mucin class of proteins and the tetraspan protein Sho1.

Ste20 is activated by Cdc42 in its active GTP-bound state, which is mainly located at the plasma membrane (Lamson *et al.*, 2002). For initiation of signalling to occur, upstream events must stimulate GTP loading of Cdc42 and recruitment of Ste20 to its vicinity in all three MAPK pathways (Chen and Thorner, 2007). A number of docking interactions based on protein domain specificity contribute to this end. The membrane-associated adaptor protein Bem1 contributes to Ste20 location to the plasma membrane via interaction of its N-terminal Src-homology-3 (SH3) domains with proline-rich motifs in Ste20 (Winters and Pryciak, 2005). The MAPKK Ste11 is recruited to the same general vicinity as activated Ste20 through its interaction with the small adaptor protein Ste50 (Wu *et al.*, 1999), which is also able to associate with Cdc42 via its C-terminal Ras-association (RA) domain (Tatebayashi *et al.*, 2006; Truckses *et al.*, 2006). Additionally, distinct

pathway-specific scaffold proteins and membrane receptors contribute to the establishment of signalling specificity upon external stimulation. While the contribution to pathway specificity by canonical scaffold and receptor proteins is well established for the pheromone response pathway, much less is known on how signalling specificity is maintained between Kss1 and Hog1 pathways.

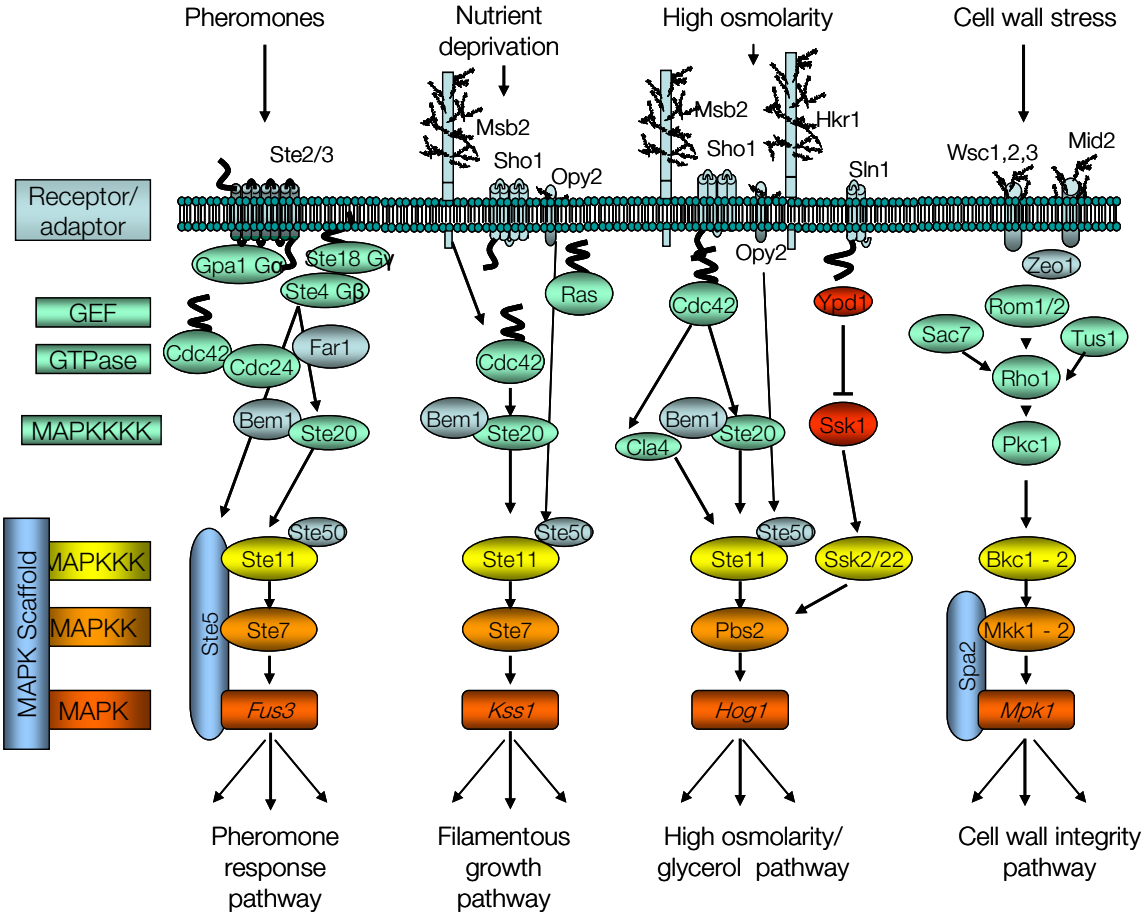


**Figure 3. MAP kinase pathways in *Saccharomyces cerevisiae*.**
Schematic diagram of MAPK signalling pathways in *S. cerevisiae*. For simplicity, not all factors and interactions are shown, connections to other pathways and processes upstream of the MAPKs are omitted, and direct targets of the MAPKs are not included. Adapted from (Chen and Thorner, 2007; Rispail *et al.*, 2009).

### 3.1.2. The pheromone response pathway

*S. cerevisiae* exists in two haploid cell types, MATa and MATα that can mate to produce diploid MATa/MATα cells. Mating regulation by the pheromone response MAPK pathway has been characterised in detail (Elion, 2000; Gustin *et al.*, 1998; Kurjan, 1993; Wang and Dohlman, 2004). Signalling for mating is initiated when α or a pheromone secreted by the haploid cells binds to the cognate cell surface receptors, Ste2 or Ste3, respectively. Pheromone receptors are coupled to a common heterotrimeric G protein, Gpa1-Ste4-Ste18, where Gpa1 is Gα and Ste4-Ste18 is the Gβγ complex. Pheromone binding induces receptor-mediated activation of Gpa1 by GTP exchange, which results in dissociation of βγ subunits Ste4 and Ste18 (Klein *et al.*, 2000). Free membrane-anchored Gβγ is then able to interact with three known effectors: Ste20, Ste5 and Far1 (Butty *et al.*, 1998; Feng *et al.*, 1998; Inouye *et al.*, 1997). Far1 binds to, and most likely activates, Cdc24, the only known GEF activator for Cdc42 (Butty *et al.*, 1998; Nern and Arkowitz, 1999; Wiget *et al.*, 2004). Cdc24 also associates with Bem1, which promotes location of Ste20 to the plasma mebrane. Ste5 is a scaffold protein that functions specifically in pheromone response by binding all three kinases of the MAPK cascade (Ste11, Ste7, and Fus3) (Choi *et al.*, 1994; Marcus *et al.*, 1994; Printen and Sprague, 1994). This protein interaction network promotes encounter of Cdc42 with its activator Cdc24 and places its target kinase (Ste20) and the downstream cascade that needs to be activated (Ste11, Ste7 and Fus3) in close proximity and at high local concentration. In addition to Fus3, pheromone stimulation also leads to transient activation of the Kss1 MAPK (Gagiano *et al.*, 2002; Ma *et al.*, 1995). Fus3 and Kss1 are the most closely related MAPKs in the yeast genome and appear to be the orthologs of mammalian ERK1 and ERK2, respectively. They belong to the yeast and fungal extracellular signal-regulated kinase (YERK1) subfamily (Kultz and Burg, 1998). While Fus3 is essential for mating, Kss1 controls invasive growth and pseudohyphal development (Madhani *et al.*, 1997). In contrast to Fus3, Kss1 can also be activated by Ste7 protein that is not bound to the Ste5 scaffold (Elion, 1998).

Phosphorylated Fus3 in *S. cerevisiae* activates downstream effectors such as Ste12, Far1 or Sst2, leading to cell cycle arrest, polarized growth and formation of specialized fusion tubes called shmoos (Elion *et al.*, 1993). Far1 mediates cell cycle arrest in response to pheromone (Peter *et al.*, 1993) and specifies direction of polarized growth during mating by linking the heterotrimeric Gβγ subunits to the polarity establishment machinery (Butty *et al.*, 1998). Ste12 is a key transcription factor downstream of the pheromone response cascade, which binds to pheromone response elements (PREs) in the upstream activating sequences of its target genes and, in cooperation with Tec1, also regulates genes involved in invasive growth (Madhani and Fink, 1997).

### 3.1.3. The filamentous growth (FG) pathway

*S. cerevisiae* cells have a spherical or ovoid (yeastlike) form and proliferate by budding under nutrient-rich conditions. When nutrients are limiting, cells become thin and elongated, and daughter cells remain adhered and connected end-to-end with the mother cell, adopting a filamentous form. This behaviour is known as the filamentous growth (FG) response (Cullen and Sprague, 2000; Gimeno *et al.*, 1992; Patankar *et al.*, 1993; Roberts and Fink, 1994). In haploid cells, this response, which leads to agar invasion, is termed invasive growth, and is activated when glucose becomes limiting. In diploids, it is termed pseudohyphal growth and is elicited by nitrogen starvation. Cellular phenotypes associated with FG include a delay in the G2 phase of the cell cycle, reorganization of cell polarity and changes in cell-cell and cell-substrate adherence (Kron *et al.*, 1994; Rua *et al.*, 2001; Verstrepen and Klis, 2006). These changes are co-regulated by several signalling pathways including the RAS-cyclic AMP-protein kinase A pathway (Mosch *et al.*, 1999; Mosch *et al.*, 1996), the target of rapamycin (TOR) pathway (Rohde and Cardenas, 2004; Vinod *et al.*, 2008) and the Kss1 MAPK pathway, commonly referred to as the FG pathway (Borneman *et al.*, 2007; Roberts and Fink, 1994).

The FG MAPK pathway shares a number of components with the pheromone response pathway, namely Cdc42, Ste20, Ste50, Ste11 and Ste7 (Figure 3). Similar to pheromone signalling, Cdc42 activation of the MAPK module Ste11/Ste7/Kss1 requires recruitment

of the Cdc42-GEF, Cdc24 to the plasma membrane. In filamentous growth, Cdc42 activation by Cdc24 is dependent on the small GTPase protein Ras2 (Mosch *et al.*, 1996), however, it is not clear how Ras2 promotes Cdc24 recruitment or how it becomes activated by its own GEF, Cdc25. Upstream of Cdc42, two integral membrane proteins, Sho1 and Msb2 are required for Kss1 activation under conditions that promote filamentous growth (O'Rourke and Herskowitz, 2002). Msb2 interacts with Sho1 and with activated GTP-bound Cdc42 (Cullen *et al.*, 2004), suggesting that the two membrane proteins may promote a scaffold module for FG pathway activation. A third transmembrane protein, Opy2, may also contribute to this scaffold function by promoting recruitment of the Ste11-adaptor protein Ste50 (Tatebayashi *et al.*, 2007). Activated Kss1 phosphorylates two repressors, Dig1 and Dig2, in the nucleus. This in turn derepresses the transcription factor Ste12 (Cook *et al.*, 1996) which is targeted to the promoters of FG genes in a heterodimeric complex with a second transcription factor, Tec1 (Madhani and Fink, 1997).

As mentioned before, several other upstream components and protein kinases contribute to establishment of the FG response. Ras2 activates membrane adenylate cyclase that converts ATP to cAMP, with the concomitant increase of intracellular cAMP levels (Gancedo, 2001). cAMP binding induces release of the three cAMP-dependent protein kinase (PKA) subunits that leads to activation of the transcription factors Flo8 and Slf1, which function as activator and repressor, respectively, of the *FLO11* gene. *FLO11* encodes a GPI-anchored cell surface glycoprotein that is required for cell-cell and cell-substratum adhesion and for filamentous growth. The 5´-AMP-activated protein kinase (AMPK) Snf1 is required for transcription of glucose-repressed genes (Hardie *et al.*, 1998; Sanz, 2003) and contributes to invasive growth of haploid cells by promoting sustained *FLO11* expression in response to glucose depression. In addition, recent evidence suggests that the protein kinase TOR may participate in regulation of Snf1 during the diploid pseudohyphal response to limiting nitrogen (Orlova *et al.*, 2006). Finally, two transmembrane proteins, Mep2 and Gpr1 (Lorenz *et al.*, 2000; Tamaki *et al.*, 2000) also take part in the filamentous growth response (Truckses *et al.*, 2004). Gpr1 is a glucose

(and sucrose)-binding G-protein coupled receptor (GPCR) that serves as a carbon sensor (Lemaire *et al.*, 2004; Lorenz *et al.*, 2000). Gpr1 associates with a distinct Gα subunit, Gpa2 (Xue *et al.*, 1998) and contributes to filamentous growth through Gpa2-mediated stimulation of PKA activation, although it is not clear whether this requires the Ras2 GTPase (Chen and Thorner, 2007). Mep2 is a high-affinity ammonium permease (Soupene *et al.*, 2001) that also regulates diploid pseudohyphal growth in response to ammonium starvation. Dominant active Gpa2 or Ras2 bypass the need for Mep2 in diploid pseudohyphal growth (Lorenz and Heitman, 1998; Van Nuland *et al.*, 2006), suggesting that Mep2 is connected both to the Kss1 MAPK and the cAMP-PKA pathways (Chen and Thorner, 2007).

### 3.1.4. The Hog1 hyperosmotic response pathway

The Hog1 pathway in *S. cerevisiae* is known as the high osmolarity glycerol (HOG) pathway and is required for growth under hyperosmotic conditions (Hohmann *et al.*, 2007; O'Rourke and Herskowitz, 2002). This pathway is regulated by two upstream branches that converge to activate the MAPKK Pbs2 and the MAPK Hog1. One branch depends on the Sho1 transmembrane protein, while the other branch depends on the two-component histidine kinase receptor Sln1. The intermediate components of the Sho1 branch are Ste20 and Ste11, and those for the Sln1 branch are Ypd1, Ssk1, Ssk2 and Ssk22 (Figure 3). Phosphorylation of Pbs2 via Ssk2 and Ssk22 occurs under severe osmotic stress (Posas *et al.*, 1996), while its activation by Ste11 takes place under less severe hyperosmotic conditions, whereby Pbs2 acts as a scaffold for Sho1, Ste11 and Hog1 (Posas and Saito, 1997).

It has been suggested that recruitment of Ste11 to the Sho1 branch of the Hog1 pathway is achieved not only by interaction with Pbs2, but also by its association with the plasma membrane via contacts with multiple components of the upstream machinery that trigger response to severe hyperosmotic stress (Chen and Thorner, 2007). It has been reported that Ste11 binds directly to the C-terminal cytosolic tail of Sho1 (Zarrinpar *et al.*, 2004). Moreover, Ste11 is tightly bound to Ste50 (Kwan *et al.*, 2006; Wu *et al.*, 1999), which can

associate with both the membrane-anchored protein Cdc42 (Truckses *et al.*, 2006) and the integral membrane protein Opy2 (Wu *et al.*, 2006). Absence of Opy2, like absence of Sho1, blocks activation of the Hog1 MAPK and the HOG response (Maeda *et al.*, 1995; Wu *et al.*, 2006). However, it is likely that the primary role of Opy2 is to recruit the Ste50 adaptor protein to the plasma membrane, since the osmosensitive phenotype of *opy2* mutants can be rescued by expression of a membrane-targeted Ste50 protein (Tatebayashi *et al.*, 2007).

The membrane mucins Msb2 and Hkr1 are redundant for HOG pathway activation and have been suggested as the potential osmosensors of the Sho1 branch of the HOG pathway (Tatebayashi *et al.*, 2007). However, the mechanims by which these proteins are able to sense osmotic changes is not yet clear.

Phosphorylated Hog1 transiently accumulates in the nucleus and activates downstream target transcription factors such as Msn2, Msn4 and Mcm1 (de Nadal *et al.*, 2002). These proteins bind to the STRE consensus in the promoters of stress response genes, resulting in expression of genes required for survival under stress conditions. Like pheromone stimulation, hyperosmotic stress also causes MAPK-mediated cell cycle arrest (Clotet *et al.*, 2006; Escote *et al.*, 2004; Zapater *et al.*, 2005). Although this arrest is only transient, it seems to be important for osmoresistance. Unlike pheromone-imposed arrest, osmostress leads to cell cycle delays in both G1 and G2 (Alexander *et al.*, 2001; Zapater *et al.*, 2005). G1 arrest is mediated primarily by Hog1-mediated phosphorylation and stabilization of the Cdk inhibitor Sic1 (Escote *et al.*, 2004), while G2 arrest is dependent on a morphogenesis checkpoint in which assembly of the septin collar at the bud neck leads to recruitment of an AMPK-related protein kinase, Hsl1. Hog1 phosphorylates Hsl1, which is then unable to phophorylate the Hls7 protein factor required for degradation of the Swe1 protein kinase that would lead to progress into M phase (Barral et al., 1999; McMillan et al., 1999; Shulewitz et al., 1999). Presumably, stress reponses are most efficiently and safely mounted when the genome is not in the

vulnerable state of either replication of segregation. In mating, only G1 arrest is appropiate since cells must maintain their haploid genomic content (Chen and Thorner, 2007).

### 3.1.5. The cell integrity pathway

The Mpk1/Slt2 cell wall integrity (CWI) cascade is responsible for modulating changes in the cell wall during the cell cycle and in response to various forms of stress (Levin, 2005). Genes under control of this pathway include those involved in the synthesis and modification of major components of the cell wall, such as glucan, mannan and chitin (Garcia *et al.*, 2004; Lesage and Bussey, 2006). Lack of an Slt2/Mpk1-dependent response causes cell lysis in the absence of an osmotic support in the medium (Torres *et al.*, 1991). Five plasma membrane proteins, Wsc1, Wsc2, Wsc3, Mid2, and Mtl1, each containing a single transmembrane segment, are important for activation of the CWI pathway, although the precise mechanisms by which they sense their direct signals/stressors are unclear. The cytoplasmic C-terminal domains of Wsc1 and Mid2 interact with Rom2 (Philip and Levin, 2001), one of three GEFs encoded in the *S. cerevisiae* genome, which is thought to be specific for the small Ras-homologous GTPase, Rho1 (Ozaki *et al.*, 1996). Like Cdc42, Rho1 is tethered to the plasma membrane. Rho1 activates protein kinase C (PKC) 1 which, in turn, activates the Bck1-Mkk1/Mkk2-Mpk1 MAPK cascade (Levin, 2005). The Spa2 scaffold protein, which interacts with Bni1, Bud6 and other plasma membrane-localised actin-associated proteins, as well as with other components of the polarisome required for polarized growth, also binds Mkk1 and Mkk2, as well as their target, the Slt2/Mpk1 MAPK (Sheu *et al.*, 1998; van Drogen and Peter, 2002). Mpk1 regulates multiple nuclear targets, including the SBF complex which is formed by DNA-binding components Swi4, Mbp1 and co-factor Swi6 and acts as a transcriptional activator of cell cycle-dependent genes (Nasmyth and Dirick, 1991). A second nuclear target of Mpk1 is the MADS box transcription factor Rlm1 which regulates expression of at least 25 genes in *S. cerevisiae*, most of which have been implicated in cell wall biogenesis (Jung *et al.*, 2002).

### 3.1.6. The MAPK network

In numerous biological contexts, MAPK pathways cooperate with other MAPK (and non-MAPK) pathways to regulate cell growth, cell remodelling and cell integrity. For instance, the CWI pathway functions in different cellular contexts (Levin, 2005). It senses and responds to cell wall stress during vegetative growth and in response to a variety of challenges including pheronome-induced morphogenesis and heat shock (Garcia-Rodriguez *et al.*, 2005; Kollar *et al.*, 1997; Levin, 2005), suggesting a connection with the pherome-response and HOG MAPK pathways. Indeed, the CWI pathway is activated during pheromone response to promote efficient mating (Buehrer and Errede, 1997; Zarzov *et al.*, 1996). The HOG and CWI pathways act sequentially in response to global cell wall damage (Bermejo *et al.*, 2008; Garcia-Rodriguez *et al.*, 2005; Garcia *et al.*, 2009; Hawle *et al.*, 2007). Slt2/Mpk1 also becomes activated in response to hyperosmotic shock in a manner that depends primarily on the O-glycosylated integral membrane protein Mid2, and also requires activated Hog1 (Bermejo *et al.*, 2008; Garcia-Rodriguez *et al.*, 2005). Sequential activation of Hog1 and Mpk1 pathways is required to regulate yeast survival to cell wall stress induced by zymolyase, which hydrolyzes the beta-1,3 glucan network (Bermejo *et al.*, 2008). Zymolyase activates Slt2/Mpk1 in a Hog1-dependent manner that requires the Sho1 branch of the HOG pathway, the redundant MAPKKs Mkk1/Mkk2, the MAPKKK Bck1, and Pkc1, but not other upstream elements such as the CWI pathway sensors and the guanine nucleotide exchange factors (Bermejo *et al.*, 2008). In some situations the FG and HOG pathways can act in parallel, such as during the response to a protein glycosylation defect (Cullen *et al.*, 2000). In protein glycosylation mutants, both the FG and Mpk1 pathways are activated and required for viability (Cullen *et al.*, 2004; Cullen *et al.*, 2000). More recently, it has been established that the CWI pathway cell surface sensors Wsc1, Wsc2, Mid2 and the MAPK Slt2/Mpk1 contribute to FG by modulating cell elongation, cell-cell adherence and agar invasion, a response that requires Msb2, Ste20 and Ste12, and only partially Sho1 (Birkaya *et al.*, 2009).

On the other side, a number of mechanisms are in place to ensure pathway fidelity for activation of distinct physiological responses. Upon pheromone stimulation, Fus3 is activated for the entire duration of the cellular response. By contrast, Kss1 is only activated transiently since Fus3 inhibits Kss1 activation though an unknown mechanism (Sabbagh *et al.*, 2001). In another set of MAPK pathways, prevention of crosstalk between the osmostress and pheromone response pathways (O'Rourke and Herskowitz, 1998) requires the kinase activity of Hog1 for phosphorylation of the shared upstream component Ste50 (Hao *et al.*, 2008; Westfall and Thorner, 2006). Kss1, together with Hog1, is transiently activated by osmotic stimulation but Hog1-phosphorylated Ste50 limits the duration of Kss1 activation and prevents invasive growth under high osmolarity growth conditions (Hao *et al.*, 2008). Under glycosylation defect conditions that induce Kss1 activation and FG (Cullen *et al.*, 2000), the Kss1 MAPK inhibits Hog1 activation, possibly through modulation of the activity of the Ptp2 phosphatase (Yang *et al.*, 2009). Cross-inhibitory events are therefore likely to be modulated by the intensity and persistance of the activating signal as well as by feedback mechanisms that activate downregulation of the pathways. In addition, MAPK cascade inhibitory mechanisms are also important to ensure that MAPKs are kept at low activation levels after the stimulus has ceased, and these include the action of phosphatases (Keyse, 2008; Martin *et al.*, 2005) and/or ubiquitin-mediated degradation of pathway components (Esch *et al.*, 2006; Sato *et al.*, 2003; Wang and Dohlman, 2002; Wang *et al.*, 2003).

## 3.2. MAPK pathways in pathogenic fungi

Fungal plant pathogens have evolved strategies to recognize suitable hosts, penetrate and invade plant tissue, overcome host defences and optimize growth in the plant. To perform these tasks correctly, the fungus must perceive chemical and physical signals from the host and respond with the appropriate metabolic and morphogenetic changes required for pathogenic development. Such changes include directed hyphal growth, adhesion to the plant surface, differentiation of specialized infection structures and secretion of lytic enzymes and phytotoxins (Knogge, 1996). Many of these responses require the synthesis of specific gene products and depend on conserved signal

transduction pathways involving the activation of G proteins (Bolker, 1998), cAMP signalling (Lee and Dean, 1993; Mitchell and Dean, 1995) and mitogen-activated protein kinase (MAPK) cascades (Xu and Hamer, 1996; Xu *et al.*, 1998). In the following sections, we review knowledge gained in the past decade on the relevance of MAPK signalling for infection-related morphogenesis and virulence in plant and human pathogens.

### 3.2.1. Homologues of the Fus3/Kss1 pathways

Among the MAPKs, the yeast and fungal extracellular signal-regulated kinase (YERK1) subfamily (Kultz and Burg, 1998) plays a key role in infection-related morphogenesis and pathogenicity. In the past decade MAPK pathways in various plant and human pathogens have been characterised and shown to regulate infection related morhogenesis and virulence (Table 4). In many cases, the MAPK pathways conserve similar function, structure and organisation, however, important differences exist that reflect the specialisation of the pathways and influence their role in virulence.

Most filamentous fungi have only one MAPK homologue to the Fus3 and Kss1 yeast MAPKs. Xu and Hamer (1996) first showed that a homolog of the *S. cerevisiae fus3* gene in the rice blast fungus *Magnaporthe grisea*, designated *Pmk1 (for pathogenicity MAP kinase)*, was essential for virulence. Subsequently, several MAPKs orthologous to Pmk1 were shown to be essential for pathogenicity in a range of biologically diverse plant pathogenic fungi, particularly during the early stages of infection (Di Pietro *et al.*, 2001; Jenczmionka *et al.*, 2003; Lev and Horwitz, 2003; Lev *et al.*, 1999; Mey *et al.*, 2002; Ruiz-Roldan *et al.*, 2001; Takano *et al.*, 2000; Zheng *et al.*, 2000). *M. grisea*, *Colletotrichum lagenarium*, *C. heterostrophus* and *Pyrenophora teres* mutants lacking the Fus3/Kss1 orthologue fail to differentiate appresoria (Lev *et al.*, 1999; Takano *et al.*, 2000; Xu and Hamer, 1996; Ruiz-Roldan *et al.*, 2001). However, these mutants also fail to grow on the host plant when inoculated into wound sites, suggesting that Pmk1 orthologues regulate other virulence functions beside appresorium development. In support of this view, fungal pathogens that penetrate their plant hosts without the need for appressoria, such as *F. oxysporum*, also require the Pmk1 orthologue for infection (Di Pietro *et al.*,

2001). In *M. grisea*, several upstream components of the Pmk1 pathway, including the MAPKKK Mst11, the MAPKK Mst7 and the Ste50 homologue, Mst50 are essential for appressorium formation and pathogenicity (Park *et al.*, 2006; Zhao *et al.*, 2007). By contrast, Mst20, a homologue of yeast Ste20, is dispensable for Pmk1 activation and virulence, suggesting a difference in the upstream components of this MAPK module between yeast and filamentous fungal pathogens (Li *et al.*, 2004). Likewise, MgCdc42, the orthologue of yeast Cdc42, is not essential for appressorium formation but it is required for plant penetration and infectious growth, possibly due to a defect of turgor and superoxide generation during the appressorial development in *Mgcdc42* deletion mutants (Zheng *et al.*, 2009). Downstream of the Mst11/Mst7/Pmk1 cascade, *M. grisea* Mst12, an orthologue of the yeast Ste12 transcription factor, is not required for appresorium formation but essential for penetration and infectious growth (Park *et al.*, 2004) and the same is true for *C. lagenarium* (Tsuji *et al.*, 2003).

In *U. maydis*, an appressorium-forming biotrophic maize pathogen, two MAPKs orthologous to Fus3/Kss1, Kpp2 (Ubc3) and Kpp6, have overlapping functions in mating and plant infection. Kpp2 is involved in appressoria development (Muller *et al.*, 2003), while Kpp6 is required for the appressorial penetration step (Brachmann *et al.*, 2003). *U. maydis* Ubc2, Kpp4/Ubc4 and Fuz7, orthologues to yeast Ste50, Ste11 and Ste7, respectively, are impaired in pheromone response and virulence (Mayorga and Gold, 2001). Similar to *M. grisea*, the Ste20 orthologue Smu1 is not directly involved in activation of the Kpp4-Fuz7-Kpp2/Kpp6 MAPK cascade and is non-essential for mating and plant infection (Smith *et al.*, 2004).

Mutations in Fus3/Kss1 orthologues in fungal plant pathogens that do not form appressoria, such as *F. graminearum*, *F. oxysporum* or the necrotrophic pathogen *Botrytis cinerea* also result in mutants that are unable to colonize plants efficiently (Di Pietro *et al.*, 2001; Jenczmionka *et al.*, 2003; Zheng *et al.*, 2000). In *F. oxysporum* the *fmk1* gene is dispensable for vegetative growth and conidiation in culture (Di Pietro *et al.*, 2001), similarly to *M. grisea Pmk1* mutants (Xu and Hamer, 1996), but in contrast with

MAPK mutants of *C. heterostrophus* and *C. lagenarium* that show severe defects in conidiation (Lev *et al.*, 1999; Takano *et al.*, 2000), while those of *B. cinerea* are reduced in vegetative growth (Zheng *et al.*, 2000).

The human pathogen *C. albicans* has two orthologues of the Fus3/Kss1 MAPKS, Cek1 and Cek2. Cek1 regulates yeast-hyphal switching, mating efficiency and virulence (Alonso-Monge *et al.*, 2006; Bennett and Johnson, 2005; Csank *et al.*, 1998; Chen *et al.*, 2002). Cek2 is partially redundant with Cek1 for regulation of mating (Chen *et al.*, 2002). Deletion of other components of the Cek1 MAP kinase cascade, such as Hst7 (*S. cerevisiae* Ste7 homologue), St20 (*S. cerevisiae* Ste20 homologue) and the transcription factors Cph1 and Tec1 (homologues to *S. cerevisiae* Ste12 and Tec1, respectively) also affects virulence and hyphal formation (Kohler and Fink, 1996; Leberer *et al.*, 1996; Liu *et al.*, 1994).

Homologues of the small GTP-binding protein Ras play a crucial role in pathogenesis in several fungi. In *C. albicans*, Ras links cellular morphogenesis to virulence by regulating the MAPK and cAMP signalling pathways (Leberer *et al.*, 2001). In *U. maydis*, expression of a dominant active allele of the *ras2* orthologue promoted pseudohyphal growth in a manner dependent on the pheromone-response MAPK cascade (Lee and Kronstad, 2002). Likewise, expression of a dominant active *ras2* allele of *M. grisea* stimulated appressorium formation on non-inductive surfaces in the wild-type strain, but not in the *pmk1* mutant, suggesting that Ras2 functions upstream of the Mst11-Mst7-Pmk1 cascade (Park *et al.*, 2006). A similar signalling role for Ras2 was proposed in *F. graminearum* (Bluhm *et al.*, 2007).

**Table 4. Fus3/Kss1 homologues characterized in pathogenic fungi.**
Adapted from (Zhao *et al.*, 2007).

| Fungal pathogen | MAPK | Major function(s) | References |
|---|---|---|---|
| *M. grisea* | Pmk1 | Appressorium formation, pathogenicity, infectious growth | (Xu and Hamer, 1996) |
| *C. lagenarium* | Cmk1 | Appressorium formation, pathogenicity, spore germination | (Takano *et al.*, 2000) |
| *P. teres* | Ptk1 | Appressorium formation, pathogenicity, conidiation | (Ruiz-Roldan *et al.*, 2001) |
| *C. heterostrophus* | Chk1 | Appressorium formation, virulence, conidiation | (Lev *et al.*, 1999) |
| *F. oxysporum* | Fmk1 | Pathogenicity, infectious growth, root attachment | (Di Pietro *et al.*, 2001) |
| *B. cinerea* | Bmp1 | Pathogenicity, normal growth rate | (Zheng *et al.*, 2000). |
| *U. maydis* | Kpp2 | Appresorium development Virulence, mating, | (Muller *et al.*, 2003) |
| *U. maydis* | Kpp6 | Appresorium penetration Virulence, mating, | (Brachmann *et al.*, 2003). |
| *F. graminearum* | Gpmk1 | Pathogenicity, infectious growth, conidiation | (Jenczmionka *et al.*, 2003) |
| *C. albicans* | Cek1 | Virulence, mating, yeast-hypha transition | (Alonso-Monge *et al.*, 2006; Bennett and Johnson, 2005; Csank *et al.*, 1998; Chen *et al.*, 2002) |
| *C. albicans* | Cek2 | Mating | (Chen *et al.*, 2002) |

### 3.2.2. Homologues of the Hog1 pathway

The role of Hog1 orthologues has been studied in different fungal pathogens. While the main function of Hog1 in *S. cerevisiae* is osmoregulation, its homologue in pathogens regulate virulence and response to several types of stresses.

*M. grisea* mutants lacking the Hog1 orthologue Osm1 are sensitive to osmotic stress, but form functional appressoria and are fully virulent on rice plants (Dixon *et al.*, 1999). In *F.*

*graminearum,* deletion mutants of MAPKKK FgOs4, MAPKK FgOs5 and MAPK FgOs2 show markedly enhanced pigmentation and fail to produce trichothecenes in aerial hyphae, although their virulence phenotype has not been determined (Ochiai *et al.*, 2007). Mutants disrupted in the *hog1* orthologous genes in *C. parasitica* and *C. lagenarium* are also sensitive to osmotic stress (Kojima *et al.*, 2002; Moriwaki *et al.*, 2006).

In *C. albicans*, the Hog1 pathway regulates adaptation to osmotic and oxidative stress and is required for virulence and hyphal morphogenesis (Alonso-Monge *et al.*, 1999; Alonso-Monge *et al.*, 2003; Enjalbert *et al.*, 2006; Monge *et al.*, 2006). Similae to yeast, Sln1, Ssk1 and Sho1 homologues are involved in oxidant adaptation (Calera *et al.*, 2000; Chauhan *et al.*, 2003; Roman *et al.*, 2009; Roman *et al.*, 2005). In contrast to yeast, CaSsk1 is the main component required for the transmission of the oxidative stress activation signal to Hog1 via the MAPKK Ssk2, and it is not critical to adaptation during osmotic stress (Chauhan *et al.*, 2003; Cheetham *et al.*, 2007). Mutants lacking CaSsk1 are avirulent and fail to adhere to human cells in a murine infection model (Calera *et al.*, 2000). The histidine kinase CaSln1 is involved in hyphal formation and virulence (Nagahashi *et al.*, 1998; Roman *et al.*, 2005). Interestingly, *C. albicans* Sho1 and Msb2 proteins contribute to the adaptation response to osmostress in a manner that appears to be independent of the Hog1 MAPK, since triple *ssk1 msb2 sho1* mutants are osmosensitive but are not affected in Hog1 activation and translocation to the nucleus (Roman *et al.*, 2009). Similar to yeast, Hog1 functions as a repressor of Cek1 activation and filamentous growth, and hog1 mutants are hyperfilamentous (Alonso-Monge *et al.*, 1999; Eisman *et al.*, 2006; Roman *et al.*, 2005).

In the human pathogen *A. fumigatus,* two Hog1 orthologues, SakA and MpkC play distinct roles in the response to oxidative and nutritional stresses, but are not required for virulence (Reyes *et al.*, 2006; Xue *et al.*, 2004). Deletion of the orthologue of *S. cerevisiae* histidine kinase Sln1, TcsB, produced no clear phenotype (Du *et al.*, 2006). Sho1 regulates hyphal growth, morphology and oxidant adaptation in *A. fumigatus* (Ma *et al.*, 2008), but is dispensable for virulence.

### 3.2.3. Homologues of the Mpk1 cell integrity pathway

Mutants in the MAPK homologous to yeast Mpk1 (Slt2) have been generated in several filamentous fungi (Bussink and Osmani, 1999; Kojima *et al.*, 2002; Mey *et al.*, 2002a; Xu *et al.*, 1998). In general, this MAPK is important for pathogenicity and cell wall integrity. In *M. grisea*, the Slt2 homologue Mps1 is essential for conidiation, appressorial penetration, and plant infection (Xu *et al.*, 1998). Similar to *S. cerevisiae*, *M. grisea mps1* mutants show increased sensitivity to cell-wall-degrading enzymes but display additional phenotypes, including reduced sporulation and fertility (Xu *et al.*, 1998). In *F. graminearum*, Mgv1 is required for hyphal fusion, cell wall integrity and pathogenicity (Hou *et al.*, 2002). In *C. lagenarium*, Maf1 is required for the early stages of appresorium formation (Kojima *et al.*, 2002). In *C. purpurea* and *B. cinerea, Stl2* orthologues Cpmk2 and Bmp3, are required for penetration and cell wall integrity (Mey *et al.*, 2002a). The *A. fumigatus* orthologue MpkA controls cell wall signalling and oxidative stress response, but is dispensable for virulence (Valiante *et al.*, 2008). *In A. nidulans*, MpkA plays an important role in conidial germination and hyphal tip growth (Bussink and Osmani, 1999). In *C. albicans*, Mpk1 orthologue Mkc1 is required for growth at high temperatures and cell wall integrity in response to several types of stresses, including cell wall antifungals, caffeine, oxidative and osmotic stress and cold-shock (Diez-Orejas *et al.*, 1997). The phosphorylation of Mkc1 in response to oxidative stress is partially dependent on the CaHog1 pathway, suggesting a cross-talk between these two pathways (Arana *et al.*, 2005). *C. albicans* Mkc1 has also been implicated in morphogenetic transition and pathogenesis (Diez-Orejas *et al.*, 1997). Reduced virulence of *mkc1* mutants in a murine model was associated with increased sensitivity to nitric oxide *in vitro* and reduced ability to inhibit NO production by macrophages (Molero *et al.*, 2005). Interestingly, Mpk1 is activated by physical surface contact in *C. albicans*, regulating invasive hyphal growth on agar medium and biofilm formation (Kumamoto, 2005).

With regards to upstream components, the role of Rho1 has been investigated in *C. albicans*, where it was found to be required for cell viability, similiar to *S. cerevisiae* (Smith *et al.*, 2002). In contrast, *rho1* knockout mutants of *F. oxysporum* were viable and

showed drastically reduced virulence on plants, but were fully virulent on immunodepressed mice (Martinez-Rocha *et al.*, 2008).

### 3.3. Pathogenicity MAPK signalling in *F. oxysporum*: The Fmk1 cascade

As reviewed in the previous sections, research on MAPK signalling in plant pathogenic fungi has established an evolutionarily conserved role of YERK1 family MAPKs among soilborne and foliar plant pathogens. In *F. oxysporum*, the *fmk1* gene encodes a YERK1 family MAPK, which is part of a signal transduction cascade involved in the formation of infection hyphae, root attachment and penetration, as well as invasive growth on living plant tissue (Di Pietro *et al.*, 2001). The Fmk1 protein shares over 90% identity with orthologous YERKs from the leaf pathogens *M. grisea*, *C. lagenarium* and *C. heterostrophus* (Di Pietro *et al.*, 2001; Lev *et al.*, 1999; Takano *et al.*, 2000; Xu and Hamer, 1996). *F. oxysporum* mutants lacking a functional copy of the *fmk1* gene grow normally on artificial media (Figure 4A), but are deficient in pathogenicity on tomato plants (Figure 4C) (Di Pietro *et al.*, 2001).

It has been shown that Fmk1 participates in the first stages of infection by controlling infection-related morphogenesis and root attachment (Di Pietro *et al.*, 2001). As described in Section 1.3, the first steps of infection in soilborne fungi usually involve spore germination in response to stimuli exuded by host roots, production of germ tubes that differentiate into infection hyphae, attachment to the roots and root penetration (Mendgen *et al.*, 1996)(Figure 2). Fmk1 is not essential for germination but it is required for correct differentiation of infection hyphae in the presence of tomato roots as well as for attachment to and penetration of tomato roots (Di Pietro *et al.*, 2001). Interestingly, the orthologous MAPK gene from *M. grisea* complemented most of the *fmk1* mutant phenotypes supporting the view of functional conservation of this MAPK signalling pathway in spite of the diversity of infection mechanisms developed (Di Pietro *et al.*, 2001).

An interesting feature of YERK1 family MAPK mutants is that, in addition to being deficient in infection-related morphogenesis and penetration, they are also unable to grow invasively on living plant tissue (Takano *et al.*, 2000; Xu *et al.*, 1999; Zheng *et al.*, 2000). *F. oxysporum fmk1* mutants have a strongly reduced ability to grow invasively on tomato fruit tissue (Figure 4B) (Di Pietro *et al.*, 2001). It was suggested that the reduced tissue maceration of these mutants may be related to alterations in the expression profile of cell-wall degrading enzymes. Indeed, transcripts of *pl1* encoding an endopectate lyase are drastically reduced in *fmk1* mutants (Di Pietro *et al.*, 2001).

Fmk1 is also required for anastomosis or vegetative hyphal fusion (VHF) (Prados Rosales and Di Pietro, 2008), an ubiquitous process in filamentous fungi whose biological function is poorly understood. VHF is not essential for plant infection, but establishment of hyphal networks may contribute to optimize virulence-related functions such as adhesion to host surfaces or exploitation of the limited nutrient resources encountered during infection (Prados Rosales and Di Pietro, 2008).

Downstream of Fmk1, the transcription factor Ste12 was recently shown to control Fmk1-mediated invasive growth in *F. oxysporum* (Rispail and Di Pietro, 2009). *F. oxysporum* mutants lacking the *ste12* gene were impaired in invasive growth on tomato and apple fruit tissue and in penetration of cellophane membranes. However, *ste12* was not required for adhesion to tomato roots, secretion of pectinolytic enzymes and vegetative hyphal fusion, suggesting that these Fmk1-dependent functions are mediated by other downstream MAPK targets.

To date, the upstream receptors that regulate Fmk1 and orthologous YERKs in plant pathogens remain unknown. This PhD work was initiated with the aim to identify putative cell surface signalling components that function upstream of the pathogenicity MAPK Fmk1 in *F. oxysporum*.

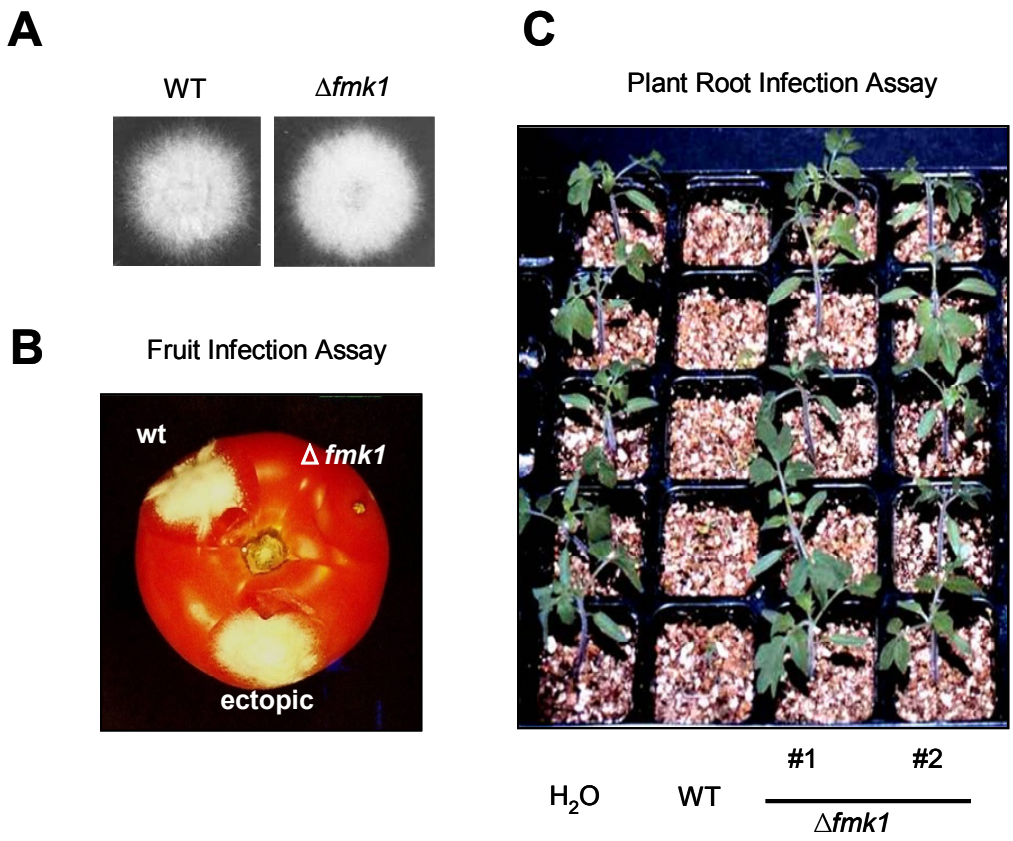


**Figure 4. The MAPK Fmk1 is dispensable for vegetative growth, but essential for invasive growth and pathogenicity of *F. oxysporum*.**
The indicated strains were tested for vegetative growth on complete medium (A), invasive growth on tomato fruit tissue (B) and pathogenicity on tomato plants (C). Figure taken from (Di Pietro *et al.*, 2001).

## 4. Mucins in signal transduction

Mucins are type I integral membrane proteins that typically have large extracellular domains containing a number of highly O-glycosylated repeat regions rich in serine and threonine residues (STR) and a short cytoplasmic tail (Agrawal *et al.*, 1998; Carraway *et al.*, 2003). The size of cytoplasmic tails on cell-surface mucins varies from 22 to 80 residues (Carraway *et al.*, 2003). It has been postulated that some cell surface mucins serve as sensors of the extracellular environment by directly sensing changes in the external conditions such as pH, ionic composition, or physical interactions and promoting intracellular signalling in response to ligand binding or conformational changes (Carraway *et al.*, 2003). Mucin-type glycoproteins are widely represented in vertebrates where they participate in important functions like cytoprotection and cell-cell interactions. In mammalian cells, mucins act as barriers to pathogen infection (Carson *et al.*, 1998) and are key factors in metastasis in a variety of human cancers (Carraway *et al.*, 2003). MUC1 and MUC4 are the prototypic human signalling mucin members which were originally identified as molecular markers of carcinoma cells (Wreschner *et al.*, 1994). MUC1 is the best characterised with respect to signal transduction. It is involved in activation of MAP kinase pathways through interactions with ErbB receptors and downstream activation of extracellular-signal-regulated kinases (ERKs 1 and 2) in mouse mammary glands (Meerzaman *et al.*, 2001; Schroeder *et al.*, 2001). In parasites, mucins have been implicated in adhesion and penetration of the mammalian host cell (Almeida *et al.*, 1994; Di Noia *et al.*, 1996).

The discovery and characterization of Msb2 as a mucin member in *S. cerevisiae* has expanded our understanding of this class of signalling molecules (Cullen *et al.*, 2004). Msb2 and Hkr1 are members of the mucin family of proteins by means of their large and highly glycosylated extracellular domains, a short cytoplasmic tail and their implication in signal transduction upstream of the the FG and HOG pathways (Cullen *et al.*, 2004; Tatebayashi *et al.*, 2007). Figure 5 represents a schematic model of the signalling mucin structure and mode of activation taken from a recent review (Cullen, 2007).

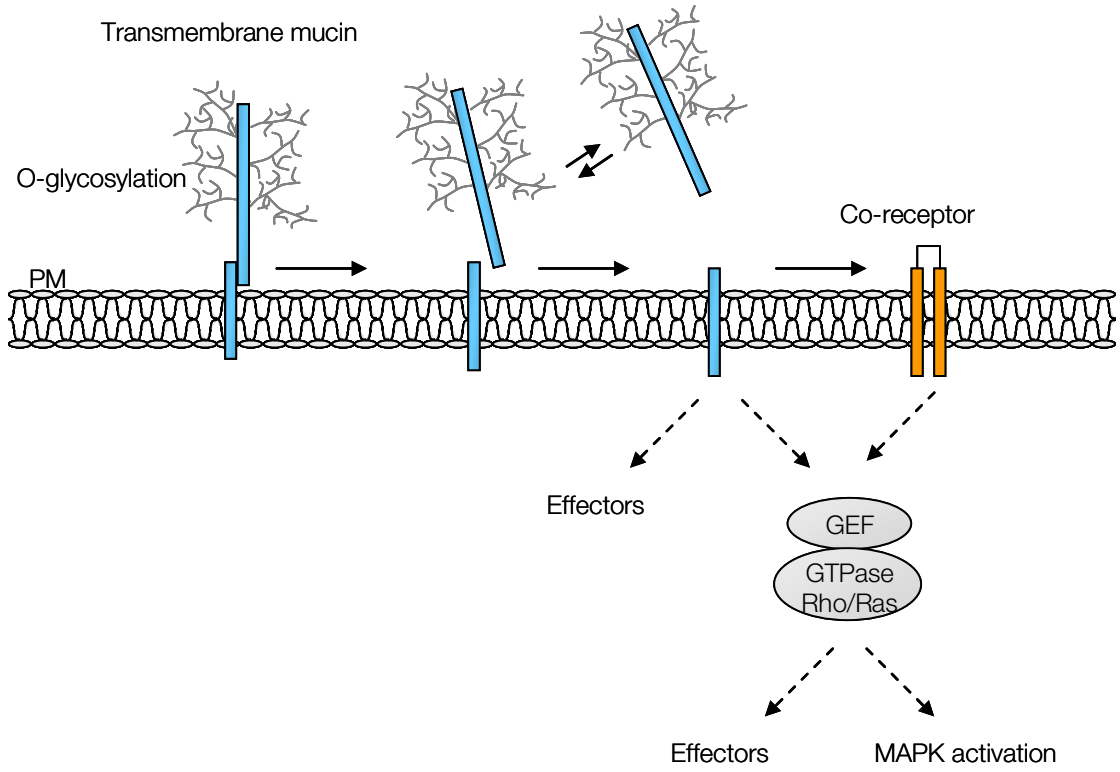


**Figure 5. General model for signalling mucin activation.**
Upon stimulation, the ectodomain of the mucin is cleaved and shed from the cell. The cleaved polypeptide activates other cell surface molecules and initiates Ras/Rho activation. These signalling events culminate in activation of mitogen-activated protein kinase pathways and other effector pathways. Adapted from (Cullen, 2007).

## 4.1. The Msb2 mucin protein

*S. cerevisiae* Msb2 was first discovered as a multicopy suppressor of a *cdc24* mutation that resulted in a budding defect (Bender and Pringle, 1992). The first report involving Msb2 signalling in a MAPK pathway was published 10 years later. O'Rourke and Herskowitz (2002) showed that the Msb2 protein was functionally redundant with the surface receptor Sho1 for activating the MAP kinase Hog1 to promote osmotolerance.

The characterisation of Msb2 as a membrane mucin and the confirmation of its role in signalling through MAPK pathways came two years later from a study by Cullen *et al.* (2004). The authors showed that the putative osmosensor for the HOG pathway, Sho1, also functions in the FG pathway and identified *msb2* as a novel FG pathway target that also functioned as the most upstream component of the Kss1 MAPK during FG. The Msb2 protein is a predicted type I integral membrane protein with six extracellular mucin repeats, that localizes to buds at the distal pole and interacts with Sho1 during FG. Cullen *et al*. also provided evidence for genetic and physical interaction of Msb2 with Cdc42, presumably to redirect cell polarity (Figure 6). Additional studies had demonstrated the interaction of Msb2 with other proteins at the cell surface, including Bni4, a protein that targets chitin deposition to sites of polarized growth by linking chitin synthase to septins, and the kinase Cla4 (DeMarini *et al.*, 1997; Drees *et al.*, 2001), further supporting the idea that Msb2 is part of the Cdc42 regulatory pathway. It was proposed that *S. cerevisae* Msb2 may function as a sensor to detect stress at the overlying cell wall, coordinating cell wall growth with other Cdc42-regulated processes such as cell polarity (Cullen *et al.*, 2004). Elegant work by Dr. Saito´s group revealed that Msb2 and a novel mucin protein called Hkr1 also functioned as the most-upstream components in the SHO1 branch of the HOG pathway (Tatebayashi *et al.*, 2007) (Figure 6). In contrast to Msb2, Hkr1 appears to function as a HOG pathway–specific factor (Pitoniak *et al.*, 2009). Hkr1 is not required for FG pathway signalling, and when overexpressed does not induce FG pathway targets. Expression of the *hkr1* gene is not induced by nutrient limitation and is not under the control of the FG pathway (Pitoniak *et al.*, 2009).

The extracellular regions of Msb2 and Hkr1 contain a positive regulatory domain (PRD) and a large Ser/Thr/Pro-rich (STR) region, referred to as the mucin homology domain (MHD), that functions as a negative regulatory domain (Vadaie *et al.*, 2008). Partial or total deletion of the MHD progressively results in constitutive FG pathway activation (Cullen *et al.*, 2004). It was shown that the extracellular MHD domain is processed and released from the surface by means of the GPI-anchored aspartyl protease Yps1p, thus activating Msb2 during FG (Vadaie *et al.*, 2008). In the HOG pathway, deletion of the STR domain of

Msb2 and Hkr1 also results in constitutive activity in the absence of osmostress, while deletion of the PRD completely abrogates induction of HOG pathway reporter genes (Tatebayashi *et al.*, 2007). It is not clear how Msb2 and Hkr1 mediate their different outputs. It has been suggested that both proteins may compete for a binding site on the Sho1 protein, since Hkr1 can inhibit the FG pathway at the level of Sho1 in the absence of Msb2 (Pitoniak *et al.*, 2009). Tatebayashi *et al.* (2007) provided evidence that Msb2 and Hkr1 cytoplasmic tail (CT) domains indeed have different implications in the HOG pathway. They established that there are two modes of activation of the SHO1 branch of the HOG pathway (Figure 6). Mode 1 requires interaction between Hkr1 (or Msb2) and Sho1 through its transmembrane (TM) domains to generate an intracellular signal through Sho1. Mode 2 is independent of the Sho1 TM domains and Hkr1, but instead requires the Msb2 cytoplasmic region. It has also been suggested that Msb2 and Hkr1 may recruit different proteins to the cell surface through their cytoplasmic signalling domains, which share little similarity to each other (Pitoniak *et al.*, 2009).

It has long been known that glycosylation defects constitutively activate an FG-like response in yeast (Cullen *et al.*, 2000; Lee and Elion, 1999). The Msb2 MHD domain is heavily modified by O-glycosylation and also has seven potential N-glycosylation sites (Cullen *et al.*, 2004;Yang *et al.*, 2009). Interestingly, disruption of the gene encoding the protein O-mannosyltransferase Pmt4 combined with N-glycosylation defects induced by tunicamycin, resulted in defective glycosylation of the Msb2 MHD and induction of the FG response (Yang *et al.*, 2009) (Figure 6). These results led the authors to speculate on the role of the Msb2 MHD as a sensor of nutrient deprivation or osmostress. Under poor nutritional conditions, underglycosylation of the MHD would unmask the PRD and initiate pathway activation, whereas under hyperosmotic conditions the physico-chemical changes in the oligosaccharide gel structure might unmask the PRD domain (Yang *et al.*, 2009). Interestingly, Sho1 is not required for glycosylation defect-dependent activation of the FG MAPK pathway. Because during mode 2, the Sho1 cytoplasmic domain is needed to activate Pbs2, and the FG response does not involve Pbs2 at all, the authors proposed that activation of the Kss1 MAPK can proceed in complete absence of Sho1 through the

mode 2 mechanism (Yang *et al.*, 2009). Therefore, Msb2 seems to behave as a membrane sensor which connects the FG and HOG pathways (Yang *et al.*, 2009).

Recently, Dr. Pla´s group has characterised the role of the Msb2 protein in the fungal pathogen *C. albicans* (Roman *et al.*, 2009). *C. albicans* Msb2, which conserves the general characteristic topology of transmembrane mucin proteins, is involved in the integrity of the cell wall and in the invasion of solid surfaces, possibly by regulating the activity of the Kss1 MAPK orthologue Cek1. Msb2 is required for Cek1 activation under conditions of cell wall stress caused by the drugs Congo red and caspofungin, and both *cek1* mutants (Eisman *et al.*, 2006; Roman *et al.*, 2005) and *msb2* mutants are hypersensitive to these drugs. *msb2*, *sho1*, *msb2 sho1* and *cek1* mutants are also sensitive to zymolyase, a glucanase-enriched enzyme preparation. The authors proposed that Msb2 may be a sensor for cell wall damage. However, the phenotypes of *sho1* and *msb2* are not identical, since *sho1* deletion has more drastic effects on Cek1 activation while *msb2* deletion has more drastic effects on morphogenesis and invasion (Roman *et al.*, 2009). Interestingly, contrary to *S. cerevisiae*, *C. albicans* Msb2 is involved in growth under conditions of high osmolarity by a mechanism independent of the activation of the Hog1 MAPK. A *ssk1 msb2 sho1* triple mutant displayed significant osmosensitivity compared to *ssk1 msb2* or *msb2 sho1* double mutants, without blocking Hog1 phosphorylation. Unlike Sho1, Msb2 is not required for virulence of *C. albicans* on mice. Based on these results, the authors propose a functional specialization of the Msb2-Sho1-Cek1 branch in filamentous fungi with respect to yeast (Roman *et al.*, 2009).

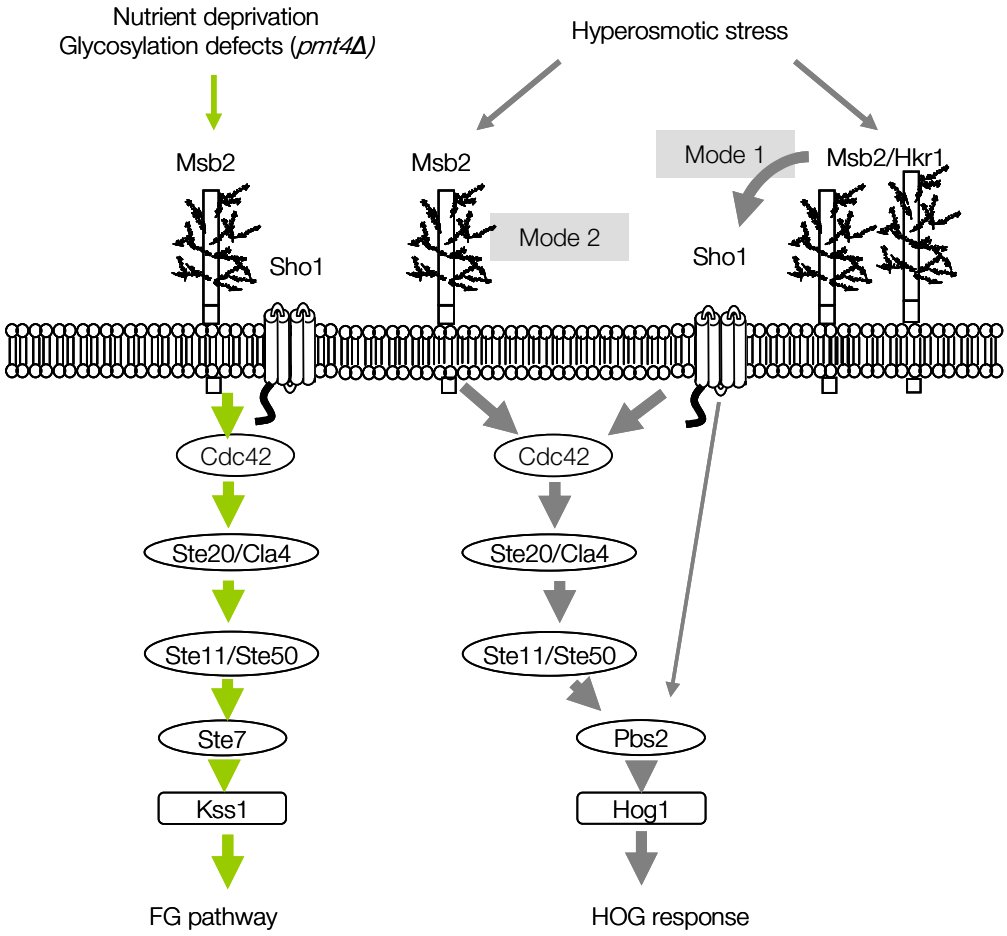


**Figure 6. Role of Msb2 and Sho1 in activation of the FG and HOG MAPK pathways in yeast.**
Adapted from (Cullen *et al.*, 2004; Tatebayashi *et al.*, 2007).

## 4.2. The Sho1 adaptor

The membrane protein Sho1 serves as an obligatory adaptor between the the Msb2/Hkr1 sensors, the Ste11/Ste50 module and the MAPKK Pbs2 (Maeda *et al.*, 1995; Marles *et al.*, 2004; Tatebayashi *et al.*, 2006; Zarrinpar *et al.*, 2004; Zarrinpar *et al.*, 2003) Sho1 predominantly localizes to the cytoplasmic membrane at areas of polarised growth, such

as the emerging bud and the bud neck (Raitt *et al.*, 2000; Reiser *et al.*, 2000). Through Ste11, Sho1 activates the Pbs2-Hog1 pathway to regulate glycerol synthesis and other adaptive stress responses, including hydrogen peroxide adaptation (Posas *et al.*, 1996; Singh, 2000), and is also required for FG pathway activity in response to nutrient limitation and protein glycosylation defects (Cullen *et al.*, 2004; Cullen *et al.*, 2000) (Figure 6).

Sho1 is a tetraspan protein with four TM domains, separated by short loops of five to eight amino acids each (Maeda *et al.*, 1995; Marles *et al.*, 2004; Zarrinpar *et al.*, 2004; Zarrinpar *et al.*, 2003). The arrangement of the tightly packed four TM domains is highly conserved across fungal Sho1 orthologue, suggesting that it may have a more specific function than simple membrane targeting (Krantz *et al.*, 2006). Indeed, in yeast, upon external high osmolarity, the Sho1 TM region is directly involved in the individual interactions with the upstream putative osmosensors Msb2 and Hkr1 during the mode 1 activation mechanism (Tatebayashi *et al.*, 2007) (Figure 6). Sho1 is then able to generate an intracellular signal through its cytoplasmic domain (Tatebayashi *et al.*, 2007). The Sho1 C-terminal cytoplasmic region contains a SH3 domain and binds both the Pbs2 MAPKK and the complex of Ste11 MAPKKK and Ste50 adaptor protein (Maeda *et al.*, 1995; Marles *et al.*, 2004; Zarrinpar *et al.*, 2004; Zarrinpar *et al.*, 2003). Thus, Sho1 has an essential scaffold function during osmostress. Interestingly, Sho1 interact with Fus1, a plasma membrane protein known to be required for septum degradation during cell fusion (Nelson *et al.*, 2004). Pheromone-induced expression of Fus1 prevents Sho1 from signaling HOG MAPK-dependent growth on high-osmolarity medium (Nelson *et al.*, 2004). A similar mechanism may also function during FG, through Msb2 recruitment of the Sho1 scaffold. In support of this idea, Sho1 can be dispensable for Kss1 activation. Thus, Sho1 overexpression can induce FG in a manner dependent on Msb2 and Ste20, however Msb2 can bypass the requirement for Sho1 in FG when overexpressed (Cullen *et al.*, 2004; Cullen *et al.*, 2000). Sho1 is also dispensable for the *pmt4*Δ-induced expression of FG-pathway reporter (Yang *et al.*, 2009). Because the FG response does not involve the MAPKK Pbs2, activation of the Kss1 MAPK by the mode 2 mechanism can proceed in the complete absence of Sho1 (Yang *et al.*, 2009).

Collectively, these data point towards a crucial role of Sho1 as an adaptor protein in conjunction with Msb2 and/or Hkr1, in polarised recruitment of the intracellular signalling and polarity machinery under conditions of cell wall reorganisation. Research on the role of Sho1 and Msb2 proteins in *C. albicans* suggests that the Msb2/Sho1/Cek1 pathway regulates cell wall biogenesis during cell growth and cell wall stress (Roman *et al.*, 2009). In addition, *C. albicans* Sho1 has Cek1-independent functions in the oxidative stress response. This function is partially independent of Hog1 phosphorylation, which mainly occurs through the Sln1/Ssk1 branch (Chauhan *et al.*, 2003; Roman *et al.*, 2005). In addition, Sho1 also plays a minor role in osmotic stress adaptation in *C. albicans*. Contrary to *S. cerevisiae ssk1 sho1* mutants, which fail to activate Hog1 under osmotic stress (O'Rourke and Herskowitz, 2002), *C. albicans ssk1 sho1* mutants still activate Hog1 under these conditions. Similarly, *A. nidulans* Sho1 is not required for Hog1 activation under hyperosmotic stress (Furukawa *et al.*, 2005).

The role of Sho1 has been studied in other fungi, including *Aspergillus fumigatus* (Ma *et al.*, 2008), *Kluyveromyces lactis* (Siderius *et al.*, 2000), *Candida utilis* (Siderius *et al.*, 2000), *Candida glabrata* (Gregori *et al.*, 2007), *Candida lusitaniae* (Boisnard *et al.*, 2008) and *Metarhizium anisopliae* (Wang *et al.*, 2008) (Table 5). In *A. fumigatus*, Sho1 is required for radial hyphal growth but it is dispensable for virulence (Ma *et al.*, 2008). Similarly to *C. albicans*, the Sho1 homologues of *A. fumigatus, C. lusitaniae* and *M. anisopliae* function in oxidative stress response (Table 5). By contrast, Sho1 was not implicated in the oxidative stresss response in *C. glabrata* (Gregori *et al.*, 2007). Interestingly, similarly to *C. albicans*, Sho1 is implicated in the cell wall stress response in *C. lusitaniae* and *M. anisopliae,* and is required for hyphal development in all these species, as well as in *A fumigatus* (Table 5), suggesting a broadly conserved function in hyphal morphogenesis. Finally, Sho1 is a virulence factor in *C. albicans* and in the insect pathogen *M. anisopliae*. At present, there is no information on the function of Sho1 in plant pathogenic fungi.

**Table 5. Sho1 homologues studied in fungi other than *S. cerevisiae*.**

| Fungal pathogen | Function(s) of Sho1 | References |
|---|---|---|
| *C. albicans* | Oxidative stress response<br>Cek1 activation<br>Minor role in resistance to osmostress and Hog1 phosphorylation<br>Morphogenesis and cell wall biogenesis during the cell wall stress response and the pseudohyphal switch<br>Required for virulence | (Chauhan *et al.*, 2003; Roman *et al.*, 2005) |
| *K. lactis and C. utilis* | Osmosensing | (Siderius *et al.*, 2000) |
| *C. glabrata* | Osmostress response only in the *C. glabrata* ATCC 2001 strain, where the Sln1 branch is inactive<br>Not implicated in oxidative stress response<br>Resistance to weak organic acids | (Gregori *et al.*, 2007) |
| *A. fumigatus* | Morphogenesis and radial growth<br>Oxidative stress response<br>Dispensable for virulence | (Ma *et al.*, 2008). |
| *C. lusitaniae* | Cell wall stress response<br>Pseudohyphal transition<br>Osmotic and oxidative adaptation, primarily during pseudohyphal morphogenesis.<br>Resistance to filamentous fungus-specific antifungals dicarboximides and phenylpyrroles. | (Boisnard *et al.*, 2008), |
| *M. anisopliae* | Osmotic, oxidative and cell wall stress adaptation<br>Appressorium and hyphal body formation of appressoria<br>Virulence | (Wang *et al.*, 2008), |

# Aims of this work

In spite of the broadly conserved role of the Pathogenicity MAPK cascade in fungal infection of plants, the upstream regulatory mechanisms of this signalliung pathway in filamentous fungal pathogens remain poorly understood. A number of fundamental questions remain unsolved: How are Pmk1 cascades able to sense external stimuli from the plant host and/or the environment? What are the key upstream receptors? What biological/molecular basis underlies the sensing ability of these putative receptors? And what is the nature of the activating signals?

Mucins are an emerging class of cell receptor molecules implicated in MAPK signalling, that has been extensively studied in mammals. Investigations on the role of mucins in fungal biology were only recently initiated. As reviewed above, recent studies point towards a pivotal role for signalling mucins in the activation of MAPK cascades in yeast and the human pathogen *C. albicans*. However, the role of membrane mucins has not been explored in any phytopathogenic species. Based on the evidence from yeast, we initiated this PhD work with the aim to identify novel upstream components implicated in regulation of the Fmk1 Pathogenicity MAPK cascade in *F. oxysporum*. We set out from the starting hypothesis that a putative mucin-type membrane receptor, orthologous to *S. cerevisiae* Msb2, may participate in regulation of the Fmk1 cascade. In addition, we present preliminary results on the characterisation of a second membrane protein, Sho1, in MAPK signalling and pathogenicity of *F. oxysporum*.

## 1. Strains and plasmids

*F. oxysporum* strains, plasmids and plant cultivars used in this work are listed in the tables below.

**Table 6. *Fusarium oxysporum* f. sp. *lycopersici* strains used in this study.**

| Strain | Background | Genotype | Reference |
|---|---|---|---|
| 4287 (FGSC 9935) | wild type, race 2 | | FGSC (1) |
| Δ*fmk1* | 4287 | *fmk1::PHLEO* | (Di Pietro *et al.*, 2001) |
| Δ*msb2* | 4287 | *msb2::HYG* | This work |
| Δ*fmk1*Δ*msb2* | Δ*fmk1* | *fmk1::PHLEO; msb2::HYG* | This work |
| Δ*msb2+msb2* | Δ*msb2* | *msb2::HYG; msb2; PHLEO (2)* | This work |
| Δ*msb2+msb2HA* | Δ*msb2* | *msb2::HYG; msb2HA; PHLEO (2)* | This work |
| Δ*msb2+msb2** | Δ*msb2* | *msb2::HYG; msb2*; PHLEO* | This work |
| Δ*msb2+Psti-msb2** | Δ*msb2* | *msb2::HYG; Pstimsb2*; PHLEO* | This work |
| Δ*sho1* | 4287 | *sho1::HYG* | This work |
| Ectopic *sho1-hph#2* | 4287 | *ectopic sho1::HYG* | This work |
| Δ*msb2*Δ*sho1* | Δ*msb2* | *msb2::HYG; sho1:: PHLEO* | This work |

(1)Fusarium Genetics Stock Center. (2)Hygromycin cassette replaced with phleomycin cassette

**Table 7. Plant cultivars used in this study.**

| Species | Cultivar | Specifications |
|---|---|---|
| Tomato (*Lycopersicon esculentum*) | Monika (seeds) Daniela (fruits) | Susceptible to *F. oxysporum* f. sp *lycopersici* race 2 |
| Apple (*Malus pumila*) | Golden Delicious | |

**Table 8. Plasmids used in this study.**

| Plasmid | Origin/Features | Reference |
|---|---|---|
| pGEM®-T | Derived from plasmid pGEM®-5Zf(+), linearized with *Eco*RV and with a T added in both 3' ends | Promega |
| pAN7-1 | Derived from pUC18; *A.nidulans gpdA* promoter; phosphotransferase hygromicin B gene from *Streptomyces spp.* (*hph*); *A. nidulans trpC* terminator | (Punt *et al.*, 1987) |
| pAN8-1 | Derived from pUC18; A.*nidulans gpdA* promoter; phleomycin resistance gene; *A. nidulans trpC* terminator | (Mattern *et al.*, 1988) |
| PBKS-hyg-lamlam_SURBamHI | Derived from pAN7-1. The *hph* cassette was amplified by PCR using primers with added *Kpn*I sites and the cassette was subcloned into the *Kpn*I site of PBKS-lamlam (Garcia-Pedrajas and Roncero, 1996). Next, the *Bam*HI site of the *A. nidulans trpC* terminator was eliminated by partial *Bam*HI digestion, followed by Klenow filling and recircularization. | Perez-Nadales and Di Pietro, 2006. |
| *msb2*-pGemT | *msb2* locus (FOXG_09254.2, 5.9 Kb) from *F. oxysporum* 4287 strain, including endogenous promoter and terminator sequences, cloned into pGemT. | This work |
| *msb2HA722*-pGemT | Derived from *msb2*-pGemT. The HA epitope coding sequence was inserted at position 722 of the Msb2 ORF. | This work |
| *msb2**-pGemT | *msb2** allele (3.6 Kb) lacking aminoacids 46 to 721 of the Msb2 ORF, including endogenous promoter and terminator sequences, cloned into pGemT. | This work |
| *sho1*-pGemT | *msb2* locus (FOXG_06120.2, 3.3 Kb) from *F. oxysporum* 4287 strain, including endogenous promoter and terminator sequences, cloned into pGemT. | This work |
| *hph(B)sho1*-pGemt | Derived from *sho1*-pGemT and PBKS-hyg-lamlam_SURBamHI | This work |
| *phleo(B)sho1*-pGemt | Derived from *sho1*-pGemT and pAN8-1 | This work |

## 2. Media and culture conditions

All media were prepared with Milli-Rho deionized water and sterilized either by autoclaving at 1.2 atm and 120 ºC for 20 min or by filtration (0.22 μm pore size, Millipore).

### 2.1. *E. coli*

For *Escherichia coli* cultures, Luria-Bertoni medium (Sambrook *et al.*, 1989) was used. Strains were incubated at 37°C and the antibiotic ampicillin was used at 100 μg/ml. For generation of recombinant plasmids, the *E. coli* strain XL1Blue was used. Screening of recombinant pGEM-T (Promega) plasmids transformed into competent *E.coli* was performed by ampicillin resistance and blue-white selection with X-gal and IPTG.

### 2.2. *F. oxysporum*

#### 2.2.1. Media and solutions

Potato Dextrose Broth (PDB): Boil 200 g of peeled potatoes in 0.6 l of water for 60 min. Stir and add 20 g of glucose and deionized water up to 1 l. Sterilize by autoclaving.

Potato Dextrose Agar (PDA): 3.9% potato dextrose agar (w/v) (Scharlau Microbiology). When needed, melt the medium and add hygromicin B (55 μg/ml) or phleomycin (5.5 $\mu g/ml^{-1}$) when the temperate is around 60ºC.

Synthetic Defined Medium (SM) (g/l): $MgSO_4$ x $7H_2O$ (0.2), $KH_2PO_4$ (0.4), KCl (0.2), $FeSO_4$ (0.01), $ZnSO_4$ (0.01), $MnSO_4$ (0.01), $NaNO_3$ (1), glucose (10) and bactoagar (15 ).

YPD (Yeast extract Peptone Dextrose) (g/l): Yeast extract (3), peptone (10) and glucose (20). Add bactoagar (15 g/l) for solid medium.

Puhalla's minimal medium (MM) (Puhalla, 1968) (g/l): $MgSO_4$ x $7H_2O$ (0.5), $KH_2PO4$ (1); KCl (0.5), $NaNO_3$ (2) and sucrose (30). Add oxoid agar (20 g/l) for solid medium. After autoclaving add trace elements (200 μl/l)

Trace elements (g/l): Citric acid (0.05), $ZnSO_4$ (0.05), $FeSO_4$ x $7H_2O$ (0.048), $Fe(NH_4)SO_4$ x $6H_2O$ (0.01), $CuSO_4$ x $5H_2O$ (0.0025), $MnSO_4$ x $H_2O$ (0.0005), $HBO_3$ (0.0005), $Na_2MoO_4$ x $2H_2O$ (0.0005). Sterilize by filtration.

**Regeneration minimal medium** (g/l): $MgSO_4$ x $7H_2O$ (0.5), $KH_2PO_4$ (1), KCl (0.5), $NaNO_3$ (2), glucose (20), sucrose (200) and oxoid agar (12.5 g/l for Petri dishes and 4 g/l for top agar).

**PGA (Polygalacturonic acid medium)** (g/l): Sodium polygalacturonate (5), sucrose (2), $(NH_4)_2SO_4$ (2) and oxoid agar (15). Prepare the sodium polygalacturonate, sucrose and $(NH_4)_2SO_4$ solution and autoclave independently of the oxoid agar. After sterilization, adjust to pH 7 with potassium phosphate buffer to a final concentration of 25 mM. Potassium phospate buffer (50 mM): Prepare 1 M $KH_2PO_4$ and 1 M $K_2HPO_4$ and autoclave. Mix 68.5 ml of the monopotassic salt with 31.5 ml of the dipotassic salt.

### 2.2.2. Growth conditions

*F. oxysporum* strains were cultured in rich (PDB and YPD), synthetic (SM) or nutrient-limiting minimal media (MM), according to specific requirements and experimental designs. For extraction of DNA, microconidium production and fungal development, cultures were grown in liquid PDB at 28°C with orbital shaking at 170 rpm. When needed, the following antibiotics were added to the culture medium: hygromicin B at 55 μg/ml or phleomycin at 5.5 μg/ml. For long-term storage of the different strains, microconidia from 3 to 4 day-old cultures were collected by filtration through a nylon filter (Monodur; mesh size 10 μm). Filtrates were centrifuged at 12000g for 10 min; Microconidia were washed in sterile deionized water and resuspended in PDN with 30% glycerol (v/v) and stored -80ºC. These suspensions were used for later inoculation to obtain fresh microconidia.

For RNA and protein extraction, $5x10^8$ freshly obtained microconidia were inoculated into 200 ml of PDB. After 14 h of incubation at 28°C and 170 rpm, mycelium was harvested, washed twice with sterile water and transferred onto three MM agar plates. Plates were incubated for the indicated times at 28°C and mycelia were harvested, frozen in liquid nitrogen and stored at -80ºC.

## 3. Molecular methodology

### 3.1. Restriction mapping and subcloning

Restriction mapping, subcloning and plasmid DNA extraction from *E. coli* were carried out according to standard methods (Sambrook *et al.*, 1989), and using the reagents according to the manufacturer´s instructions. Restriction enzymes were provided by Roche (Barcelona, Spain). Ligations were carried out using T4 DNA ligase from Roche. DNA fragments were isolated from TAE electrophoresis gels using the QIAquick Gel extraction Kit (QIAGEN). *E. coli* competent cells were transformed with purified plasmids by the heat shock method described by (Hanahan, 1985).

### 3.2. Nucleic acid extraction from *F. oxysporum*

Genomic DNA was extracted from *F. oxysporum* mycelium using the CTAB method (Torres *et al.*, 1993), with some modifications. Briefly, approximately 100 mg of mycelium were ground to a fine powder in a prechilled (−80°C) mortar and pestle under liquid nitrogen and transferred to a 2 ml Eppendorf centrifuge tube with 1 ml of CTAB extraction buffer (1) and vortexed. Next, 4 µl of β-mercaptoethanol (Merck) and 500 µl of a chloroform:octanol 24:1 (v/v) solution were added and the mix was incubated at 65ºC for 30 minutes and left at room temperature for 15 minutes. The tube was centrifuged for 5 minutes at 10000 g. The supernatant was then precipitated with 1 ml of 100% ice-cold ethanol and incubated at -20ºC for 10 minutes, followed by centrifugation for 5 minutes at 7500 g and two consecutive washes with 1 ml of 200 mM sodium acetate in 75 % aqueous ethanol and 1 ml of 10 mM sodium acetate in 75 % aqueous ethanol. Finally, the pellet was resuspended in 75 µl of sterile deionised water with 4 µl de RNase (10 mg/ml) and incubated at 37ºC for 30 minutes.

For RNA extraction, 100 mg of frozen mycelium were ground as described above and transferred to a pre-chilled 2 ml-vial with 1 ml of Tripure Isolation Reagent (Roche), follwed by vortexing and centrifugation at 4ºC for 10 minutes and 12000 *g*. The supernantant

was transferred to a new vial and incubated at 0ºC for 5 minutes to allow complete separation of nucleoprotein complexes. Then, 200 µl of chloroform were added and the mix was vortexed for 15 seconds, incubated at 0ºC for 15 minutes and centrifuged at 4ºC for 15 minutes at 12000 g, which results in the formation of three phases: upper aqueous phase, middle phase and organic phase. The middle phase is tightly condensed so that it is easy to remove the upper clear phase with high-quality RNA. This clear phase was transferred to a new clean vial, 500 µl of isopropanol were added and the tube was mixed by inversion followed by incubation at 0ºC for 10 minutes and centrifugation at 4ºC for 10 minutes and 12000 g to precipitate RNA. The pellet was washed with 1 ml of 75% ethanol (v/v). Finally, the tube was centrifuged at 4ºC for 5 minutes and 7500 *g*, dried, the pellet resuspended in 50 µl of RNase-free water and incubated at 55-60 ºC for 10-15 minutes.

(1) CTAB extraction buffer: 12.1 g/l Trizma base; 7.44 g/l EDTA; 81.8 g/l NaCl y 20 g/l Cetyltrimethylammonium bromide. Heat to 60 ºC to dissolve and adjust to pH 8.0 with NaOH. Keep at 37 ºC to avoid precipitation.

## 3.3. Nucleic acid quantification

DNA and RNA were quantified in a Nanodrop® ND-1000 spectrophotometer at 260nm and 280 nm wavelength, respectively. In addition, the quality of the DNA and RNA obtained was monitored by electrophoresis in a 0.7% and 1% agarose gel (w/v), respectively.

## 3.4. Southern blot analysis

Southern analysis and probe labelling were carried out as described (Di Pietro and Roncero, 1998) using the non-isotopic digoxigenin labelling kit (Roche Diagnostics SL, Barcelona, Spain).

## 3.5. Amplification reactions

### 3.5.1. Standard PCR

PCR amplifications were performed in a termocycler using the thermostable DNA polymerase of the Roche Expand High Fidelity PCR System. Each reaction contained 300 nM primers, 2.5 mM de MgCl2, 0.8 mM dNTPs mix and 0.05 U/μl of polymerase. Genomic DNA was added at 20 ng/μl and plasmid DNA at 2 ng/μl. PCR cycling conditions were: an initial step of denaturation (5 min, 94ºC) followed by 35 cycles of 35 s at 94ºC, 30 s at the calculated primer annealing temperature and 35 s at 72ºC (or 68ºC for templates larger than 3Kb), and a final extension step at 72ºC (or 68ºC) for 10 minutes. For PCR amplification of fragments higher than 7 Kb and/or with high GC, the more robust iProof High-Fidelity DNA Polymerase (BioRad) was used, following the manufacturer´s instructions.

### 3.5.2. Reverse transcriptase PCR

Prior to complementary DNA (cDNA) synthesis, the RNA was treated with DNaseI (Fermentas). First strand cDNA was synthesized with Moloney murine leukemia virus reverse transcriptase following the instructions of the manufacturer (Invitrogen S.A., Spain). Briefly, 1 μg of total RNA was added in a final volume of 20 μl with 100 pmol oligodT primer, which was incubated at 70 ºC for 10 minutes for RNA denaturation. Next, the tube was transferred to ice and 0.4 mM dNTPs, 1x First Strand Buffer (Invitrogen), 4 U/μl of RNAsas RNasin® Plus RNase Inhibitor (Promega) and 5 mM dithiothreitol (DTT) were added and the mix was incubated at room temperature for 10 minutes. Then, the retrotransciptase (10 U/μl) was added follwed by a 50 minute incubation at 37ºC and a final 15 minute incubation at 70ºC to inactivate the enzyme.

### 3.5.3. Real time quantitative PCR

Real-time quantitative PCR reactions (qPCR )were performed in an iCycler apparatus (BioRad, USA) using iQ SYBR Green Supermix (BioRad, USA), 400 ng cDNA template

and 300 nM of each gene-specific primer in a final reaction volume of 12.5 µl. All primer pairs amplified products of 160 – 200 bp. The following PCR program was used for all reactions: an initial step of denaturation (5 min, 94ºC) followed by 40 cycles of 30 s at 94ºC, 30 s at 60ºC, 30 s at 72ºC, and 20 s at 80ºC for measurement of fluorescence emission. A melting curve program was run for which measurements were made at 0.5ºC temperature increments every 5 s within a range of 55 – 95ºC.

Once Ct values were obtained (Ct=number of cycles required for the fluorescent signal to cross the threshold), comparison of multiple samples was performed using relative quantification by the $2^{-\Delta\Delta Ct}$ method (Livak and Schmittgen, 2001; Pfaffl, 2001). For this, the wild type strain was chosen as the calibrator and the expression of the target gene in all other strains was expressed as an increase or decrease relative to the calibrator. To determine the relative expression of a target gene in the test sample and calibrator sample, a reference gene (*actin*) was used as the normalizer (see Table 9).

**Table 9. Ct values required for relative quantification with reference gene as the normalizer.**

| | Test | Calibrator (cal) |
|---|---|---|
| Target gene | Ct(target, test) | Ct(target, cal) |
| Reference gene | Ct(ref, test) | Ct(ref, cal) |

For calculation of PCR amplification efficiencies (E), a standard curve was generated using a 10-fold dilution of a cDNA template amplified on the iCycler iQ® real-time system, with each dilution assayed in triplicate. Mean CT values were plotted against the log of the starting quantity of template for each dilution. E is calculated from the slope of the standard curve using the formula: $E = 10^{-1/slope}$. All PCR amplification reactions were optimized to achieve efficiencies of 90–105%. Whenever lower reaction efficiencies were obtained, new primers were designed until optimal reaction conditions were achieved.

Primers pairs act-2/act-q6 (E=99%), msb2ORF-s/msb2ORF-as (E=101%), 09795-for /09795-rev (E=98%), ChsV-20/ChsV-36B (E=92%), Chs3-12/Chs3-18 (E=96%), Gas-1/Gas-5 (E=98%), FOXG_14695-F/FOXG_14695-R (E=99%) and sho1-for4/sho1-rev5 (E=101%) were used to detect actin, *msb2, fpr1, chsV, chs3, gas, pg1* and *sho1* transcripts, respectively.

Once established that all target and the reference genes had similar and nearly 100% amplification efficiencies, the relative difference in expression level of the target gene in different samples was determined using the steps below:
First, the Ct of the target gene was normalized to that of the reference (ref) gene, for both the test sample and the calibrator sample:
$\Delta$Ct(test) = Ct(target, test) – Ct(ref, test)
$\Delta$Ct(calibrator) = Ct(target, calibrator) – Ct(ref, calibrator)
Second, the $\Delta$Ct of the test sample was normalized to the $\Delta$Ct of the calibrator:
$\Delta\Delta$Ct = $\Delta$Ct(test) – $\Delta$Ct(calibrator)
Finally, calculate the expression ratio:
$2^{-\Delta\Delta Ct}$ = Normalized expression ratio

The result obtained is the fold increase (or decrease) of the target gene in the test sample relative to the calibrator sample and is normalized to the expression of a reference gene.

Data from three independent experiments, including two qPCR technical replicates were analysed with the software SPSS 15.0 for Windows® (LEAD Technologies, Inc., Charlotte, North Carolina). Kruskal-Wallis ANOVA and the Mann-Whitney test were executed to assess statistically relevant differences among strains for each gene at $p \leq 0.05$.

### 3.5.4. Fusion PCR

Fusion PCR or overlap extension represents a new approach to genetic engineering (Ho *et al.*, 1989; Yang *et al.*, 2004). The method is schematically represented in Figure 7.

Complementary oligodeoxyribonucleotide (oligo) primers and the polymerase chain reaction are used to generate two DNA fragments with overlapping ends. These fragments are combined in a subsequent 'fusion' reaction in which the overlapping ends anneal, allowing the 3' overlap of each strand to serve as a primer for the 3' extension of the complementary strand. The resulting fusion product is amplified further by PCR.

In this work, this technique was used for several purposes: 1. Generation of the *msb2* gene knockout construct, where part of the ORF of the gene was replaced with the hygromycin resistance cassette; 2. In-frame insertion of the HA epitope sequence in the *msb2* gene; 3. In-frame substitution of a large nucleotide fragment within the *msb2* ORF region by the HA epitope nucleotide sequence. In each specific case, the PCR protocol was adapted to achieve optimal results. In general, we found that fusion of two PCR fragments was best achieved by first purifying the fragments with the comercial GENECLEAN Turbo Nucleic Acid Purification kit and then using equimolar quantities of the purified products as templates for subsequent PCR reactions, using standard conditions (see Section 3.5.1). For PCR fusion of templates with high GC content or final fusion fragments larger than 5 Kb, the more robust iProof High-Fidelity DNA Polymerase (BioRad, Madrid, Spain) was used, following the manufacturer´s instructions.

### 3.5.5. Synthetic oligonucleotides

Oligonucleotides used in amplification and sequencing reactions were designed with the software Oligo (version 6.65; Molecular Biology Insights, Inc. USA), analyzing internal stability, duplex and hairpin formation and different physicochemical parameters (Tm, %G+C, %A+T) in each case. Oligonucleotides were synthesized by different companies (MWG-Biotech and Bonsai Technologies). Oligonucleotides used in this work are listed in Table 10. Lower case italic letters do not belong to the original sequence and were introduced to generate a restriction enzyme cutting site. Similarly, underlined nucleotides do not belong to the original sequence and were introduced to generate M13 complementary sequences or the HA coding sequence.

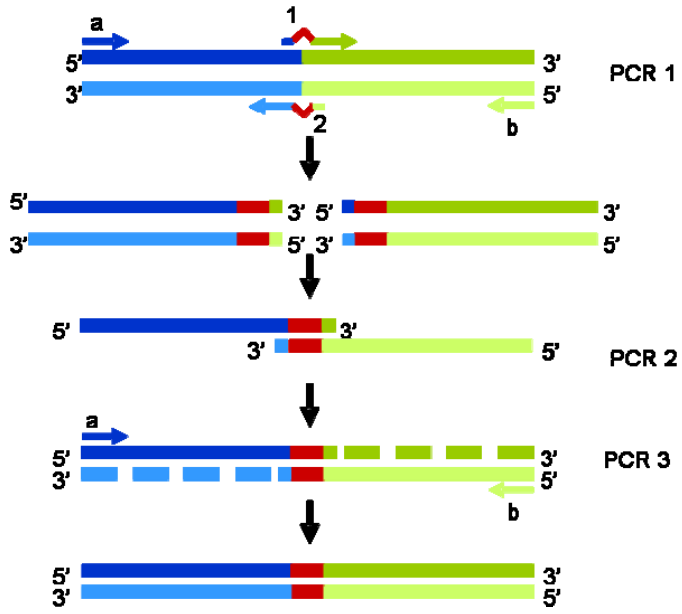


**Figure 7. Schematic representation of the Fusion PCR technique.**
Two initial PCR reactions are performed with primer sets a/2 and 1/b, using genomic or plasmid DNA as a template. The PCR products obtained are used as templates for a second PCR reaction with no oligos, resulting in annealing of complementary template sequences and extension by the polymerase. The final reaction uses the PCR2 product as a template for amplification with the external primer set a/b.

**Table 10. Oligonucleotides used in this study.**
Added restriction sites not present in the orginal DNA sequence are indicated in lower case. HA epitope nucleotide sequences and sequences complementary to M13 primers are underlined.

| Plasmid/gene | Name | Sequence 5'-3' |
|---|---|---|
| pGemT | M13for | CGCCAGGGTTTTCCCAGTCACGAC |
| | M13rev | AGCGGATAACAATTTCACACAGGA |
| hph/phleo | gpdA-15b | ggatccCGAGACCTAATACAGCCCCT |
| cassettes | trpter-8b | ggatccAAACAAGTGTACCTGTGCATTC |
| | gpdA-9 | GTGATGTCTGCTCAAGCGG |
| *msb2* | msb2-5'-HA-s | GCAGATGGAGGCGCTGAAGCAT |
| | msb2-5'-HA(722)-as | GGCATAGTCAGGAACGTCATATGGATAAGTCTCGGTGGCAGGGCTGCC |

| | | |
|---|---|---|
| | msb2-5'-HA-as | GGCATAGTCAGGAACGTCATATGGATAATTCTCTGGGGCGACTGGAGCAT |
| | msb2-3'-HA-s | TATCCATATGACGTTCCTGACTATGCCACTGATGCGGAGACCAACGGCAC |
| | msb2-3'-HA-as | CTGAACAACACCACCGCTTCCC |
| | msb2-for2 | GAGATTCCAACAATAGCAGATG |
| | msb2-comp2 | GCAATCCGCGCCCAATAGAC |
| | msb2-ORF-s | TGCCCCCACAGATGAGCAAC |
| | msb2-HA-s | CCATATGACGTTCCTGACTATG |
| | msb2-nest3 | CAAGCATCAAAGGCGTCGTC |
| | msb2-nest4 | CTCACGCCTAACGCCTCCAA |
| | msb2-knock1 | GTGACTGGGAAAACCCTGGCGAGTTGGATACTGTTTGGTGATTG |
| | msb2-knock2 | TCCTGTGTGAAATTGTTATCCGCTACTCGTTAGCAAGATTGTTCCTC |
| *sho1* | sho1-for1 | GTTACCAAGAAGTACAGCACG |
| | sho1-for1 | GTTACCAAGAAGTACAGCACG |
| | sho1-for3 | TATCGATACCAATAAACCATCAC |
| | sho1-M13r-rev1 | TCCTGTGTGAAATTGTTATCCGCTTGTTGCTCATCTGAATGCCCTT |
| | sho1-rev2 | GCATTCCAATAATCATCGTGTTC |
| qPCR | 09795-for (*fpr1*) | CCCAAGAAGAACCCTGCTCC |
| | 09795-rev (*fpr1*) | GAGTAGGGGTTGGAGCCGC |
| | msb2-ORF-s | TGCCCCCACAGATGAGCAAC |
| | msb2-ORF-as | GGATCTTGGCGAGAGCAGTG |
| | Chs3-12 | GTGTCATGGGGAACAAAGGG |
| | Chs3-18 | CCTGTAACCCCAAAAGTATGT |
| | Gas-1 | GACTCCGACCTCTGCGACT |
| | Gas-5 | TCCGAGGCGTAACCGACACC |
| | FOXG_14695-F (*pg1*) | GCAGCGTCACTGACTACTCC |
| | FOXG_14695-R (*pg1*) | GTTAGAACCTTCGCCATCCCA |
| | ChsV-20 | GCACAATTTGGCTGAGCTTAT |
| | ChsV-36B | GGATCCCTACAATTGGCCAGAAAGCA |
| | act-2 | GAGGGACCGCTCTCGTCGT |
| | act-q6 | GGAGATCCAGACTGCCGCTCAG |

## 4. Protein methods

### 4.1. Protein purification from *F. oxysporum* mycelia

Approximately 100 mg of frozen mycelium were ground to a fine powder in a pre-chilled mortar and pestle under liquid nitrogen. For analysis of cytosolic proteins in whole cell extracts, the ground mycelium was resuspended in 200 to 500 µl of ice-cold protein extraction buffer A, containing 10% glycerol, 50 mM Tris-HCL pH7.5, 150 mM NaCl, 0.1 % SDS, 1% Triton, 5 mM EDTA, 1 mM PMSF and Protease inhibitor cocktail (Sigma, P8215), vortexed to ensure sample homogenisation and centrifuged at 4°C to pellet cell debris. The supernantant was either quantified and used in subsequent experiments or stored at -80°C. For analysis of phosphogroups in proteins, ground mycelium was homogenised in buffer A including the following phosphatase inhibitors: 50mM NaF, 5 mM sodium orthovanadate, 50 mM beta-glycerophosphate, 1mM Sodium Orthovanadate, and PhosSTOP Phosphatase Inhibitor Cocktail tablets from Roche. Tomato plant roots with adhering mycelium were treated as normal mycelium.

For generation of protein samples for subcellular fractionation experiments, liquid-nitrogen ground mycelium was homogenised in detergent-free protein extraction buffer B, containing 10% glycerol, 50 mM Tris-HCL pH7.5, 150 mM NaCl, 5 mM EDTA, 1 mM PMSF and Protease inhibitor cocktail (Sigma, P8215) and the lysate was processed as described in Section 4.7.

### 4.2. Protein purification from *F. oxysporum* culture supernatants

For detection of secreted Msb2-HA protein in culture supernantants, germlings from PDB were obtained as described in Section 2.2, washed twice in sterile water, transferred to liquid MM and incubated for 8 h at 28ºC at 120 rpm. Cultures were harvested, sterile filtered (0.22 µm pore size), dialyzed against various changes of distilled water for 3 days at 4ºC and lyophilized. Samples were resuspended in double distilled water and submitted to western blot analysis (see below).

## 4.3. Determination of protein concentration

Protein concentration of cell extracts was determined with the Bio-Rad protein assay reagent, using bovine serum albumin as standard and following the manufacturer´s instructions.

## 4.4. Western blot analysis

For western blot analysis, one hundred microgram of total protein was resuspended in protein loading buffer (50 mM Tris-HCl, pH 6,8; 8% glycerol (v/v); 1,6% SDS w/v; 4% β-mercaptoetanol (v/v); 0,1% bromophenol blue) and separated in 5 to 20% gradient SDS-polyacrylamide gels (Laemmli, 1970) at constant voltage, using Tris-HCl/glycine/SDS (50mM, 400 mM, 0.02%, respectively) as running buffer. The gel was transferred to nitrocellulose membranes (Bio-Rad) using the Mini Trans-blot® Cell (Bio-Rad) and a transfer buffer containing 48mM Tris-HCl pH 7.5, 39 mM glycine, 0.0375% SDS and 20% methanol at constant voltage (100 V at room temperature for 2 hours for MAPK analysis or 30V at 4°C overnight for Msb2-HA analysis). For Western blot analysis, membranes were blocked using 5% non-fat skimmed milk for 1 h. p44/42 MAP kinases were detected using the Phospho Plus p42/p44 MAP Kinase (Thr202/Tyr204) Antibody kit (Cell Signaling Technology, Beverly, MA) according to the manufacturer´s instructions, except that ECL Plus immunoblotting reagent (GE Healthcare, Barcelona, Spain) was used for detection. Monoclonal α-actin antibody from Sigma (A3853) was used as a loading control.

For Western blot analysis of Msb2-HA, the following modifications of the above protocol were applied: protein separation was performed in 7% SDS-polyacrilamide gels and membranes were blocked using 1% non-fat skimmed milk for 1 h at 25°C and probed with α-HA-Peroxidase High Affinity antibody (Roche) according to the manufacturer´s instructions, followed by detection with ECL Plus reagent.

## 4.5. Colony inmunoblot

For colony inmunoblot assays (Pitoniak *et al.*, 2009), germlings from PDB were obtained as described in Section 2.2, washed twice in sterile water, resuspended in 1 ml of MM, transferred as a colony onto 0.2 µm pore-filters placed over an MM agar plate overlaid with a nitrocellulose filter and incubated for 8 h at 28°C. The 0.2 µm pore-filters with the colonies were removed carefully, the nitrocellulose membranes were washed with running water and submitted to western blotting with $\alpha$ HA-antibody.

## 4.6. Analysis of N-glycosylation

N-glycosylation was examined by EndoH and Tunycamycin treatment. Whole cell extracts were treated for different time periods with EndoH (New England Biolabs, Ipswich, MA), following the manufacturer's instructions. The N-glycosylation inhibitor Tunicamycin (Sigma Chemicals, Madrid, Spain) was added at 25 µg/ml to 14 h-old germlings in PDB and cultures were incubated for an additional 2 h before harvesting.

## 4.7. Subcellular fractionation studies

Protein samples used for subcellular fractionation studies were prepared from frozen mycelium as described above (Section 4.1) and processed as described by (Horazdovsky and Emr, 1993). The protein lysate was centrifuged at 500 x g for 5 min to remove unbroken cells. The supernatant (S5) was subsequently spun at 14,000 x g for 10 min at 4°C to generate a supernatant (S14) and a pellet (P14) fraction. The P14 was suspended in lysis buffer B and equivalent aliquots of S14 and P14 were reserved for western blot analysis. The remainder of the S14 was centrifuged at 100,000 x g for 50 min, to generate a supernatant (S1OO) and a pellet (P100) fraction. These fractions were analyzed by Western blot. To determine the nature of the association of Msb2-HA with the P14 fraction, equal aliquots of a P14 fraction were adjusted to 5% SDS/8 M urea, 1 M NaCl, 1% Triton X-100, 0.1 M $Na_2C0_3$ (pH 11.0) or left untreated and incubated for 10 min on ice. Samples were then subjected to the 14,000 x g spin. The supernatant fraction was

carefully removed and the protein products precipitated with trichloroacetic acid at a final concentration of 5% (NaCl, Triton X-100) or 10% (urea and $Na_2C0_3$). Trichloroacetic acid pellets were suspended in protein loading buffer (Section 4.4) and subjected to Western blotting.

## 5. Generation of *F. oxysporum* transformants

### 5.1. Generation of *F. oxysporum* protoplasts

Protoplasts were obtained following the protocol described by (Powell and Kistler, 1990), with minor modifications. Briefly, $5x10^8$ microconidia were inoculated into 200 ml of PDB. After 14-15 h incubation, germlings were harvested by filtration with a Monodur and washed throroughly but carefully with an MgP solution (1). A sterile spatula was used to tranfer germlings from the monodur to a sterile 50 ml Falcon tube, containing 20 ml of MgP with 0.5% (w/v) Glucanex® (Novozymes) as the protoplasting enzyme. The protoplasts were incubated in the enzyme solution for 45 minutes at 30ºC with slow shaking (60 rpm), and protoplast accumulation was monitored under the microscope. When optimal number and quantity of protoplasts were achieved, the sample was filtered through a double layer of Monodur nylon filters and washed with two volumes of STC solution (2). The the flow-through containing the protoplasts was collected in pre-chilled ice-cold 50 ml centrifuge tubes. Filtrates were centrifuged at 4ºC and 1500 *g* for 15 minutes to collect protoplats, which were carefully resuspended in 1 ml STC and counted. The protoplast suspension was adjusted to a final concentration of 2 x $10^8$ protoplastos/ml and stored as 100 µl aliquots in Eppendorf tubes to be used for transformation. For long-term storage at -80ºC, 0% of PEG (3) (v/v) and 1% DMSO (Merck) (v/v) were added.

1. MgP solution: 1.2 $MgSO_4$; 10 mM $Na_2HPO_4$, pH 5.8-6.0 adjusted with orthophosphoric acid .
2. STC solution: 0.8 M sorbitol; 50 mM $CaCl_2$ y 50 mM Tris-HCl, pH 7.5.
3. PEG solution: 60% polyethylene glycol MW 4000 (p/v) in 0.6 M MOPS.

## 5.2. Transformation of *F. oxysporum*

Transformation was performed as described (Malardier *et al.*, 1989), with minor modifications. 2 μg of transforming DNA were mixed with 10 μl of 0.1 M aurintricarboxylic acid, a potent inhibitor of nucleases, in a final volume of 60 μl with TEC solution(1). For cotransformation experiments, 1 μg of the DNA construct conferring antibiotic resistance was added. The mix was incubated on ice for 20 minutes. In parallel, 100 μl protoplasts ($2x10^7$) generated as described above, were incubated on ice for 20 minutes. Next, protoplasts and DNA solutions were carefully mixed and incubated a further 20 minutes on ice. Then, 160 μl of PEG solution were added and mixed carefully, followed by a 15-minute incubation at room temperature, after which 1 ml of STC solution was added. The tube was centrifuged for 5 minutes at 3000 rpm to pellet protoplasts, which were resuspended in 200 μl of STC. Next, 50 μl aliquots were mixed with 3 ml of top agar (2) at 45ºC and spread onto plates containing 25 ml of solid regeneration minimal medium. Plates were incubated at 28ºC for 2 hours or 16 hours before addition of 3 ml of top agar containing 2 mg of hygromycin B or 160 μg of phleomycin, respectively. Incubation at 28ºC was prolongued for 4-5 days until transformant colonies became were visible. Colonies were transferred to PDA plates with selective medium, and transformants were submitted to two consecutive rounds of single monoconidial purification on selective PDA plates.

1. TEC solution: 10 mM Tris-HCl, pH 7.5; 1 mM EDTA and 40 mM $CaCl_2$.
2. Top agar: 0.4% agar (Oxoid) (w/v) in regeneration minimal medium.

## 5.3. Generation of Δ*msb2* and Δ*msb2*Δ*fmk1* strains

The *F. oxysporum msb2* gene disruption construct was generated by the fusion PCR technique. A 1559 bp upstream fragment and a 1716 bp downstream fragment relative to the *F. oxysporum msb2* open reading frame (ORF) were amplified from genomic DNA using PCR with primer pairs msb2-for2 and msb2-knock1and msb2-knock2 and msb2-comp2, respectively. The hygromycin B resistance gene, under the control of the

*A. nidulans gpdA* promoter and *trpC* terminator (Punt *et al.*, 1987) cloned into the pGEM-T vector was amplified with the universal primers M13-For and M13-Rev. The three obtained PCR fragments were used for a final fusion PCR using primers msb2-nest3 and msb2-nest4 (Figure 8).

For targeted gene knockout, the *F. oxysporum msb2-hph* fusion construct was used to transform protoplasts of *F. oxysporum* wild type strain 4287 and of the Δ*mk1* mutant. Hygromycin-resistant transformants were selected and purified by monoconidial isolation as described above. Gene knockout was confirmed by Southern blot and PCR analysis.

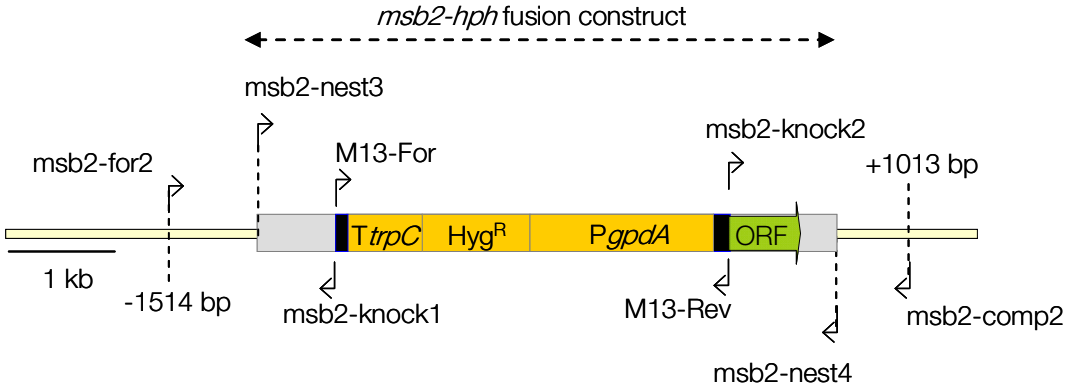


**Figure 8. Representation of the *msb2-hph* fusion construct with relative positions of primers used.**

## 5.4. Generation of Δ*msb2*+*msb2* strains

A 5.3 PCR fragment encompassing the entire *msb2* gene was obtained by PCR amplification from genomic DNA with primers msb2-for2 and msb2-comp2 and cloned into pGemT (Figure 9A). *msb2*-pGemT was used for subsequent PCR amplification of the *msb2* fragment, which was introduced into protoplasts of the Δ*msb2* strain by co-transformation with the phleomycin resistance cassette amplified from plasmid pAN8-1 (Punt *et al.*, 2008), and phleomycin-resistant transformants were isolated as described before.

## 5.5. Generation of Δ*msb2* + *msb2-HA* strains

The hemagglutinin (HA) sequence was inserted into the *msb2* open reading frame at aa position 722 located in the extracellular domain. A 3707 bp upstream and a 1954 downstream PCR fragment were generated by amplification from genomic DNA with primers msb2-5'HA-s and msb2-5´HA722-as and msb2-3´HA-s and msb2-3´HA-as, respectively. Primers msb2-5'HA-s and msb2-3´HA-as were used for fusion PCR of the two fragments (Figure 9B). Due to PCR restrictions, primers were designed to generate in-frame insertion of the HA-epitope followed by a threonine residue not present in the original ORF. The 5.6 Kb fusion fragment was digested with *Cla*I/*Xba*I and subcloned into the *Cla*I/*Xba*I sites of *msb2*-pGemT (Figure 9A) to generate plasmid *msb2-HA*-pGemT, which was sequenced to confirm in-frame insertion of the HA coding sequence. As a result of the combined fusion PCR and subcloning strategy, the *msb2-HA*-pGemt plasmid lost the *Xba*I/*Xba*I sequence region from *msb2*-pGemT, including the binding site for primer msb2-3´HA-as (Figure 9A). The *msb2-HA* construct was amplified by PCR from plasmid *msb2-HA*-pGemt with primers msb2-5'HA-s and msb2-comp2 and introduced into protoplasts of the Δ*msb2#62* strain by co-transformation with the phleomycin resistance cassette amplified from plasmid pAN8-1 (Punt *et al.*, 2008). Phleomycin-resistant transformants were isolated and analysed by PCR Figure 20B).

## 5.6. Generation of the Δ*msb2* + *msb2** strain

The HA-tagged *F. oxysporum msb2** allele lacking part of the extracellular region from glutamine 46 (Q46) to glutamate 721 (E721) of the ORF was generated by fusion PCR. A 1660 bp upstream fragment and a 1956 bp downstream fragment from the *F. oxysporum msb2* locus were amplified from genomic DNA using PCR with primer pairs msb2-5'HA-s and msb2-5´HA-as and msb2-3´HA-s and msb2-3´HA-as, respectively. The two obtained PCR fragments were used for a final fusion PCR using primers msb2-5'HA-s and msb2-3´HA-as. This product was cloned into pGemt to generate *msb2*HA*-pGemT.

For targeted gene replacement, the *F. oxysporum msb2*-HA* construct and the phleomycin resistance cassette amplified from plasmid pAN8-1 (Punt *et al.*, 2008) were used for cotransformation of protoplasts of a *F. oxysporum* Δ*msb2* mutant. Phleomycin-resistant transformants were isolated, purified by monoconidial isolation as described above and examined by PCR analysis (Figure 26).

## 5.7. Generation of Δ*sho1* and Δ*msb2*Δ*sho1* strains

A 5.3 PCR fragment encompassing the entire *sho1* gene was obtained by PCR amplification from genomic DNA with primers sho1-for3 and sho1-rev2 and cloned into pGemT to generate sho1-pGemT (Figure 10). The hygromycin and phleomycin resistance cassettes were amplified from plasmids PBKS-hyg-lamlam and pAN8-1 (Punt *et al.*, 2008), respectively, with primers gpdA-15B and trpter-8B with added *Bam*HI sites and the amplification products were treated with the *Bam*HI restriction enzyme and subcloned into the single *Bam*HI site of *sho1*-pGemT, located immediately after the second intron of *sho1*. Next, part of the ORF was eliminated by PCR amplification of the plasmid with primers gpdA-15B and sho1-M13rev-rev1, using iProof High-Fidelity DNA Polymerase (BioRad). The blunt-ended PCR-generated DNA fragment was self-ligated and used to transform *E. coli*. Clones were screened following standard methods (Sambrook *et al.*, 1989) until the *hph(B)sho1*-pGemT vector was identified. For generation of the *phleo(B)sho1*-pGemT plasmid, the phleomycin resistance cassette amplified with primers gpdA-15B and trpter-8B, was treated with *Bam*HI and used to replace the hygromycin resistance cassette in *hph(B)sho1*-pGemT. The *sho1-hph* and *sho1-phleo* deletion constructs were generated by PCR amplification from plasmids *hph(B)sho1*-pGemT and *phleo(B)sho1*-pGemT, respectively with primers sho1-for1 and sho1-rev2.

The *F. oxysporum sho1-hph* construct was used to transform protoplasts of *F. oxysporum* wild type strain 4287 and the *F. oxysporum sho1-hph* construct was used to transform protoplasts of *F. oxysporum* Δ*msb2* mutant. Transformants were selected and purified by monoconidial isolation. Gene knockout was confirmed by PCR analysis.

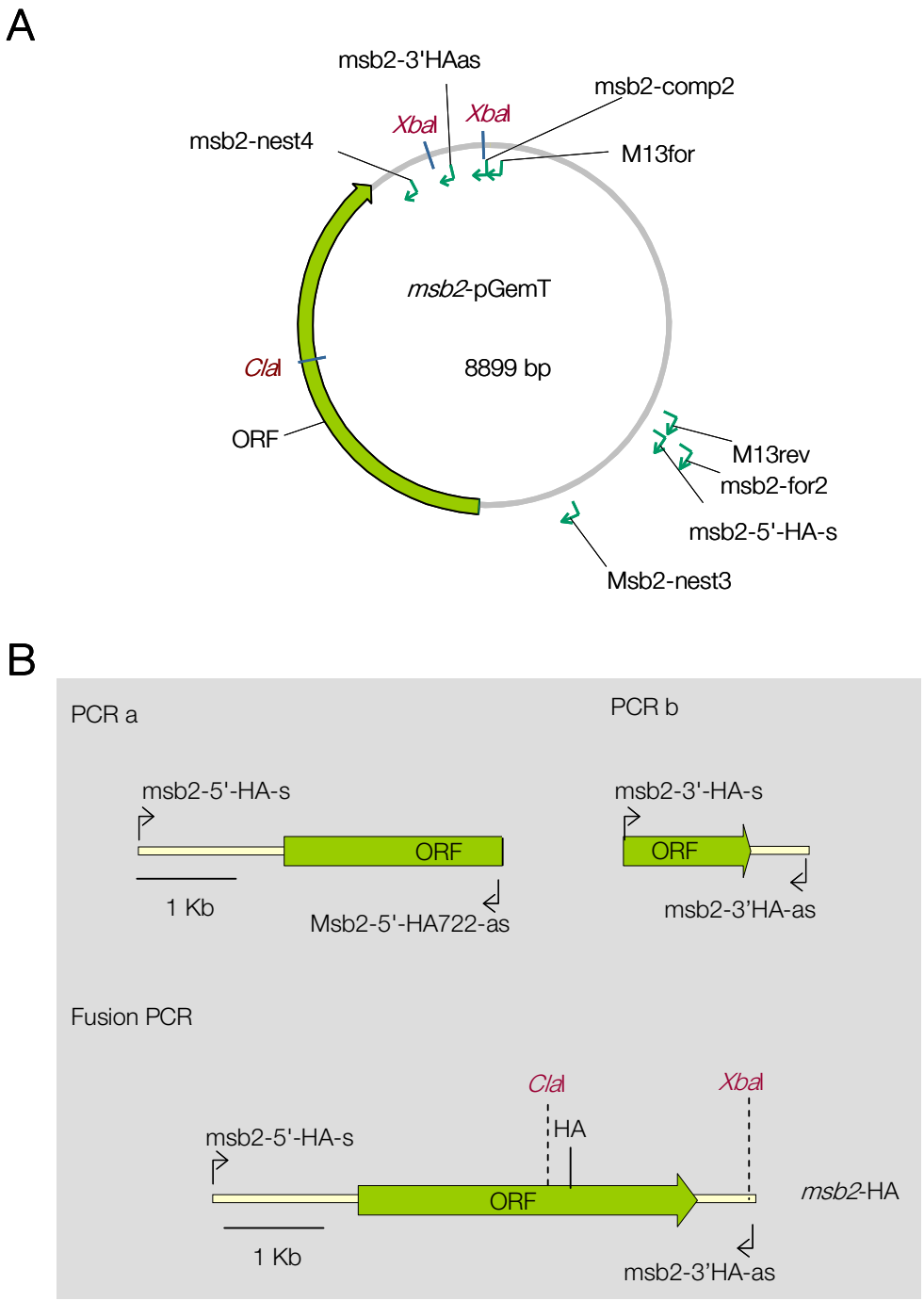


**Figure 9. Generation of the *msb2-HA*-pGemT plasmid.**
*msb2-HA* was derived from *msb2*-pGemt (**A**) by a combined strategy of fusion PCR (**B**) and subcloning. Relative positions of PCR primers and restriction sites are indicated.

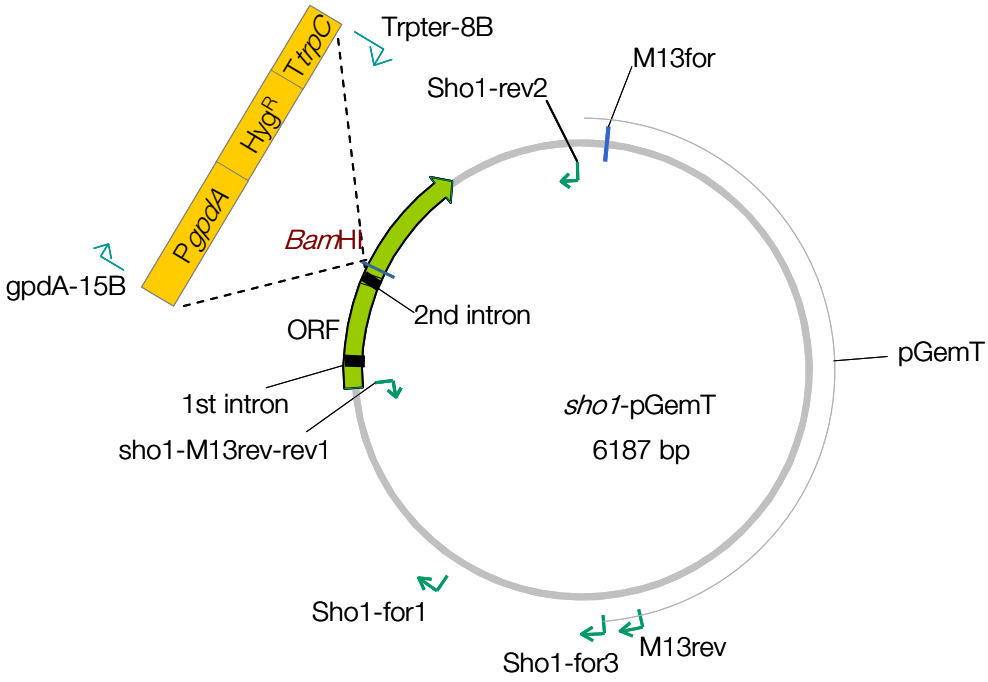


**Figure 10. The *sho1*-pGemT vector.**
Relative positions of primers used for generation of *sho1-hph* and *sho1-phleo* deletion constructs from *sho1*-pGemt are indicated (see text for details).

## 6. Colony growth assays

For phenotypic analysis of colony growth, drops of water containing 2 x $10^5$ microconidia were spotted onto YPD or MM agar plates and plates were incubated at 28°C for 3 days. For cell wall stress assays, 50 µg/ml Congo Red (Sigma) or 40 µg/ml Calcofluor white (Sigma) were added to 50 mM MES-buffered SM agar, pH 6.5 (Ram and Klis, 2006), with or without 1M Sorbitol. For osmotic or oxidative stress assays, YPD agar plates were supplemented with 0.4M, 0.8M and 1.2 M NaCl or 10 µg/ml menadione, respectively. Preparation of stock solutions from these compounds is summarized in Table 11. All experiments included three replicates and were performed at least three times with similar results.

**Table 11. Preparation of stock solutions of cell wall stress and oxidative stress agents.**

| Compound/Company | Preparation | Storage |
|---|---|---|
| Congo red (CR); Sigma | 1% (w/v) in water | -20ºC in the dark |
| Calcofluor white (CFW); Sigma | 1% (w/v) with 0.5% (w/v) KOH and 83% glycerol (v/v) | -20ºC in the dark |
| Menadione; Sigma | 1.6% (w/v) in ethanol | -20ºC in the dark |

## 7. Virulence related assays

### 7.1. Cellophane penetration

For cellophane invasion assays (Prados-Rosales and Di Pietro, 2008), autoclaved cellophane sheets were placed on MM plates and the center of each plate was inoculated with a drop of water containing 2 x $10^5$ microconidia. After 3 days at 28°C, the cellophane sheet with the fungal colony was removed carefully. The presence or absence of fungal mycelium on the underlying medium was recorded after incubation of the plates for an additional 24 h at 28°C. All experiments included three replicates and were performed three times with similar results.

### 7.2. Pectinolytic activity assay

Plate assays for secreted pectinolytic activity (Delgado-Jarana *et al.*, 2005) were performed by determining the clear halo surrounding fungal colonies after precipitation of the substrate polygalacturonic acid. Aliquots of 2 x $10^5$ microconidia were spotted onto solid PGA medium prepared as described in Section 2.2.1. Colonies were grown for three days at 28ºC. PGA plates were precipitated 5 min with 0.4 N HCl and washed thoroughly with water. All experiments included three replicates and were performed three times with similar results.

### 7.3. Vegetative hyphal fusion

Presence of vegetative hyphal fusion was determined as decribed (Prados Rosales and Di Pietro, 2008), using a Leica DMR microscope and the Nomarski technique. Photographs were recorded with a Leica DC 300F digital camera. All assays were done in triplicate, and experiments were performed twice with similar results.

## 8. Infection assays

### 8.1. Msb2-HA expression in infected roots

For analysis of Msb2 expression in *F. oxysporum* during infection of tomato plants, roots of 2 week old plants of the susceptible cultivar Monika (Syngenta Seeds, Almeria, Spain) were immersed into microconidial suspensions of the different strains in sterile water (2.5 x $10^6$ $ml^{-1}$) for 48 h at 28°C. Roots with adhering mycelium were collected, frozen in liquid nitrogen and processed as normal mycelium for western analysis.

### 8.2. Fruit infection

Invasive growth assays on tomato fruits (cultivar Daniela) and apple slices (cultivar Golden Delicious) were carried out as described (Di Pietro *et al.*, 2001; Sánchez López-Berges *et al.*, 2009), using three replicates.

### 8.3. Plant root infection

Tomato root infection assays were performed in a growth chamber as described (Di Pietro and Roncero, 1998), using the susceptible cultivar Monika (Syngenta Seeds, Almeria, Spain). Briefly, two week-old tomato seedlings were inoculated with *F. oxysporum* strains by immersing the roots in a microconidial suspension, planted in vermiculite and maintained in a growth chamber. At different times after inoculation, severity of disease symptoms was recorded with indices ranging from 1 (healthy plant) to

5 (dead plant) (Figure 11) (Huertas-González *et al.*, 1999)). Twenty plants were used for each treatment. All infection experiments were performed three times with similar results.


**Figure 11. Disease index in tomato plants infected with *F. oxysporum f. sp. lycopersici.***

## 9. Bioinformatic analysis

### 9.1. Sequence retrieval

The *F. oxysporum* Msb2 and Sho1 proteins were identified by BLASTp search in the Fusarium Comparative Database of the Broad Institute http://www.broadinstitute.org/annotation/genome/fusarium_group/MultiHome.html) with the *S. cerevisiae* protein sequences. Identification of putative Msb2 ortologues from other fungi was performed as described (Rispail *et al.*, 2009).

### 9.2. Bioinformatic topology prediction

Protein alignments were made using ClustalW (Thompson *et al.*, 1994), and protein domain predictions were made using the Prosite database (ExPASy; Swiss Institute of

Bioinformatics) and SMART analysis (Simple Modular Architecture Research Tool; http://smart.embl-heidelberg.de/). Presence of a signal peptide was determined with SignalP version 3.0 (Bendtsen *et al.*, 2004), using a standardized threshold value of 0.5. Putative N-glycosylation and O-glycosylation sites were identified with NetNGlyc 1.0 and NetOGlyc 3.1 (Julenius *et al.*, 2005), respectively. Prediction of transmembrane helices in proteins was done with TMHMM (Krogh *et al.*, 2001). Calculations of sequence identity percentages was performed using the online EMBOSS Pairwise Alignment Algorithms. For promoter analysis of Tec1 and Ste12 sites, sequences 1,000 bp upstream of the coding region were analysed using the regulatory sequence analysis tools website at http://rsat.ulb.ac.be/rsat/.

## 9.3. Genome-wide analysis of PTS domains

The predicted *F. oxysporum* proteins were downloaded from the Fusarium Comparative Database of the Broad Institute. The PTSpred algorithm (Lang *et al.*, 2004) was used for the identification of mucin domains, which examines the frequency of the amino acids Ser, Thr, Pro. The basic principle of the program is that a protein sequence is analyzed by moving a window, typically 100 amino acids long, along the sequence and determining the composition of Ser, Thr and Pro in that window. The window is moved by default in steps of 10. If the composition of S+T and P, respectively, is above a certain threshold value it is recorded as a potential PTS domain. If two or more such domains overlap they are merged in the output. Typical threshold values are 40% S+T and 5% P. The output from the program is a list of hits ordered by the length of the PTS-rich region.

## 9.4. Phylogenetic analysis

Full-length sequences were aligned with Clustal W (Thompson *et al.*, 1994) and manually inspected. Only fully aligned parts of the multiple sequence alignment were used. The tree was made by using the Modelgenerator algorithm. A maximum likelihood tree was built from the alignment by PhyML version 4.0 using both parsimony and distance analysis (neighbor joining) with 1000 bootstrap replicates (Guindon and Gascuel, 2003).

## 10. Software

Data management and processing was performed using different software products listed in Table 12.

**Table 12. Software products used in this work.**

| Program | | Application |
|---|---|---|
| LaserGene (DNA-Star) | EditSeq | Sequence editor |
| | SeqBuilder | ORF and restriction sites analyzer |
| | MegAlign | Sequence alignment |
| | SeqMan | Sequence assembly and analysis |
| Vector NTI | | Sequence edition |
| BioEdit | | Sequence edition and alignment |
| Oligo 6 | | Synthetic oligonucleotides design |
| Modelgenerator | | Model of substitution analyzer |
| PhyIml | | Phylogenetic trees computation |
| Dendroscope | | Phylogenetic trees representation |
| Leica IM 500 and Leica QWin | | Edition and analysis of microscope and binocular images |
| Fujifilm Image Reader | | Obtaining, edition and analysis of chemiluminescence images |
| Kodak 1D Image Analysis | | Obtaining, edition and analysis of DNA and RNA gel images |
| Espson Scan | | Image scanning |
| Bio-Rad iQ5 | | Obtaining and analysis of real time RT-PCR data |
| Microsoft Office | Word | Word processing |
| | PowerPoint | Image presentation and processing |
| | Excel | Data processing |
| EndNote | | Reference and bibliography editor |
| Adobe Photoshop Elements | | Image processing |

# Results

## 1. *F. oxysporum msb2* encodes a predicted transmembrane protein with a large extracellular mucin homology domain and a short intracellular region.

A BLAST search of the complete genome database of *F. oxysporum* (http://www.broad.mit.edu/annotation/genome/fusarium_group.1/MultiHome.html) with the amino acid sequence of the *S. cerevisiae* Msb2 protein identified a single putative ortologue, *FOXG_09254,* encoding a hypothetical protein of 1129 amino acids with a molecular mass of 117,5 kDa and a pI of 4,48. The predicted *F. oxysporum* Msb2 protein has a domain architecture similar to *S. cerevisiae* Msb2 (Figure 12A), including an N-terminal signal sequence (SS, 20 amino acids), a large extracellular domain (amino acids 21 to 991) with a Ser/Thr/Pro-rich region predicted to be highly O-glycosylated (mucin homology domain (MHD), amino acids 106 to 836), a positive regulatory domain (PRD, 176 amino acids), a single transmembrane domain (TM, 22 amino acids) and a short cytoplasmic tail (CT, 95 amino acids). The overall sequence identity between *F. oxysporum* and *S. cerevisiae* Msb2 proteins was 20.2%. The MHD, defined as the extracellular region extending from the first to the last amino acid predicted to be O-

glycosylated by the NetOGlyc algorithm, showed the lowest sequence identity (19%). In contrast to *S. cerevisiae* Msb2, no exact repeats were found in the MHD domain of the *F. oxsyporum* protein. However, two regions containing non-exact repeats (RPT) were detected using the Prospero algorythm implemented in the SMART program (Mott, 2000) (Figure 12B). Higher identity values were found in the cytoplasmic tail (25.7 %) and in a region of approximately 100 amino acids located upstream of the transmembrane domain (25.8 %), named PRD for positive regulatory domain (Cullen *et al.*, 2004). Msb2 orthologues were also detected in the genome sequences of other ascomycetes including plant and human pathogens (Rispail *et al.*, 2009), displaying a similarly conserved domain architecture as *F. oxysporum* Msb2. While *S. cerevisiae* and *Ashbya gossypii* have two paralogues, Msb2 and Hkr1, the other ascomycete species surveyed contain only one Msb2 orthologue (Figure 14 and Figure 13, Hkr1 orthologues not shown). Sequence identity scores among these orthologues were highest in the TM, PRD and CT regions, with values above 50% for TM and CT regions between most filamentous ascomycetes and *F. oxysporum* (Table 13). Collectively, these results suggest that *FOXG_09254* encodes a structural orthologue of *S. cerevisiae* Msb2, and that Msb2 is conserved in ascomycetes.

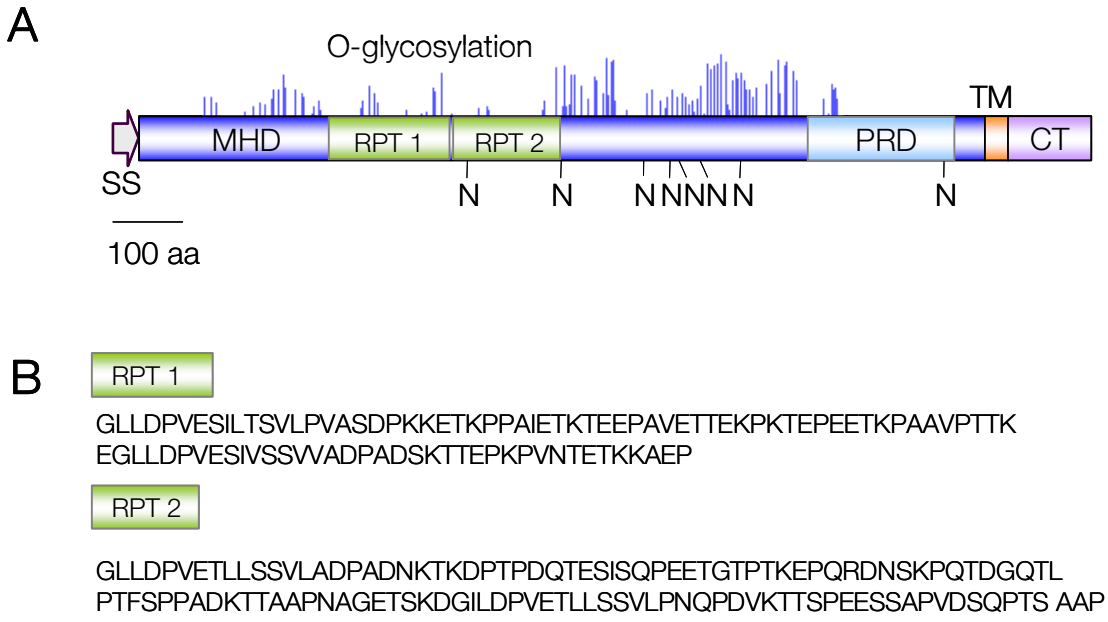


**Figure 12. Predicted domain architecture of the Msb2 protein.**
(**A**) Shown are the N-terminal signal sequence (SS), the extracellular Ser/Thr/Pro-rich mucin homology domain (MHD), the internal repeats (RPT), the positive regulatory domain (PRD), the transmembrane domain (TM), and the cytoplasmic tail (CT). N-glycosylation sites were predicted by NetNGlyc 1.0. O-glycosylation sites (blue peaks) are represented as predicted by NetOGlyc 3.1 Each peak represents the score value calculated for an S or T residue in the sequence above the limiting threshold. The higher the score the more confident the prediction. aa: amino acids. (**B**) Aminoacid sequence of the two internal RPT in (A), as detected by the Prospero program.

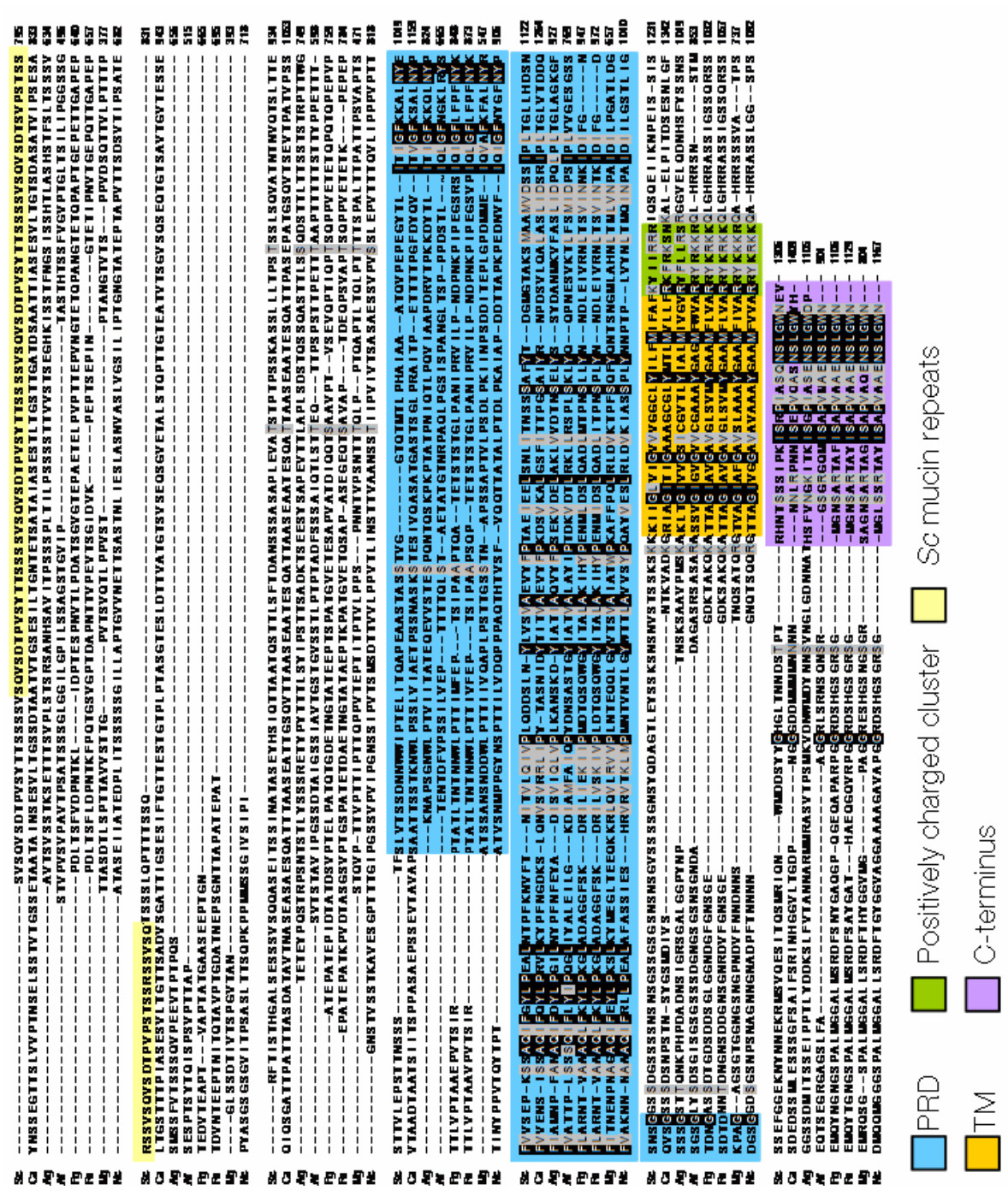


**Figure 13. Sequence alignment of fungal Msb2 proteins.**
The alignment shows the predicted amino acid sequences of Msb2 orthologues from the indicated species (abbreviations as in Table 13). Highly conserved residues are shaded in black, moderately conserved residues are shaded in grey.

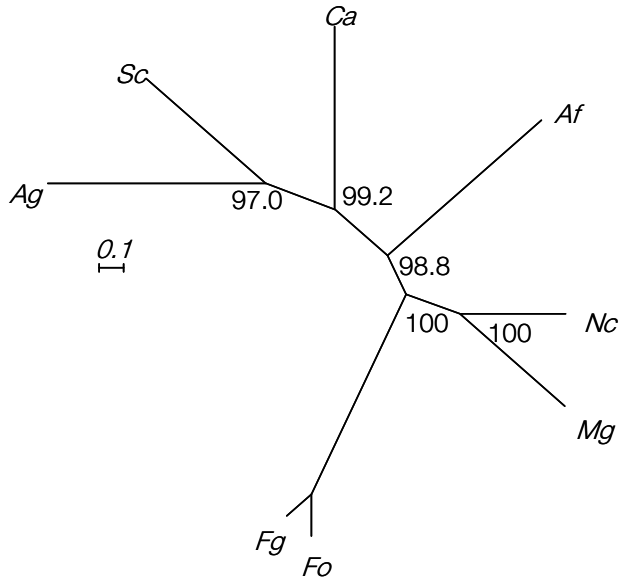


**Figure 14. Phylogram of Msb2 proteins from ascomycetes.**
Shown are putative orthologues of Msb2 in the indicated species. Percentage bootstrap values obtained from 1000 replicates are indicated at the nodes. Scale bar indicates the relative length of each branch. *S. cerevisiae (Sc), C. albicans (Ca), A. gossypii (Ag), A. fumigatus (Af), F. graminearum (Fg), F. oxysporum (Fo), M. grisea (Mg) and N. crassa (Nc)*.

**Table 13. Sequence identities of Msb2 domains of different ascomycetes assessed by pair-wise analysis against Msb2 proteins of *S. cerevisiae* (A) and *F. oxysporum* (B).**
(FL, full-length protein, MHD, extracellular; PRD, homology region; TM, transmembrane; CT, cytoplasmic). Values represent identity scores obtained after pairwise analysis using the needle method (global) of the EMBOSS pairwise analysis server. Abbreviations as in Figure 14.

A

| Sc | Ag | Ca | Af | Fg | Fo | Mg | Nc |
|---|---|---|---|---|---|---|---|
| Msb2 (FL) | 27,0 | 27,0 | 22,5 | 19,2 | 20.2 | 19,6 | 24,2 |
| MHD | 25.9 | 24.8 | 20.8 | 17.9 | 19.0 | 17.6 | 24.3 |
| PRD | 43.7 | 43.8 | 33.6 | 23.3 | 25.8 | 33.1 | 26.8 |
| TM | 39.1 | 39.1 | 29.2 | 20.0 | 20.0 | 17.9 | 10.7 |
| CT | 31.9 | 23.0 | 17.0 | 26.1 | 25.7 | 23.9 | 17.2 |

B

| Fo | Sc | Ag | Ca | Af | Fg | Mg | Nc |
|---|---|---|---|---|---|---|---|
| Msb2 (FL) | 20.2 | 23.1 | 23.2 | 26.0 | 66.8 | 23.4 | 28.6 |
| MHD | 19.0 | 21.5 | 22.0 | 23.1 | 60.9 | 16.3 | 21.6 |
| PRD | 27.1 | 27.1 | 28.9 | 30.1 | 89.3 | 32.8 | 38.5 |
| TM | 20.0 | 30.4 | 34.8 | 50.0 | 100.0 | 66.7 | 65.2 |
| CT | 25.7 | 25.9 | 25.5 | 36.5 | 88.8 | 60.6 | 73.7 |

## 2. Genome-wide analysis of *F. oxysporum* proteins with mucin-type domains

We took a bioinformatic approach to study the presence of putative mucin-type proteins in the genome of *F. oxysporum*. First, we performed a genome-wide analysis of proline-serine-threonine rich (PTS) domains which are characteristic for mucins. Predicted proteins from the *F. oxysporum* genome were downloaded from the *Fusarium* Comparative Database of the Broad Institute and analysed with the PTSpred algorithm (Lang *et al.*, 2004) (see Materials and Methods, Section 9.3). The analysis retrieved 356 proteins (Table 14, Supplementary Table 1) that were subsequently tested with the SignalP program (Bendtsen *et al.*, 2004) to determine the presence of a putative signal peptide. Sequences with a predicted signal peptide cleavage site within 28 amino acids from the N terminus and a confidence value of the Hidden Markov Model prediction equal to or >90% were retrieved, resulting in the selection of 132 proteins. Next, TargetP (Emanuelsson *et al.*, 2000) was used to remove proteins predicted to be targeted to mitochondria, resulting in the selection of 116 non-mitochondrial proteins. TMHMM (Krogh *et al.*, 2001) and PredGPI software (Pierleoni *et al.*, 2008) were used to identify putative transmembrane and GPI-anchored proteins, respectively, resulting in the retention of a set of 15 putative transmembrane mucins, 13 of which had one single predicted TM domain, 1 had two predicted TM domains and 1 had seven TM domains. Moreover, we detected 17 putative GPI-modified and 84 putatively secreted mucin proteins.

It is worth noting that the PTSpred analysis did not retrieve FOXG_09254, the yeast Msb2 orthologue identified by blastp search (see previous section). We suspect that this is due to the absence of exact repeat sequences in the extracellular MHD domain of *F. oxysporum* Msb2.

Even taking into account the preliminary nature of this analysis, and being aware that more detailed studies on these predicted candidates are required to determine whether they actually represent putative mucin-like proteins, the results of this genome-wide

approach suggest that mucin-type surface or extracellular proteins may be widespread in filamentous fungal pathogens such as *F. oxysporum*.

**Table 14. Results of genome-wide analysis of putative mucins in *F. oxysporum* using the PTSpred algorythm.**

| Predicted *F. oxysporum* proteins | Proteins with PTS domains | Putative signal petide (SignalP) | Non-mitochondrial proteins (Target P) | + (TMHMM + PredGPI) | | |
|---|---|---|---|---|---|---|
| | | | | TM domain | GPI-anchored | Secreted |
| 17735 | 356 | 132 | 116 | 15 | 17 | 84 |

## 3. Targeted deletion of *msb2* in the wild type and Δ*fmk1* backgrounds.

To explore the biological role of Msb2 in *F. oxysporum,* we generated a Δ*msb2* allele by replacing most of the open reading frame with the hygromycin resistance cassette (Figure 15A). This construct was introduced into the wild type strain and into the Δ*fmk1* mutant to study possible epistatic relationships between the two genes. Southern blot analysis identified several transformants in which the 9.7 kb *Eco*RI fragment corresponding to the wild type *msb2* allele had been replaced by a fragment of 5.5 kb (Figure 15B), demonstrating homologous insertion in these transformants which were named Δ*msb2* and Δ*fmk1*Δ*msb2*, respectively. For complementation of the Δ*msb2* mutation, a 5,3 kb DNA fragment encompassing the complete *msb2* gene was amplified by PCR with primer set msb2-for2/msb2-comp2 from the *msb2*-pGemT plasmid and introduced into the Δ*msb2#62* mutant by cotransformation with the phleomycin resistance marker. Several phleomycin-resistant transformants produced a PCR amplification product with primer set msb2-nest3/msb2-ORFas, identical to that obtained from the wild type strain but not from the Δ*msb2#62* mutant, suggesting that these strains, named Δ*msb2*+*msb2* had integrated an intact copy of the *msb2* gene into their genome (Figure 15C).

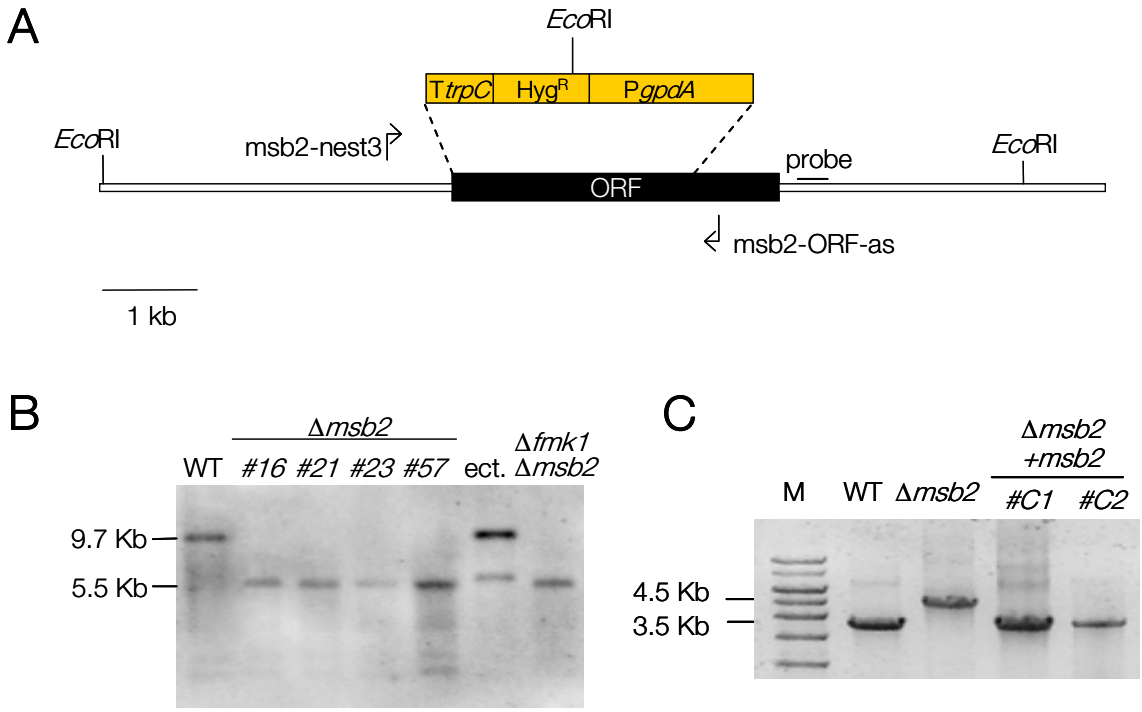


**Figure 15. Targeted disruption of the *F. oxysporum msb2* gene.**
(**A**) Physical maps of the *msb2* locus and the gene replacement construct obtained by PCR fusion (Δ*msb2* allele). Relative positions of the primers used for generation of the gene disruption construct and PCR analysis of transformants and complemented strains and the probe used for Southern analysis are indicated. (**B**) Southern blot hybridization analysis of the wild type strain 4287, different Δ*msb2* mutants and an ectopic transformant. Genomic DNA treated with *EcoRI* was hybridized with the probe indicated in (A). Molecular sizes of the hybridizing fragments are indicated on the left. (**C**) Amplification of genomic DNA of the indicated strains using forward primer nest3 and msb2-ORF-as indicated in (A), to differentiate the wild type PCR product from that corresponding to the Δ*msb2* allele.

## 4. Msb2 contributes to hyphal growth on nutrient limiting solid medium

To test the role of Msb2 in vegetative hyphal growth, colony diameter was determined on rich (YPD) or nutrient-limiting solid medium (MM) medium. On MM, colonies of the Δ*msb2* mutants displayed a significantly slower growth rate than the wild type strain, a phenotype that was completely restored in the Δ*msb2*+*msb2* complemented strain (Figure 16). By contrast, no differences in growth rate were detected on nutrient-rich solid medium

(YPD). The Δ*fmk1* and Δ*fmk1*Δ*msb2* strains displayed the same decrease in hyphal growth rate as Δ*msb2*, suggesting absence of an additive effect in the double mutant. Colonies of Δ*msb2*, Δ*fmk1* and Δ*fmk1*Δ*msb2* mutants also developed less aerial hyphae than those of the wild type strain (Figure 16A).

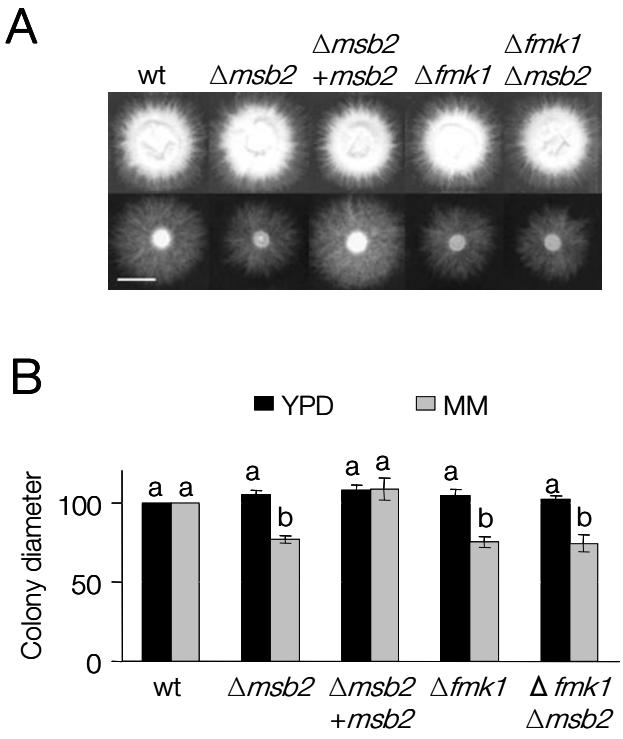


**Figure 16. Msb2 contributes to hyphal growth under conditions of nutrient limitation.** (**A**) Colony phenotype of the indicated strains grown on yeast peptone glucose (YPD) or minimal medium (MM). Plates were spot-inoculated with $10^5$ microconidia, incubated 3 days at 28°C and scanned. Scale bar, 1 cm. (**B**) Colony diameter was measured after 5 days and plotted relative to the wild type strain (100%). Bars represent standard errors calculated from 4 plates. Values with the same letter are not significantly different according to Mann-Whitney test ($p \leq 0.05$).

In order to compare growth of the different strains in submerged culture, growth curves were obtained in nutrient-rich (PDB) or nutrient-limiting medium (MM), by measuring optical density at 595 nm in microtiter plates at different time points after inoculation. No

significant differences in growth rates were observed between the strains either in PDB or MM liquid culture (Figure 17).

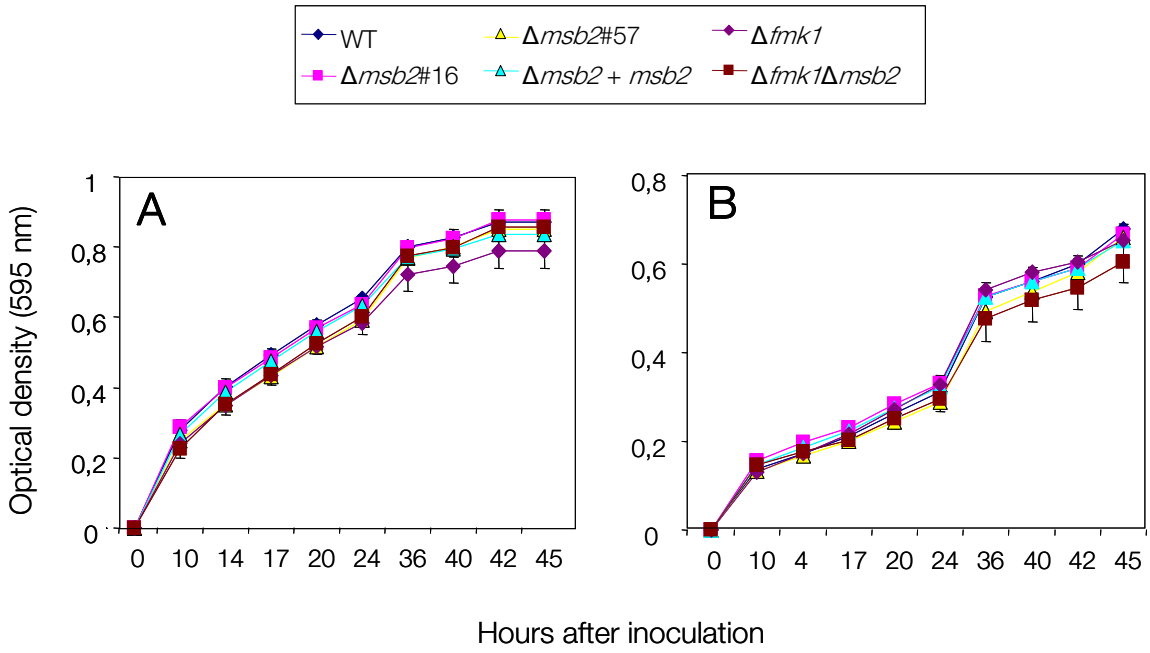


**Figure 17. Growth of different strains in submerged culture.**
Growth of the wild type strain (blue diamonds), Δ*msb2#16* (pink squares), Δ*msb2#57* (yellow triangles), Δ*msb2*+*msb2* (blue triangles), Δ*fmk1* (purple diamonds) and Δ*fmk1* Δ*msb2* (brown squares) was measured in microtiter wells containing liquid YPG (A) or MM (B), by determining the optical density at 595 nm at different time points after inoculation. Bars represent standard errors calculated from 3 wells.

## 5. Δ*msb2* strains are affected by cell wall stress

The Δ*msb2,* but not the Δ*fmk1* strains were more sensitive to the cell wall targeting compounds Congo Red (CR) and Calcofluor White (CFW) than the wild type strain (Figure 18). Addition of 1M Sorbitol partially rescued the growth inhibition by CR and CFW. Strikingly, the Δ*fmk1*Δ*msb2* double mutant was significantly more sensitive to the two drugs than each of the single mutants, revealing a genetic interaction between Msb2 and

Fmk1 in the regulation of the cell wall integrity response. No differences between strains were detected on menadione (oxidative stress) or different concentrations of sodium chloride (osmotic and salt stress) (Figure 19). We conclude that *F. oxysporum* Msb2 is specifically required for hyphal growth under conditions of nutrient limitation or cell wall stress, but not of other types of stresses.

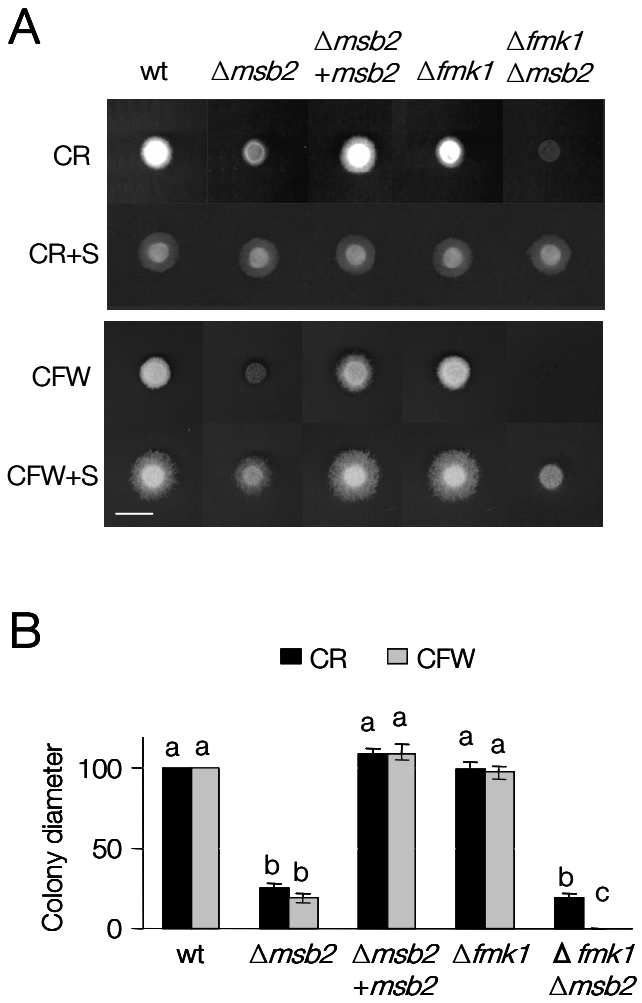


**Figure 18. Msb2 contributes to growth under conditions of cell wall stress.**
(**A**) Colony phenotype of the indicated strains grown on YPD supplemented with 50 μg/ml Congo Red (CR) or 40 μg/ml Calcofluor White (CFW) in the absence or presence of 1 M Sorbitol (S). Scale bar, 1 cm. (**B**) Colony diameter was measured after 5 days and plotted relative to the wild type strain (100%). Bars represent standard errors calculated from 4 plates. Values with the same letter are not significantly different according to Mann-Whitney test ($p \leq 0.05$).

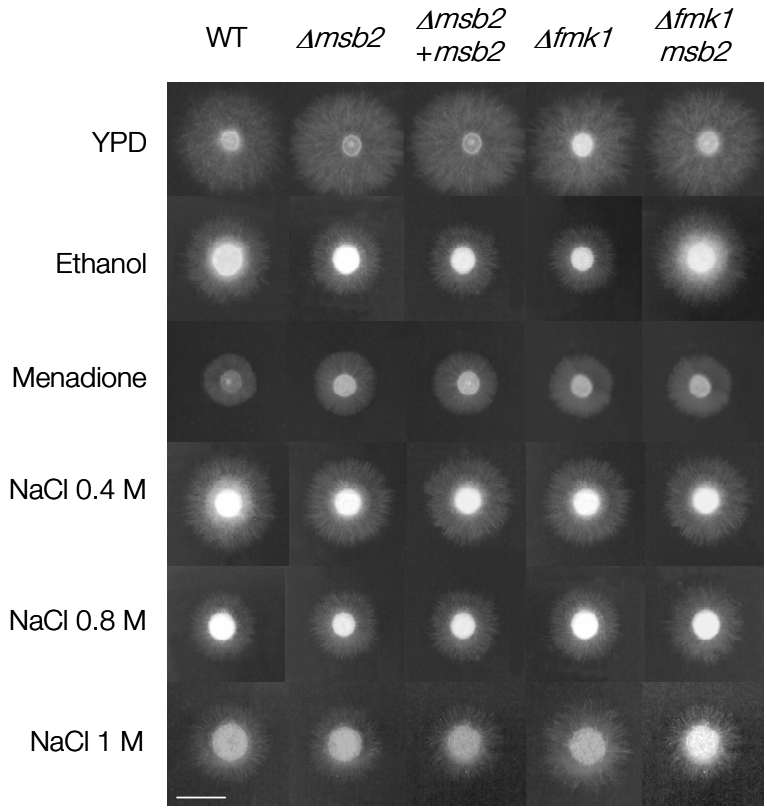


**Figure 19. Msb2 is not required for oxidative and osmotic (salt) stress response.**
Colony phenotype of the indicated strains grown on yeast peptone glucose (YPD) or YPD supplemented with 10 µg/ml menadione or with the indicated concentrations of NaCl. Plates were spot-inoculated with $10^5$ microconidia, incubated 3 days at 28°C and scanned. Scale bar, 1 cm.

## 6. Msb2 is an integral membrane protein

In order to study the subcellular localization of Msb2, we generated an epitope-tagged allele by inserting the HA epitope downstream of amino acid residue 722 located in the extracellular MHD domain (Figure 20A). The msb2-HA allele was intoduced into the Δ*msb2*#62 strain (see Section 5.5 in Materials and Methods). PCR analysis with primer HA-s, specific for the HA epitope nucleotide sequence and reverse primer msb2-3´HA-as confirmed integration of the allele in several transformants (Figure 20B). As shown in Figure 20C, introduction of the tagged *msb2*-HA allele fully restored the wild type growth

phenotype on MM and in the presence of CR and CFW, suggesting that Msb2-HA is functional in *F. oxysporum*.

Western blot analysis with an α-HA antibody of crude cell extracts from cultures of the Δ*msb2*+*msb2-HA* strain detected a robust hybridization signal in the Δ*msb2*+*msb2-HA* strain, but not in the wild type (Figure 21A). Time course analysis revealed that Msb2-HA was continuously expressed during growth of *F. oxysporum* on solid MM (Figure 21B).

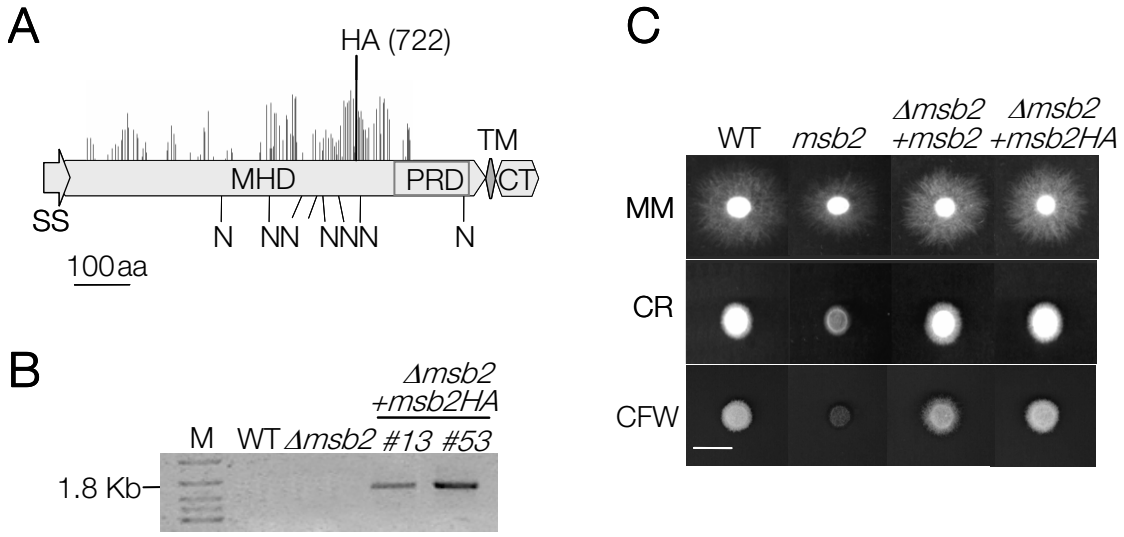


**Figure 20. An HA-tagged version of Msb2 is functional in *F. oxysporum.***
(**A**) Schematic representation of the Msb2-HA protein carrying the HA epitope at amino acid 722 located in the MHD region. Symbols and abbreviations are as in Figure 12. (**B**) PCR amplification of genomic DNA of the indicated strains using forward primer HA-s, specific for the HA epitope nucleotide sequence and reverse primer msb2-3′HA-as. M. Molecular marker. (**C**) Colony phenotype of the indicated strains grown on minimal medium (MM) in the absence or presence of 50 μg/ml Congo Red (CR) or 40 μg/ml Calcofluor White (CFW). Experimental conditions were as in Figure 18.

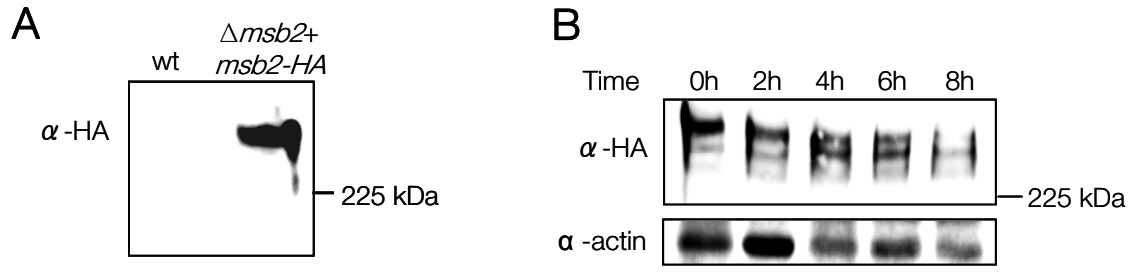


**Figure 21. Msb2-HA is expressed during growth under nutrient-limiting conditions.**
(A) Western blot analysis of cell lysates from the indicated strains germinated 14 hours in potato dextrose broth (PDB) and transferred for 8 additional hours onto MM plates. Samples were separated by SDS PAGE and subjected to immunoblot analysis with monoclonal α-HA antibody. (B) Western blot analysis of cell lysates from the Δ*msb2*+*msb2*-HA strain germinated as described in (A) and transferred onto MM plates for the indicated time periods.

Yeast Msb2 as well as mammalian mucins are heavily glycosylated (Cullen *et al.*, 2004; Silverman *et al.*, 2001). We noted that the apparent molecular mass of *F. oxysporum* Msb2-HA (>250 kDa) was substantially higher than the predicted one (117.5 Kda). Moreover, the presence of multiple hybridizing bands (Figure 21B) suggested that Msb2 may be present in differentially glycosylated isoforms. *F. oxysporum* Msb2 contains eight putative sites for N-linked glycosylation and multiple predicted sites for O-linked glycosylation (see Figure 12). We tested the effect of treating crude cell extracts or fungal mycelia, respectively, with Endo H, an enzyme that cleaves N-linked glycosyl side chains, or with the N-glycosylation inhibitor tunicamycin. None of these treatments however caused a detectable shift in the electrophoretic mobility of Msb2 (Figure 22).

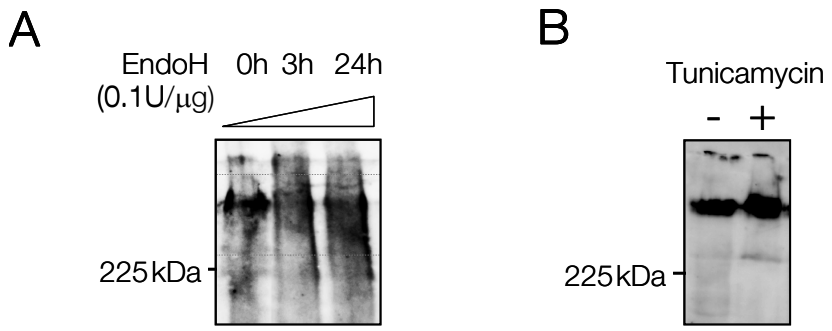


**Figure 22. Treatment with Endo H or tunicamycin does not affect electrophoretic mobility of Msb2.**
(**A**) Cell extracts from the *msb2-HA* strain obtained as described in Figure 21A were treated with 0.1 U/mg Endo H for the indicated time periods and submitted to immunoblot analysis with α-HA antibody. (**B**) Cell extracts were obtained as described in Figure 21A from the *msb2-HA* strain grown in the absence or presence of 25 μg/ml tunicamycin and submitted immunoblot analysis with α-HA antibody.

Western analysis of different subcellular fractions detected almost all of the Msb2 protein in the P14 fraction, a location consistent with the plasma membrane and associated proteins (Figure 23A). Only treatments that disrupt the membrane lipid layer such as SDS/Urea and Triton released the Msb2 protein from the P14 to the soluble fraction, thus confirming the bioinformatic prediction that *F. oxysporum* Msb2 is an integral membrane protein (Figure 23B).

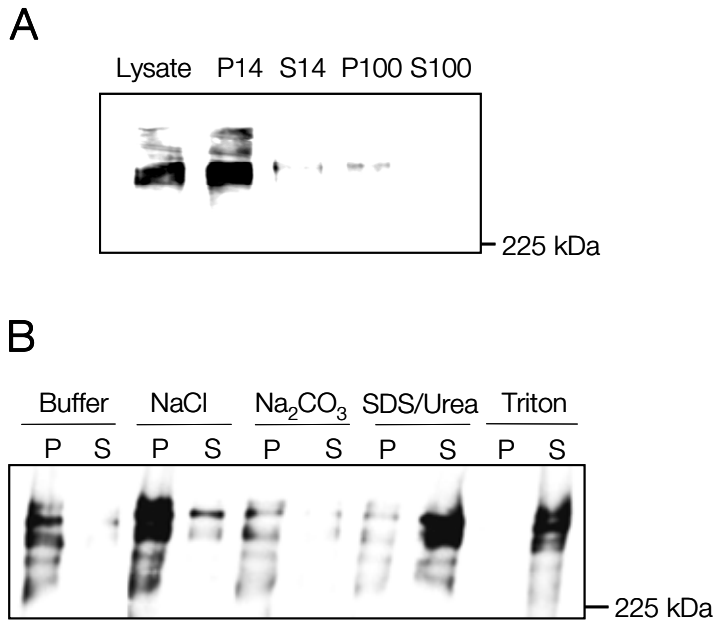


**Figure 23. Msb2 is an integral membrane protein.**
(**A**) Western blot analysis of cell lysates from the the Δ*msb2*+*msb2-HA* strain generated as described in Figure 21A and separated by centrifugation. Lysate, supernatant (S), and pellet (P) fractions are shown. [14] 14,000 x g; [100] 100,000 x g. (**B**) P14 fraction analysis. Treatments were: lysis buffer alone (Buffer) or with 0.5 M NaCl, 100 mM $Na_2CO_3$ at pH 11, 5% SDS / 8 M urea, or 1% Triton.

## 7. Msb2 is shed from the cell surface

While studying the subcellular localization of Msb2, we noted that treatments which solubilize peripheral membrane proteins, such as high salt and sodium bicarbonate, consistently released a fraction of the membrane-bound protein into the supernatant (Figure 23B). This finding suggested that a proportion of the total Msb2 protein may be peripherally associated rather than integral to the membrane. Recent work in *S. cerevisiae* showed that Msb2p is processed by proteolytic cleavage and the extracellular domain is shed from the cells (Vadaie *et al.*, 2008). Using Western blot analysis, we detected a hybridizing band of the expected size in culture supernatants of the Δ*msb2*+*msb2-HA*

strain, but not in the negative controls (wild type and Δ*msb2* strain) (Figure 24A). Shedding of *F. oxysporum* Msb2 was confirmed by colony blot analysis (Pitoniak *et al.*, 2009), revealing a strong hybridizing signal underneath the colonies of the Δ*msb2*+*msb2-HA* strain, but not under those of the wild type and the Δ*msb2* strains (Figure 24B).

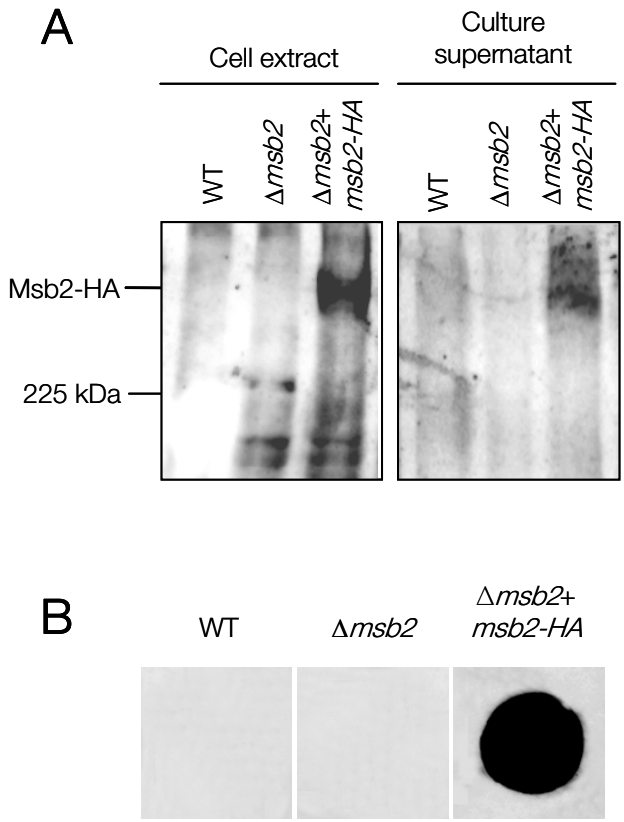


**Figure 24. Msb2 is shed from the cell surface.**
(**A**) Western blot analysis of cell lysates and culture supernatants of the indicated strains with monoclonal α-HA antibody. (**B**) Colony inmunoblot assay. Fresh microconidia of the indicated strains were germinated for 14 h in PDB, harvested and washed twice in distilled water, transferred as a colony onto 0.2 µm pore-filters placed over an MM agar plate overlaid with a nitrocellulose filter, and incubated for 8 h at 28°C. The 0.2 µm pore-filters with the colonies were carefully removed, nitrocellulose membranes were washed with running water and submitted to western blotting with α HA-antibody.

## 8. A version of Msb2 lacking the MHD domain appears to cause a deleterious effect in *F. oxysporum*

The MHD domain of *S. cerevisiae* has been shown to negatively regulate Msb2 activation. To investigate the role of the MHD domain in *F. oxsyporum* Msb2, we generated a protein version named Msb2*HA, in which most of the MHD domain was replaced with the HA epitope (Figure 26). Plasmid *msb2*HA*-pGemT was generated as described in Section 5.6 of Materials and Methods and sequenced with primer ORFas, confirming the correct replacement of amino acid residues 46-721 of the MHD domain with the HA-coding sequence. A 3,6 Kb PCR product was amplified from this plasmid with primer set msb2-5'HA-s/msb2-3'HA-as and co-transformed (2 μg) with the amplified phleomycin resistance cassette (1.5 μg) into the Δ*msb2#62* mutant. A total of 24 transformants were obtained from two independent transformation events (Table 15), which were routinely transferred to a PDA plate supplemented with phleomycin and allowed to grow for 2 days. At this stage a replica plate was generated by transferring approximately a small piece of colony to a new PDA-phleomycin plate, and the remaining of the colony was used for genomic DNA extraction andy PCR analysis with primer set msb2-nest3/msb2-ORFas. Twelve transformants showed the presence of a 1.8 kb band corresponding to the *msb2*HA* allele (see one representative transformant in Figure 25), indicating a frequency of co-transformation of approximately 50%, in line with previous results obtained in our laboratory. The presence of a 4.5 kb PCR product in some of the transformants corresponds to the *msb2-hph* knockout construct present in the Δ*msb2#62* mutant (Figure 25).

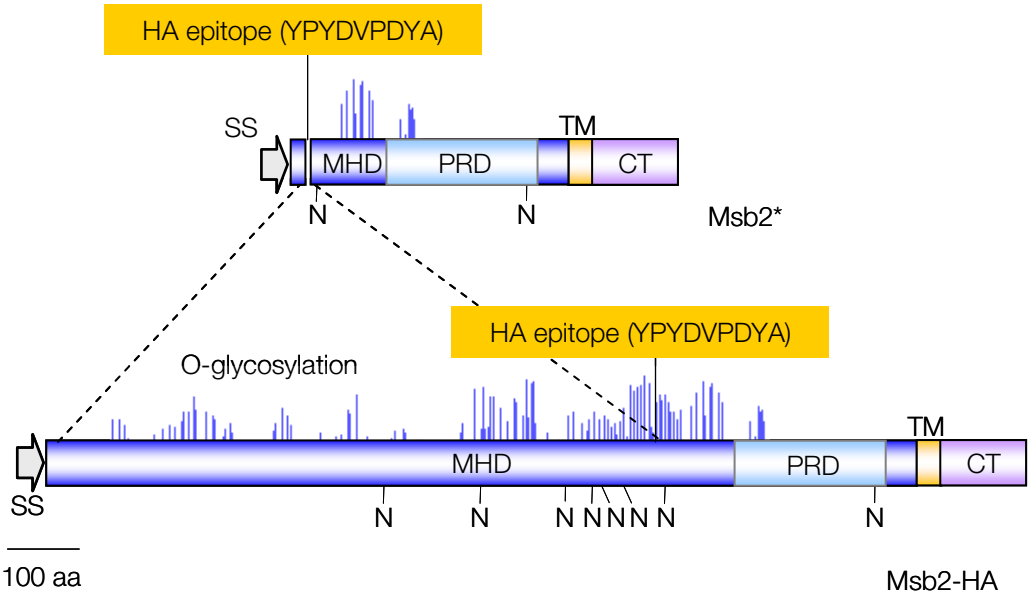


**Figure 25. Schematic representation of the Msb2* protein**
Most of the MHD domain of Msb2-HA was replaced with the HA epitope to generate the shorter Msb2* protein. Symbols and abbreviations are as in Figure 12.

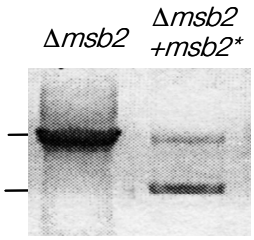


**Figure 26. PCR analysis of *Δmsb2 +msb2*HA* strains.**
Amplification of genomic DNA of the indicated strains using forward primer nest3 and msb2-ORF-as to differentiate the *Δmsb2* allele from that corresponding to the *msb2*HA* allele introduced by cotransformation.

The 12 identified cotransformants were submitted to monoconidial purification, and isolated colonies were transferred to liquid PDB for routine propagation. After 7 day

incubation at 28°C, we noted that 5 out of the 12 cultures showed none or very low microconidia production and unusual mycelial development (Table 15). Mycelial aggregation is sometimes observed as an artefact if too much residual agar is inoculated with the colony from the single-sporing plates. However, we observed similar phenotypes following inoculation of other colonies from the single-sporing plates. Unexpectedly, PCR analysis of DNA extracted from PDB cultures of the 7 transformants showing normal growth, now revealed absence of the *msb2*HA* allele, which had been detected at the previous stage (data not shown). One explanation to this phenomenon is that *msb2*HA* nuclei may have been represented at a low rate with respect to Δ*msb2#62* nuclei in the original PDA-plate-grown culture. Alternatively, it is possible that the *msb2*HA* allele may confer a disadvantage during monoconidial isolation and/or passage through submerged culture. This hypothesis was supported by the fact that the *msb2*HA* allele was detected in DNA from the remaining 5 cultures, all of which showed a defect in development during submerged culture. In order to examine expression of the Msb2*HA protein, the abnormally shaped mycelium from these 5 cultures was used for protein extraction. However, it was only possible to obtain sufficient protein for Western analysis from two of the transformants, *msb2*HA#4* and *msb2*HA#5*. The α-HA antibody detected the presence in both strains of several hybridising bands migrating slightly above the 52 KDa marker (close to the predicted molecular weight of 48.9 kDa of the Msb2*HA protein) (Figure 27). No hybridizing signal was detected in the Δ*msb2#62* strain used as a negative control. Conidia from the *msb2*HA#4* and *msb2*HA#5* strains were collected and stored at -80°C. Upon inoculation from these -80°C stocks into PDB, we observed even a more extreme growth defect than previously found for the two strains, with no conidial production and formation of a white mycelial aggregate (Figure 28A). Western analysis confirmed that Msb2*HA was still being expressed in these strains (Figure 28B). Due to lack of microconidia, it was not possible to stably store these strains at -80°C. Based on these preliminary results, we put forward the hypothesis that Msb2*HA may cause a dominant deleterious effect on fungal growth.

**Table 15. Summary of analysis of Δ*msb2* + *msb2*HA* transformants.**

| Analysis step: | | DNA analysis before single sporing | Single sporing and propagation in PDB | DNA and Protein analysis after single sporing | |
|---|---|---|---|---|---|
| Trans-formation event | Number of trans-formants | Transformants with *msb2*HA* PCR band | Conidia/mycelium production in submerged culture | Transformants with *msb2*HA* PCR band | Western analysis of Msb2*HA expression |
| #1 | 14 | 7 | 7 Apparently normal | 0 | N/A |
| #2 | 10 | 5 | 2 Very low conidia production and mycelial aggregates | 2 | 2 |
| | | | 3 No conidia and sparce ball-like mycelium | Insufficient material to obtain DNA or protein | |
| TOTAL | 24 | 12 | | | |

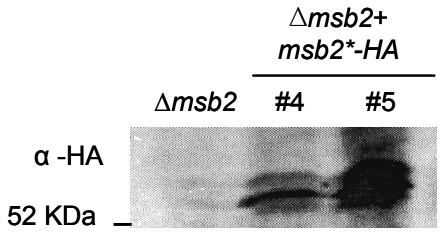


**Figure 27. Western blot analysis of Δ*msb2*+*msb2*HA* strains**
The indicated strains were submitted to monoconidial purification, and isolated colonies were transferred to liquid PDB and incubated for 7 days. Mycelia were collected and obtained cell extracts were subjected to immunoblot analysis with monoclonal α-HA antibody.

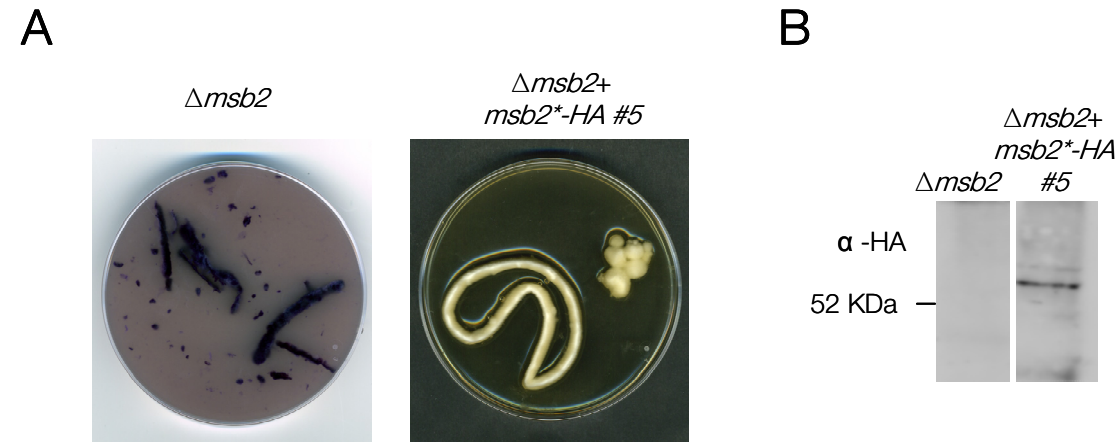


**Figure 28. Growth phenotype of Δ*msb2*+*msb2*HA* strains.**
(A) Conidia from the indicated strains stored at -80°C were inoculated into PDB and 5-day-old cultures were scanned. (B) Mycelia were used for protein extraction and immunoblot analysis with monoclonal α-HA antibody.

## 9. Msb2 regulates phosphorylation levels of Fmk1

We previously observed that the Δ*fmk1* and Δ*msb2* mutants shared similar phenotypes on solid nutrient-limiting medium (Figure 16). We therefore used these growth conditions to investigate the hypothesis that Msb2 functions upstream of the Pathogenicity MAPK cascade. Western blot analysis with commercial α-phospho-p44/42 MAPK antibody detected a rapid and transient increase of Fmk1 phosphorylation levels in the wild type strain, upon transfer from submerged culture to solid minimal medium (Figure 29A). This increase was even more sustained in the presence of the cell wall targeting compound CR. Interestingly, Fmk1 was underphosphorylated in two independent Δ*msb2* mutants, but not in the complemented strain, 30 min after transfer to solid medium (Figure 29B), suggesting that Msb2 is required for maintaining full levels of phosphorylation of Fmk1 during growth on solid nutrient-limited substrate.

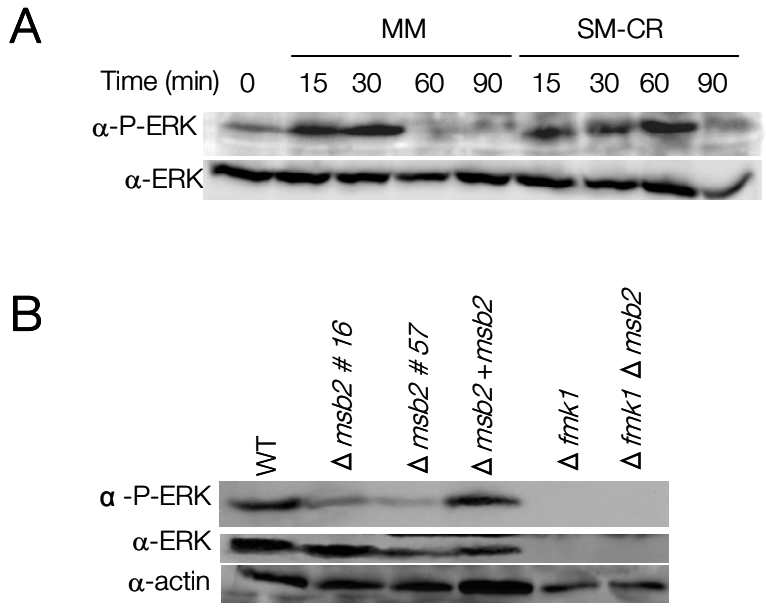


**Figure 29. Msb2 controls phosphorylation of the MAPK Fmk1.**
(**A**) Transfer to solid medium produces a transient increase in Fmk1 phosphorylation. Total protein extracts from the wild type strain germinated as described in Figure 21A and transferred onto plates containing MM or MM with 50 μg/ml Congo Red (CR) for the indicated time periods were submitted to immunoblot analysis with anti-phospho-p44/42 MAPK antibody (α-P-ERK), or anti-p44/p42 MAPK antibody (α-ERK) as a loading control. (**B**) Msb2 is required for full levels of Fmk1 phosphorylation. Total protein extracts from the indicated strains transferred for 30 min onto MM plates were submitted to immunoblot analysis as described in (A). Actin protein was detected using a α-*S. cerevisiae*-actin monoclonal antibody.

## 10. Msb2 controls expression of Fmk1-regulated effector genes

In *S. cerevisiae*, *msb2* expression is regulated by the FG pathway. We examined whether Fmk1 also regulates expression of *msb2* in *F. oxysporum*. Quantitative real time PCR analysis revealed that *msb2* transcript levels in the Δ*fmk1* mutant were not significantly different from those of the wild type strain, suggesting that Msb2 itself is not a transcriptional target of the Fmk1 MAPK cascade (Figure 30). We noted that expression

of *msb2* in the complemented strain was higher than in the wild type, possibly due to a positional effect of the ectopic integration site of the complementing allele.

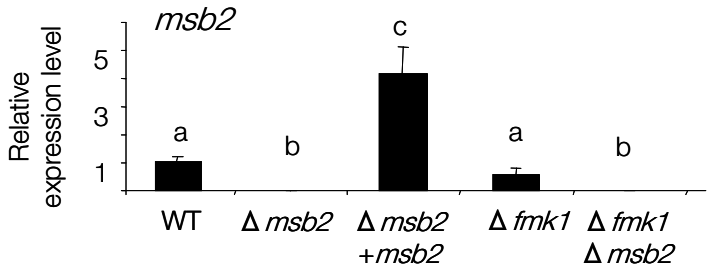


**Figure 30. Fmk1 regulates *msb2* expression.**
mRNA abundance of the *msb2* gene was measured upon transfer of the indicated strains to MM plates for 6 hours, using quantitative real time PCR. Relative expression levels represent mean ΔCt values normalized to *actin* gene expression levels and relative to expression values in the wild type strain. Bars represent standard errors calculated from three biological replicates. Different small letters represent significant differences between strains ($p \leq 0.05$).

To further investigate the possible role of Msb2 as an upstream component of Fmk1, we examined expression of *fpr1,* a gene encoding a secreted protein with an SCP-PR-1-like domain that was previously shown by northern blot analysis to be transcriptionally regulated by the Fmk1 MAPK cascade (Prados-Rosales and Di Pietro, unpublished). In agreement with the previous results, *fpr1* transcript levels were significantly lower in the Δ*fmk1* mutant, showing a five-fold reducion compared to the wild type strain (Figure 31). Interestingly, the Δ*msb2* mutant had ten-fold lower *fpr1* transcript levels than the wild type, while in the Δ*fmk1*Δ*msb2* double mutant had a hundred-fold lower levels (Figure 31). Transcript levels of the *chsV* gene, which encodes a class V chitin synthase required for pathogenicity of *F. oxysporum* (Madrid *et al*., 2003), were only significantly reduced in the Δ*msb2* and Δ*fmk1*Δ*msb2* mutants, showing a synergistic effect in the case of the double mutant (Figure 31). By contrast, the *chs3* gene encoding a different class of chitin synthase did not show significant differences in transcript levels between the different strains (Figure 31). Δ*fmk1* and Δ*msb2* mutants showed significantly reduced levels of

expression of the *gas1* gene, encoding a putative β-1,3-glucanosyltransferase essential for pathogenicity of *F. oxysporum*. Interestingly, *gas1* transcript levels were significantly lower in the Δ*fmk1*Δ*msb2* than in the single mutants. These results suggest that Msb2 controls expression of Fmk1-regulated effector genes.

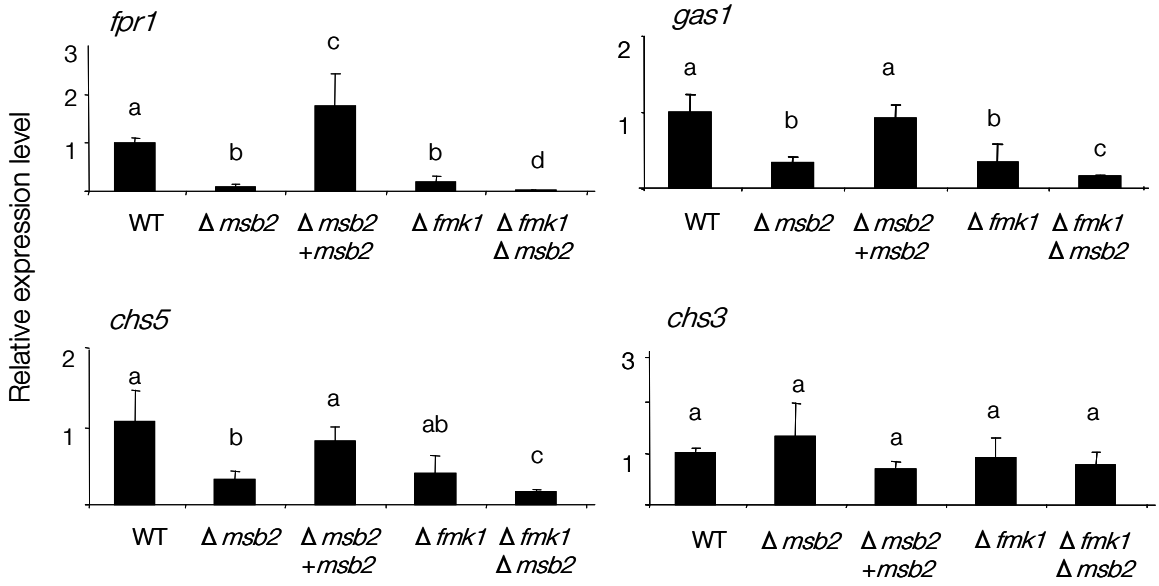


**Figure 31. Msb2 and Fmk1 regulate expression of the *fpr1*, *chsV* and *gas1* genes.**
mRNA abundance of the indicated genes was measured upon transfer of the indicated strains to MM plates for 6 hours, using quantitative real time PCR. Relative expression levels represent mean ΔCt values normalized to *actin* gene expression levels and relative to expression values in the wild type strain. Bars represent standard errors calculated from three biological replicates. Different small letters represent significant differences between strains ($p \leq 0.05$).

## 11. Msb2 controls Fmk1-dependent virulence functions

We investigated the role of Msb2 in controlling virulence-associated functions upstream of Fmk1 by systematically comparing phenotypes in the Δ*fmk1*, Δ*msb2* and Δ*fmk1*Δ*msb2* mutants. One of these functions is vegetative hyphal fusion (Prados Rosales and Di Pietro, 2008). Hyphal fusion in submerged culture of the wild type strain leads to the production of mycelial networks that are macroscopically visible as aggregates (Figure

32). By contrast, the Δ*fmk1* mutants failed to undergo hyphal fusion and to form aggregates as previously described (Prados Rosales and Di Pietro, 2008). Two independent Δ*msb2* mutants produced aggregates similar to the wild type strain, indicating that they were still competent for vegetative hyphal fusion. These results were corroborated by microscopic examination of the germlings of different Δ*msb2* strains, revealing hyphal fusion bridges and germ tube fusion events at frequencies similar to those of the wild type strain, whereas no such events were observed in the Δ*fmk1* and Δ*fmk1*Δ*msb2* mutants.

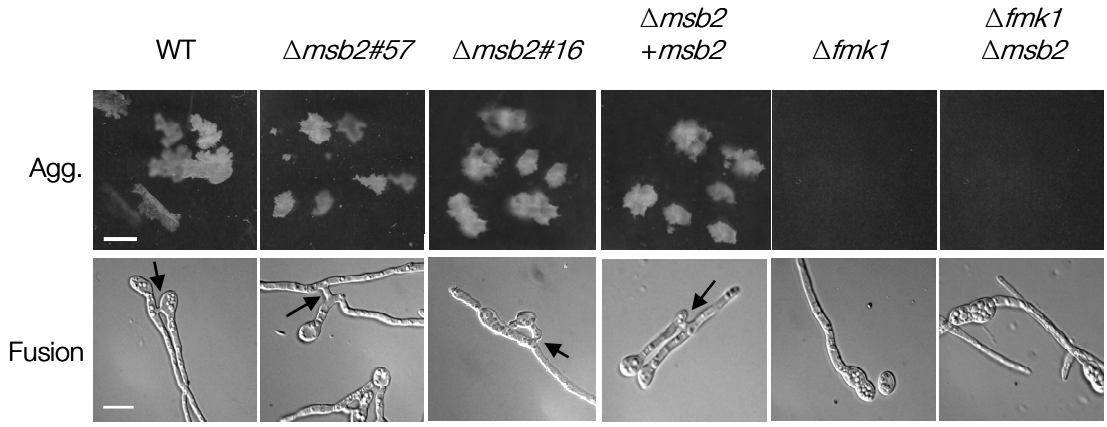


**Figure 32. Msb2 is not required for hyphal agglutination and vegetative hyphal fusion.** Strains were grown overnight in PDB diluted 1:50 with water and supplemented with 20 mM glutamic acid. Upper: The fungal culture was transferred to a Petri dish and photographed. Note the presence of mycelial aggregates (agg.) in the wild type and Δ*msb2* strains. Bar 1 cm. Lower: Fungal cultures were observed in a Leica DMR microscope using the Nomarsky technique. Note the presence of vegetative fusions between hyphae and microconidial germ tubes of the wild type and Δ*msb2* strains. Bar 10 μm.

The Δ*fmk1* mutant is impaired in multiple functions associated with invasive growth on plant tissue. Firstly, Δ*fmk1* mutants have dramatically reduced extracellular pectinolytic activity during growth on plates containing polygalacturonic acid (PGA), as shown by a lack of clear halo production (Delgado-Jarana *et al.*, 2005) (Figure 33A). Two independent

Δ*msb2* mutants showed intermediate phenotypes with a partial reduction in pectinolytic activity (Figure 33A). Secondly, the Δ*fmk1* mutant is impaired in penetration of cellophane membranes (Prados Rosales and Di Pietro, 2008). Interestingly, the Δ*msb2* strains were also reduced in their capacity to penetrate cellophane membranes, although they still retained a low invasive ability in contrast to the Δ*fmk1* and Δ*fmk1*Δ*msb2* mutants (Figure 33B).

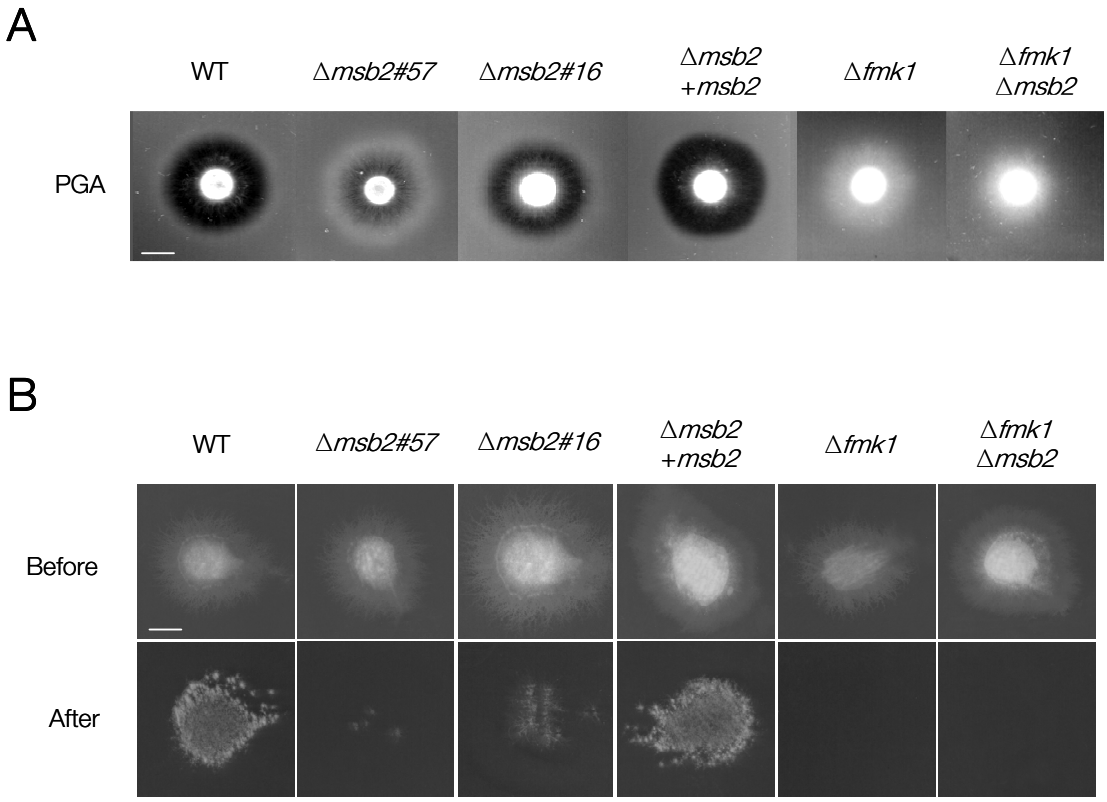


**Figure 33. Msb2 contributes to extracellular pectinolytic activity and penetration of cellophane membranes.**
Microconidial suspensions of the indicated strains were spot-inoculated on different substrates for invasive growth assays. (**A**) Extracellular pectinolytic activity on plates containing polygalacturonic acid (PGA) was visualized as a contrasting halo underneath the fungal colony. (**B**) To determine penetration of cellophane membranes, colonies were grown for 4 days on a plate with minimal medium covered by a cellophane membrane (before), then the cellophane with the colony was removed and plates were incubated for an additional day (after). Scale bar 1 cm.

The Δ*fmk1* mutant is impaired in invasion and colonization of living fruit tissue (Di Pietro *et al.*, 2001; Rispail and Di Pietro, 2009) (Figure 34). Again, the Δ*msb2* mutants had an intermediate phenotype, showing a reduced capacity to grow invasively on tomato fruits or apple slices (Figure 34). All the virulence-related functions were completely restored in the Δ*msb2*+*msb2* complemented strain.

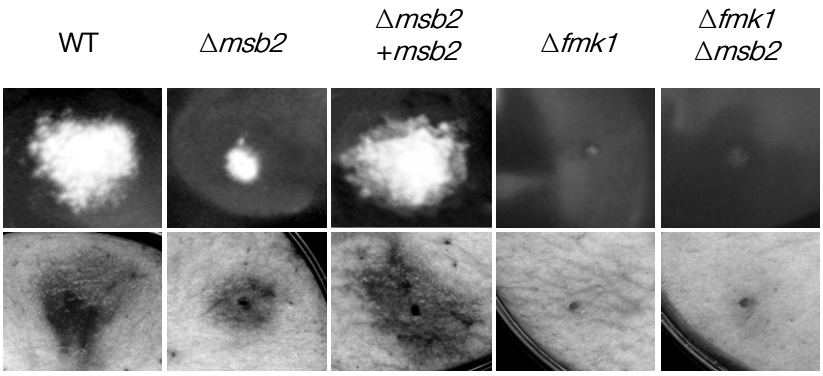


**Figure 34. Msb2 contributes to invasive growth on living fruit tissue.**
Tomato (upper) and apple fruits (lower) were inoculated with $5 \times 10^4$ microconidia of the indicated strains and incubated at 28ºC for 4 days.

To test whether Msb2 plays a role in plant pathogenicity, we first monitored the presence of the protein during early stages of infection of tomato plants in two independent *F. oxysporum* strains carrying an HA-tagged *msb2* allele. Western blot analysis of total cell extracts detected a robust signal in the Δ*msb2*+*msb2-HA* strains, but not in the negative controls (wild type, Δ*msb2*, uninoculated plants), suggesting that Msb2 is expressed by *F. oxysporum* during early stages of infection (Figure 35).

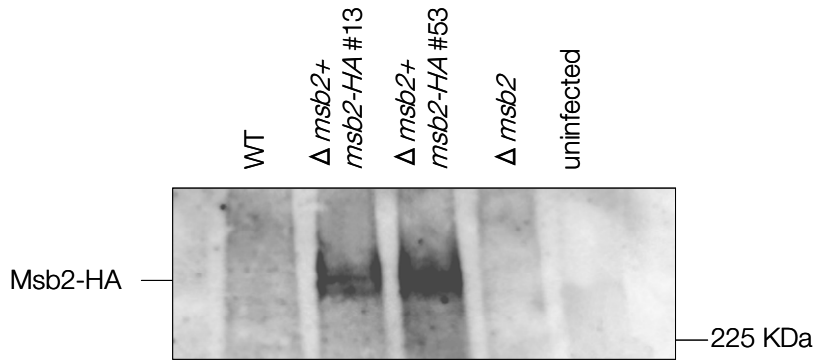


**Figure 35. Msb2 is expressed during early stages of infection.**
Total protein extracts obtained from tomato roots 48 hours after inoculation with microconidia of the indicated strains or from uninoculated roots were submitted to immunoblot analysis with α HA-antibody.

Tomato plants inoculated with the wild type strain showed a continuous increase in wilt disease symptoms, and most of the plants were dead 20 days after inoculation (Figure 36). As reported previously (Di Pietro *et al.*, 2001), plants inoculated with the Δ*fmk1* mutant failed to develop disease symptoms. Three independent Δ*msb2* mutants were significantly reduced in virulence, although disease ratings were higher than those of the Δ*fmk1* strain (two representative mutants are shown in Figure 36). Complementation with the wild type *msb2* gene or the *msb2-HA* allele fully restored virulence. The Δ*fmk1*Δ*msb2* double mutant had the same phenotype as the Δ*fmk1* single mutant. These results indicate that Msb2 controls Fmk1-regulated invasive growth functions and virulence of *F. oxysporum* on tomato plants.

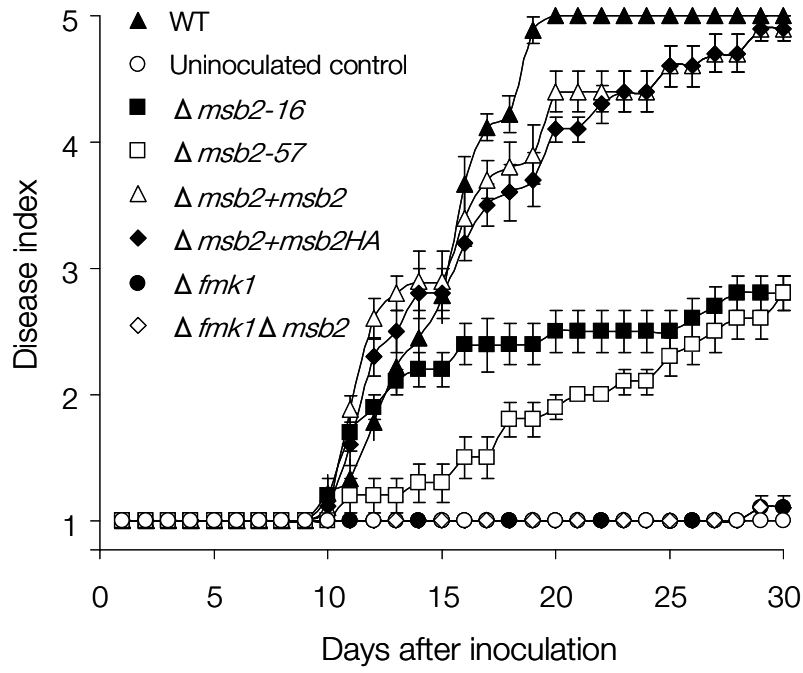


**Figure 36. Msb2 is required for virulence of *F. oxysporum* on tomato plants.**
Incidence of *Fusarium* wilt on tomato plants (cultivar Monica) inoculated with the indicated strains. Severity of disease symptoms was recorded at different times after inoculation, using an index ranging from 1 (healthy plant) to 5 (dead plant). Error bars represent standard deviations calculated from 20 plants.

## 12. The *F. oxysporum* Sho1 protein

The *F. oxysporum sho1* gene was identified through BLASTP search of the complete genome database of *F. oxysporum* (accession no. *FOXG_06120.2*). It consists of a 933-bp open reading frame encoding a predicted 311-amino-acid protein homologous to Sho1 proteins from *S. cerevisiae* (28.0 % identity), *C. albicans* (27.3% identity), *U. maydis* (29.2% sequence identity), *A. gossypii* (30.6%), *A. fumigatus* (54.2 % identity), *M. grisea* (62.3 % identity), *N. crassa* (55.5 % identity) and *F. graminearum* (93.6 % identity). SMART analysis (http://smart.embl-heidelberg.de/) revealed a conserved domain architecture between Sho1 from *F. oxysporum* and fungal orthologous from all these species (Figure 37 and Figure 39), including four putative transmembrane domains (amino

acids 22 to 44, 64 to 83, 88 to 110, and 123 to 145) near the N terminus, a linker domain between these domains, and an SH3 domain at the C terminus (amino acids 254 to 310) that in yeast is believed to interact with the Pbs2p MAPK kinase (Raitt *et al.*, 2000). As expected, sequence conservation was highest in the transmembrane regions.

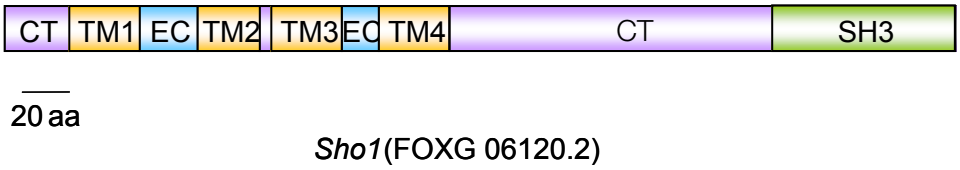


**Figure 37. Predicted domain architecture of the Sho1 protein**
Shown are the cytoplasmic domain (CT), the four the transmembrane domains (TM), the short extracelular loops (EC) and the SH3 domain. aa: amino acids.

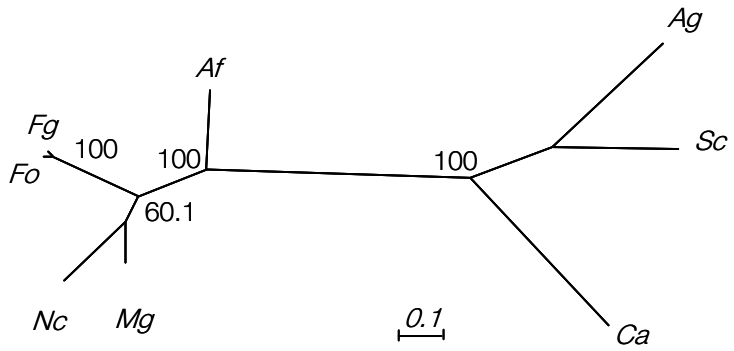


**Figure 38. Phylogram of Sho1 proteins from ascomycetes.**
Shown are putative orthologues of Sho1 in the indicated species. Percentage bootstrap values obtained from 1000 replicates are indicated at the nodes. Scale bar indicates the relative length of each branch. *S. cerevisiae (Sc), C. albicans (Ca), A. gossypii (Ag), A. fumigatus (Af), F. graminearum (Fg), F. oxysporum (Fo), M. grisea (Mg)* and *N. crassa (Nc)*.

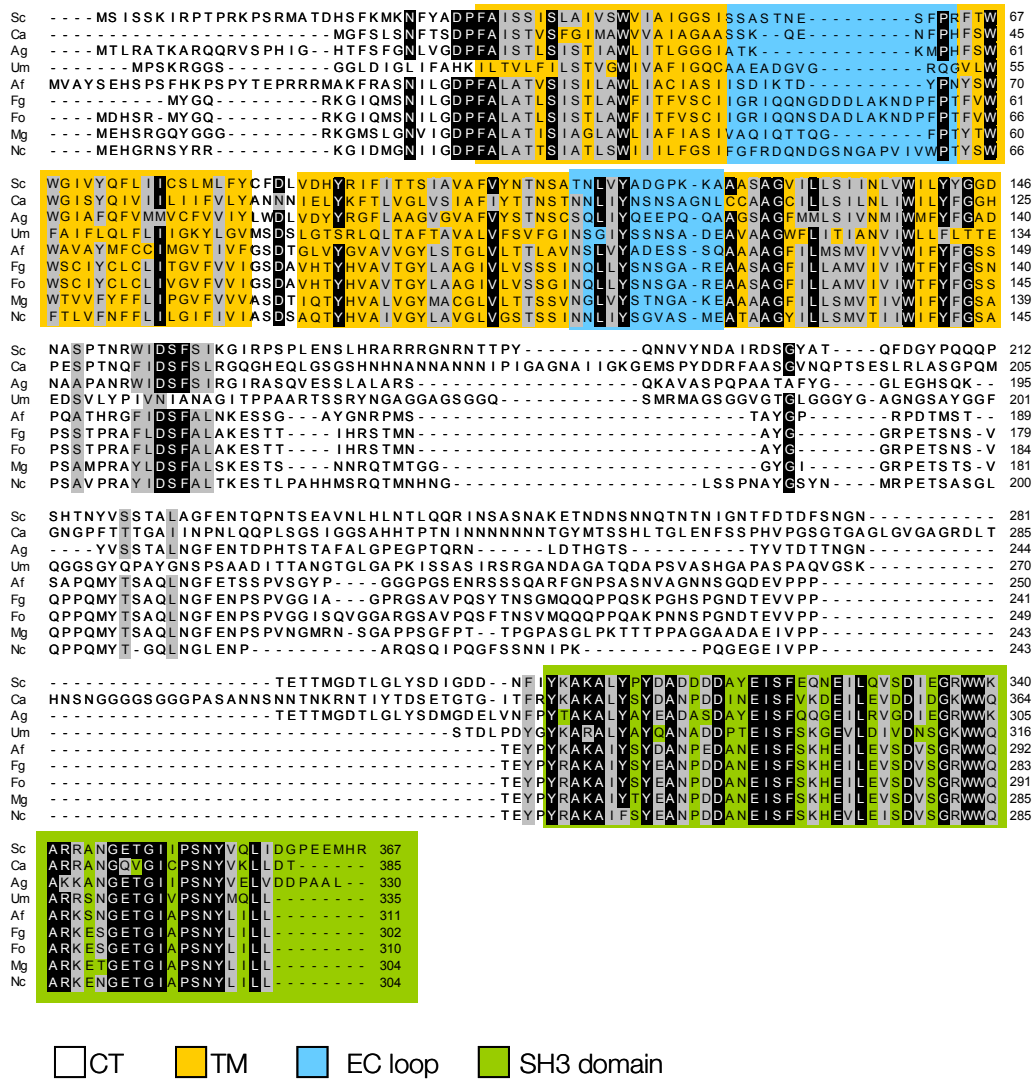


**Figure 39. Sequence alignment of fungal Sho1 proteins.**
The alignment shows the predicted amino acid sequences of Sho1 orthologues from *S. cerevisiae* (Sc), *C. albicans* (Ca), *A. gossypii* (Ag), *U. maydis* (Um), *A. fumigatus* (Af), *F. graminearum* (Fg), *F. oxysporum* (Fo), *M. grisea* (Mg) and *N. crassa* (Nc). Highly conserved residues are shaded in black, moderately conserved residues are shaded in grey. Cytoplasmic (CT), transmembrane (TM), extracelular (EC) regions and the SH3 domain are highlighted in light yellow, dark yellow, blue and green, respectively.

## 13. Deletion of *sho1* in *F. oxysporum.*

To examine the function of Sho1 in *F. oxysporum*, we generated a *sho1* deletion construct by replacing most of the ORF of the *F. oxysporum sho1* gene with the hygromycin *or* the phleomycin resistance cassette (see Section 5.7 in Materials and Methods and Figure 40A). We also deleted the gene in a *msb2* genetic background to analyze the possible genetic interactions between *sho1* and *msb2* (Section 5.7). Transformation of the wild type and Δ*msb2#57* with the *sho1-hph* and *sho1-phleo* constructs, respectively, yielded 11 and 10 transformants (Figure 40B). PCR analysis with primers sho1-for3 and sho1-rev2 designed to amplify the *sho1* locus both in wild type and mutant strains (Figure 40A) revealed that one Δ*msb2+sho1-phleo* transformant and two Δ*msb2+sho1-hph* transformants produced a 5.1 Kb and 5.6 Kb PCR amplicon, respectively, corresponding to the interrupted alleles, but not the 3.2 kb wild type band (Figure 40B). Additionally, primers designed to amplify the predicted *sho1* replacement only in case of homologous recombination produced a 2.8 Kb PCR band in these three mutants but not in the wild type or ectopic transformants (Figure 40C), thus confirming them as Δ*sho1* strains.

## 14. Sho1 contributes to hyphal growth on nutrient limiting solid medium

We performed preliminary experiments to test the role of Sho1 in vegetative hyphal growth on nutrient-limiting solid minimal medium (MM). On MM, colonies of the Δ*sho1* mutants displayed a slower growth rate and developed less aerial hyphae than the wild type strain or the ectopic strain, similar to the Δ*fmk1,* Δ*msb2* and Δ*msb2*Δ*sho1* strains (Figure 41). Deletion of *sho1* in a *msb2* background did not result in enhanced sensititivity to the limiting nutrient conditions of the plates, suggesting that the two proteins have redundant functions for this particular trait (Figure 41).

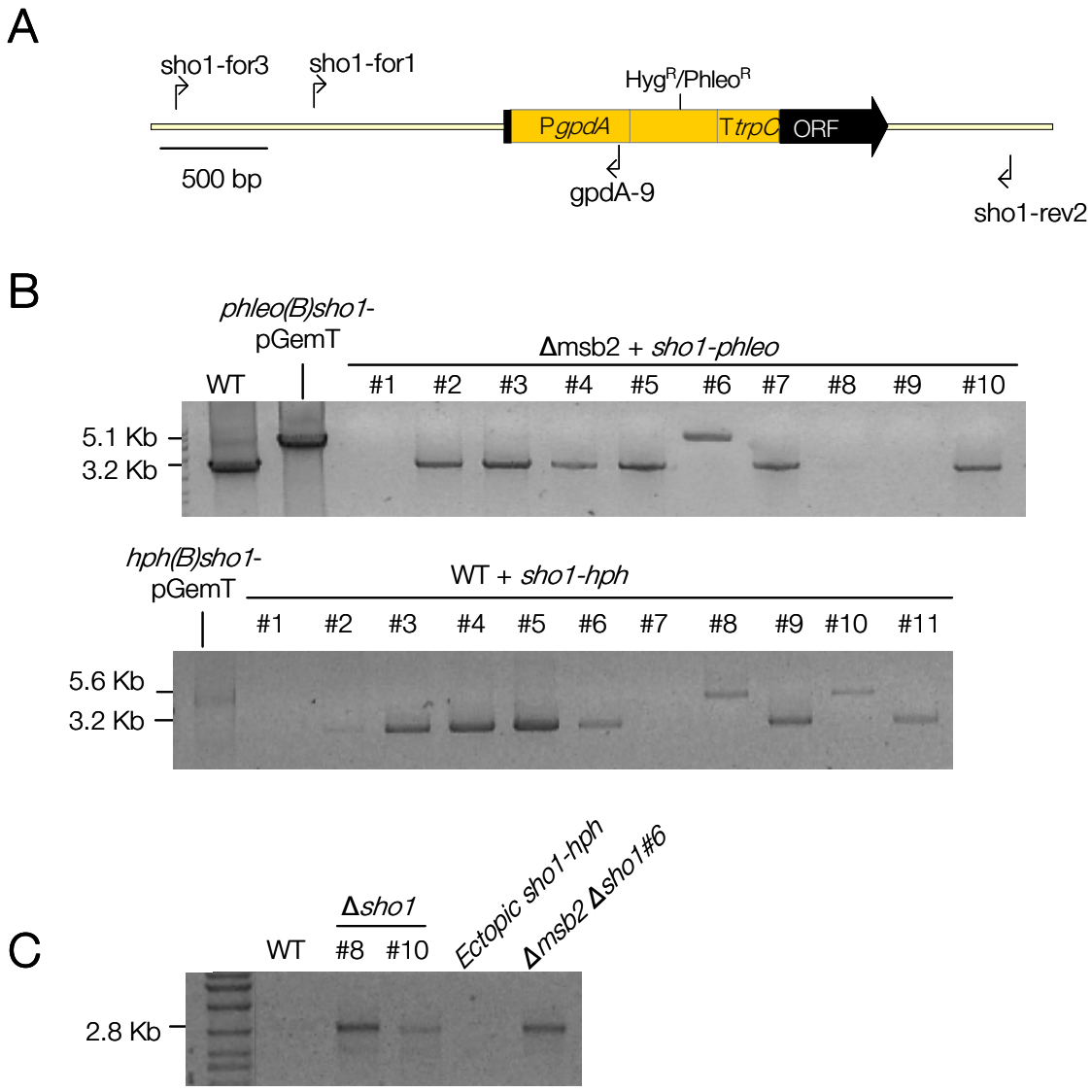


**Figure 40. Targeted disruption of the *F. oxysporum sho1* gene.**
(**A**) Physical maps of the *sho1* locus and the gene replacement construct obtained by PCR amplification from plasmids *hph(B)sho1*-pGemt and *phleo(B)sho1*-pGemT (Δ*sho1* allele). Relative positions of the primers used for PCR analysis of transformants are indicated. Scale bar, 500 base pairs. (**B**) PCR amplification of genomic DNA of the indicated mutant strains and plasmids using primers sho1-for3 and sho1-rev2 indicated in (A) to differentiate the wild type PCR product from that corresponding to the Δ*sho1* allele. (**C**) PCR amplification of genomic DNA of the indicated strains from (B) using forward primer sho1-for3 and reverse primer gpdA-9, specific of the *gpdA* promoter to confirm homologous insertion of the disruption construct at the *sho1* locus.

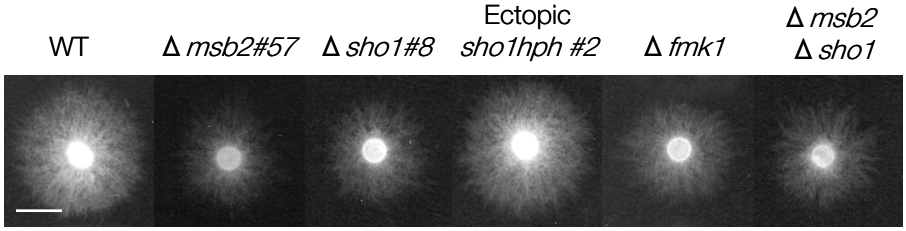


**Figure 41. Sho1 contributes to hyphal growth under conditions of nutrient limitation.** Colony phenotype of the indicated strains grown on minimal medium (MM). Plates were spot-inoculated with $10^5$ microconidia, incubated 3 days at 28°C and scanned. Scale bar, 1 cm.

## 15. Δ*sho1* mutants are affected by cell wall stress, similarly to *msb2* mutants

To analyze the role of *sho1* in response to cell wall stress, we performed a preliminary growth assay in the presence of Congo Red (Figure 42). It is worth noting the more sensitive phenotype observed for the Δ*msb2*#57 and Δ*fmk1* strains in this particular experiment, as compared to previous experiments (Figure 18A). This suggests that the effective concentration of CR in this isolated assay may have been higher than normal. Δ*sho1* and Δ*msb2*Δ*sho1* strains showed similar sensitivity to CR as the Δ*msb2*#57 mutant. The three mutants were more sensitive than the wild type strain, ectopic transformant and Δ*fmk1* strain. Interestingly, Figure 42 highlights that Fmk1 is indeed required for full growth under these conditions, as previously suggested by the additive growth defect observed in the Δ*fmk1*Δ*msb2* strain on CR and CFW (Figure 18). Addition of 1M Sorbitol partially rescued the growth inhibition by CR in all strains. The assay did not reveal detectable differences in sensitivity to CR between the single *msb2* and *sho1* mutants and the double *msb2sho1* mutant, suggesting partially redundant roles for the two proteins. However it will be necessary to test these strains in additional replicate assays to evaluate the statistical significance of these results. We conclude that *F. oxysporum* Sho1 contributes to hyphal growth under conditions of cell wall stress, similarly to Msb2.

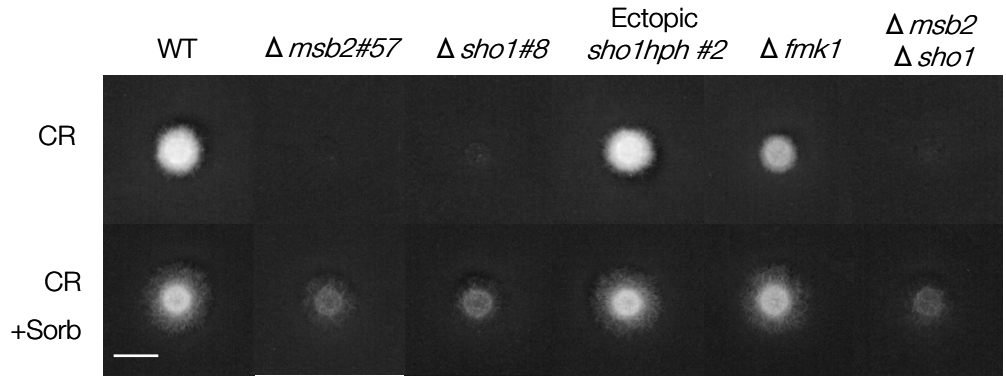


**Figure 42. Sho1 is required for growth under conditions of cell wall stress.**
Colony phenotype of the indicated strains grown on YPD supplemented with 50 μg/ml Congo Red (CR) in the absence or presence of 1 M Sorbitol (S). Scale bar, 1 cm.

## 16. Sho1 controls expression of Fmk1-regulated effector genes

We examined whether Msb2 and Fmk1 regulate expression levels of *sho1* in *F. oxysporum*. Quantitative real time PCR analysis revealed that this was not the case (Figure 43). The possible role of Sho1 as an upstream component of Fmk1 was examined by analyzing expression of *fpr1, gas1, chs5* and *chs3*. Interestingly, similar to the Δ*msb2* mutant, the Δ*sho1* strain had siginificantly reduced *fpr1* transcript levels compared to the wild type, and these levels were even more reduced in the Δ*msb2*Δ*sho1* double mutant to levels similar to those of the Δ*fmk1*Δ*msb2* double mutant (Figure 43). Similar results were observed for transcript levels of the *chsV* and *gas1* genes. By contrast, no significant differences between strains were detected for *chs3* gene.

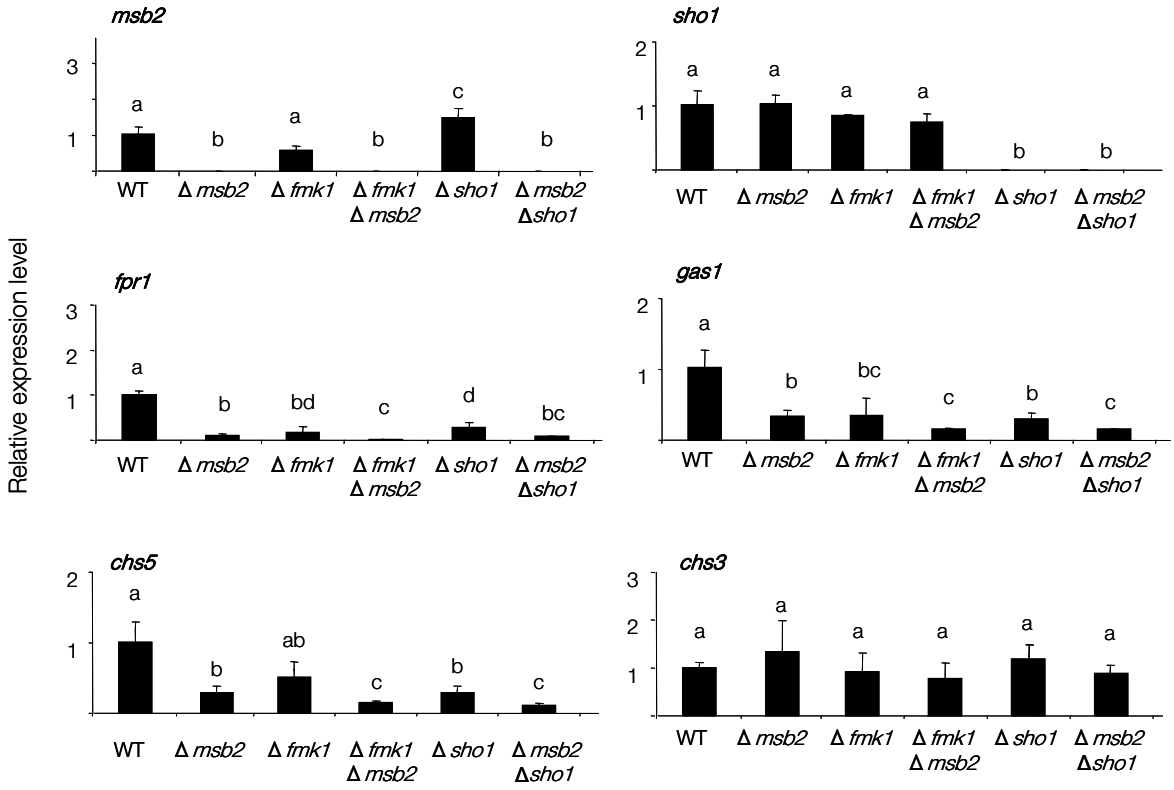


**Figure 43. Sho1 regulate expression of the *fpr1*, *chsV* and *gas1* genes.**
mRNA abundance of the indicated genes was measured upon transfer of the indicated strains to MM plates for 6 hours, using quantitative real time PCR. Relative expression levels represent mean ΔCt values normalized to *actin* gene expression levels and relative to expression values in the wild type strain. Bars represent standard errors calculated from three biological replicates. Different small letters represent significant differences between strains ($p \leq 0.05$).

## 17. Sho1 controls Fmk1-dependent virulence functions

As mentioned before, Δ*fmk1* mutants have significantly reduced extracellular pectinolytic activity during growth on plates containing polygalacturonic acid (PGA) (Delgado-Jarana *et al.*, 2005) and Δ*msb2* mutants showed an intermediate phenotype with a partial reduction in pectinolytic activity (Figure 33A). Preliminary data indicated that a Δ*sho1* mutant had a more reduced pectinolytic activity than Δ*msb2* and this phenotype was slightly more pronounced in the double Δ*msb2*Δ*sho1* mutant. Because the reduction in pectinolytic activity of the Δ*msb2*Δ*sho1* mutant was not as dramatic as that in the Δ*fmk1*

strain, we speculate that additional signalling components must contribute to regulation of this response upstream of Fmk1.

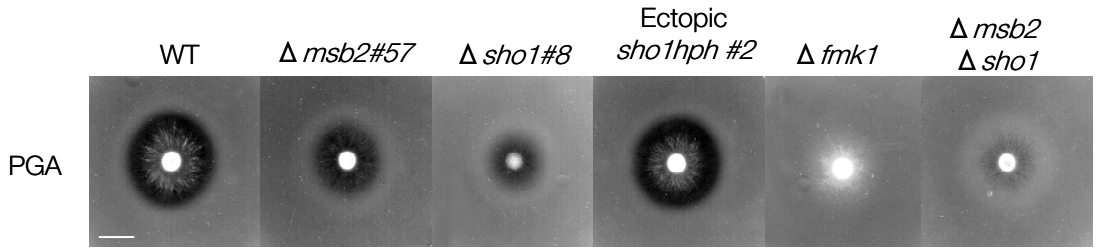


**Figure 44. Sho1 contributes to extracellular pectinolytic activity.**
Microconidial suspensions of the indicated strains were spot-inoculated on polygalacturonic acid (PGA) plates. Extracellular pectinolytic activity was visualized as a contrasting halo underneath the fungal colony. Scale bar, 1 cm.

We also tested the capacity of the Δ*sho1* strains for invasive growth on fruit tissue. The single Δ*sho1* mutant showed a delayed invasion, similarly to the Δ*msb2* mutant, while the ectopic strain behaved like the wild type (Figure 45). We noted that there was a slightly more severe effect in the double Δ*msb2*Δ*sho1* mutant, suggesting additive contributions of the two proteins to invasive growth. However, confirmation of this hypothesis will require more detailed analysis of the mutant phenotypes. Collectively, these preliminary data show that Sho1 contributes to invasive growth of *F. oxysporum*.

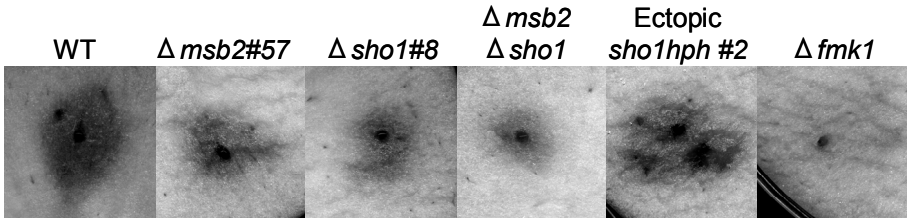


**Figure 45. Sho1 contributes to invasive growth on living fruit tissue.**
Tomato (upper) and apple fruits (lower) were inoculated with $5 \times 10^4$ microconidia of the indicated strains and incubated at 28ºC for 4 days.

We tested the role of Sho1 in plant pathogenicity. Two independent Δ*sho1* mutants were significantly reduced in virulence on tomato plants compared to the *sho1::hph* ectopic, the wild type and the Δ*msb2 + msb2HA* strains used as positive controls (Figure 46). Interestingly, virulence levels of the Δ*sho1* mutants were not significantly different from those of the Δ*msb2* mutants. Strikingly, plants infected with the Δ*msb2*Δ*sho1* double mutant showed significantly reduced wilt symptoms with respect to either single mutant, similar to those infected with the Δ*fmk1* strain. The fact that the Δ*msb2*Δ*sho1* double mutant behaved like the Δ*fmk1* strain throughout the infection suggests that Msb2 and Sho1 may interact to regulate different aspects of Fmk1-mediated pathogenicity in *F. oxysporum*.

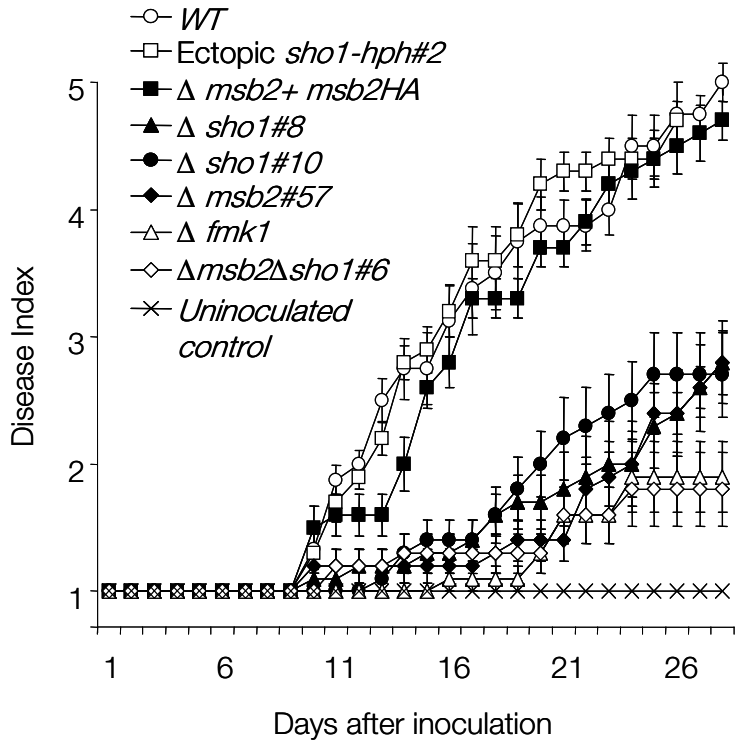


**Figure 46. Sho1 and Msb2 have non-redundant functions in virulence of *F. oxysporum* on tomato plants.**
Incidence of *Fusarium* wilt on tomato plants (cultivar Monica) inoculated with the indicated strains. Severity of disease symptoms was recorded at different times after inoculation, using an index ranging from 1 (healthy plant) to 5 (dead plant). Bars represent standard errors calculated from 20 plants.

# Discussion

In *S. cerevisiae*, the FG pathway is regulated by the signalling mucin Msb2, a cell-surface glycoprotein that mediates signalling through the GTPase Cdc42p (Cullen *et al.*, 2004). Msb2 is situated upstream of and physically interacts with the Sho1 membrane protein (Cullen *et al.*, 2004). Msb2 is processed in its extracellular domain by the aspartyl protease Yps1, and release of this extracellular domain is required for FG pathway activation (Vadaie *et al.*, 2008).

In the fungal plant pathogen *F. oxysporum* the Fmk1 MAPK, orthologous to *S. cerevisiae* Fus3/Kss1, is part of a pathogenicity signalling cascade essential for plant infection (Di Pietro *et al.*, 2001).

The aim of this work was to characterize the role of the Msb2 membrane protein in signal transduction and virulence of *F. oxysporum*. We present evidence that Msb2 (i) is a transmembrane mucin, (ii) mediates hyphal growth on solid nutrient limiting media, (iii) interacts genetically with Fmk1 to control cell wall integrity and (iv) regulates Fmk1-dependent invasive growth and virulence. In addition, we present preliminary data on the role of the Sho1 adaptor protein, indicating that Sho1 interacts genetically with Msb2 to

regulate growth of *F. oxysporum* on solid surfaces, cell wall integrity and pathogenicity. The results obtained in this work can be accommodated in the model proposed in Figure 47, in which Msb2 and Sho1 function together upstream of the MAPK Fmk1 to promote invasive growth and virulence, while other Fmk1-controlled functions such as vegetative hyphal fusion are activated independently. In this model, Msb2 and Sho1 contribute to cell integrity through a distinct pathway.

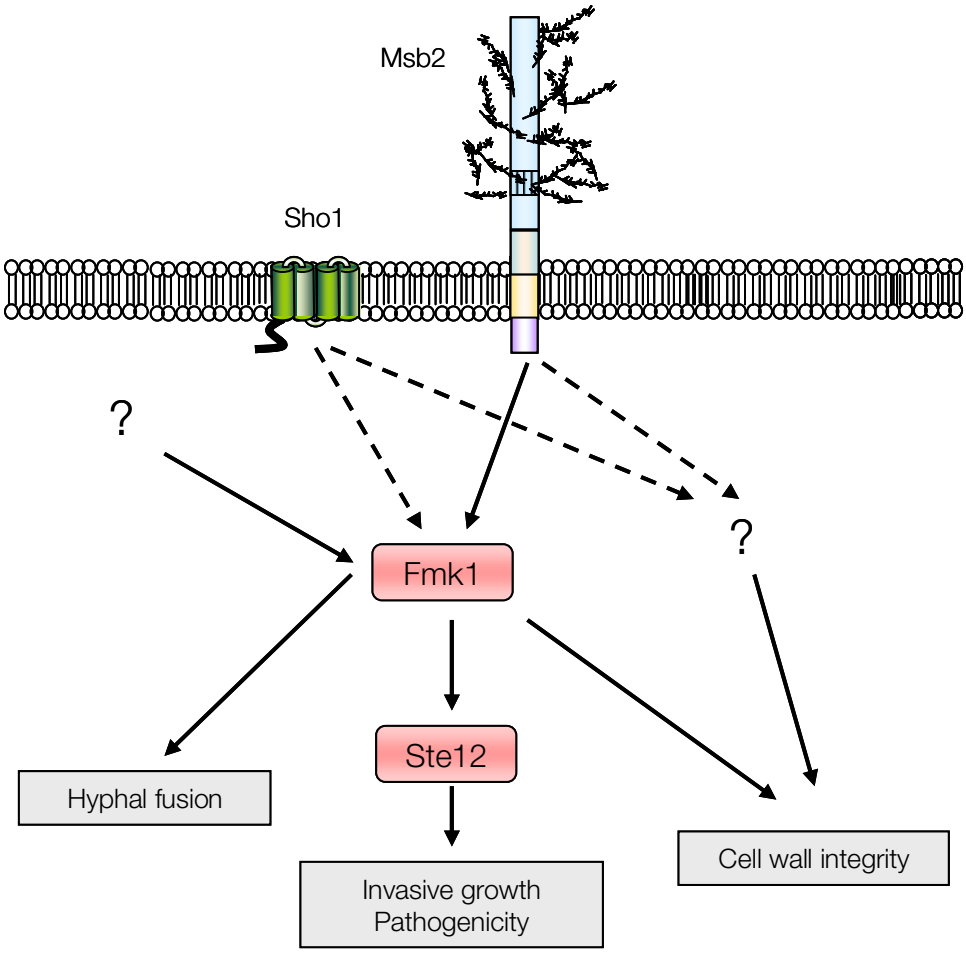


**Figure 47. Model for the role of Msb2 and Sho1 in MAPK signalling and pathogenicity of *F. oxysporum*.**
Msb2, and possibly Sho1, function upstream of the MAPK Fmk1 to promote invasive growth and virulence. Other Fmk1-controlled functions such as vegetative hyphal fusion are regulated independently. In addition, Msb2 and Sho1 contribute to cell integrity through a distinct pathway.

## 1. *F. oxysporum* Msb2 is a transmembrane mucin

*F. oxysporum* Msb2 was identified by its homology to the Msb2 protein from *S. cerevisiae* (Cullen *et al.*, 2004). Although the amino acid sequence identity between the two proteins is fairly low, several lines of evidence suggest that they are structural orthologues. *F. oxysporum* and yeast Msb2 have a conserved domain structure. Both contain a signal peptide, an extracellular MHD, a so-called positive regulatory domain, a transmembrane region and an intracellular cytoplasmic tail at the C-terminus. The presence of an N-terminal signal sequence and a single transmembrane domain suggests that *F. oxysporum* Msb2 is an integral membrane protein. This hypothesis was experimentally confirmed using a HA-tagged Msb2 version, thus corroborating the results from *S. cerevisiae* (Cullen *et al.*, 2004).

Interestingly, another parallel between the two species is that *F. oxysporum* Msb2 is shed from the cell surface into the surrounding medium. Shedding was particularly evident during growth on solid surfaces, as detected by the robust hybridyzing signal from the secreted Msb2 protein after removal of the fungal colony. The mechanism of Msb2 shedding in *F. oxysporum* is currently unknown. In *S. cerevisiae*, this process involves cleavage of the extracellular Msb2 domain by the glycosylphosphatidyl-inositol (GPI)-anchored aspartyl protease Yps1p, a member of the yapsin family (Vadaie *et al.*, 2008). A genome-wide inventory of the predicted GPI-anchored proteins in *F. oxysporum* detected several aspartic proteases, one of which, FOXG_09428, is a putative orthologue of Yps1p (Prados-Rosales *et al.*, 2009). Thus, a mechanism for Msb2 cleavage similar to that described in *S. cerevisiae* could also be operating in filamentous ascomycetes. Treatment of *F. oxysporum* colonies with an aspartyl protease inhibitor or a protein inhibitor cocktail previous to analysis by the colony blot assay did not clearly block Msb2 shedding (EPN and ADP, unpublished data). However, involvement of a protease in the process of Msb2 shedding in *F. oxysporum* can not be discarded at this stage, since the reversible protease inhibitors used in these preliminary experiments could have been removed by dilution over the 8 h incubation time of the colony blot assay. It will be necessary to perform more detailed studies, including a genetic approach, to fully clarify the possible

role of proteases in Msb2 shedding and MAPK pathway activation. In *S. cerevisiae*, some controversy exists on the requirement of Yps1-mediated cleavage for mucin activation (Yang *et al.*, 2009). Proteolytic degradation of overexpressed Msb2, as revealed by shedding of the Msb2 ectodomain, was highly but not completely blocked in a *yps1*Δ mutant and this mutant was only partially defective in activating the FG pathway (Vadaie *et al.*, 2008). It was recently shown that deletion of *YPS1* does not prevent the induction of FG-pathway reporters by glycosylation defects (Yang *et al.*, 2009). At present, the possible relationship between Yps1-dependent cleavage and glycosylation defects in activating the Kss1 MAPK cascade remains unsolved. Likewise, the biochemical events that regulates Msb2 secretion in *F. oxysporum* remain to be determined.

The overall structure of Msb2 was conserved in putative orthologues from other ascomycetes, including plant and human pathogens (Rispail and Di Pietro, 2009; Roman *et al.*, 2009). TM, PRD and CT regions show the highest sequence identity scores while the large extracellular region (730 residues in *F. oxysporum*) named MHD for mucin homology domain (Cullen *et al.*, 2004; Vadaie *et al.*, 2008) shows higher sequence divergency. Interestingly, the three conserved domains are relevant for mucin signalling activity in *S. cerevisiae*. The TM functions to anchor the mucin receptor to the plasma membrane and is directly involved in signal transduction by interacting with Sho1 (Cullen *et al.*, 2004; Tatebayashi *et al.*, 2007). The *S. cerevisiae* CT domain interacts with the Cdc42 protein (Cullen *et al.*, 2004; Tatebayashi *et al.*, 2007) and is involved in signalling osmostress as part of a mechanism independent of the Sho1 TM domain (Cullen *et al.*, 2004; Tatebayashi *et al.*, 2007). Interestingly, in *C. albicans*, dominant activating allles of Cdc42 are able to stimulate the Cek1 MAPK pathway via the Hst7 MAPK kinase (Rispail and Di Pietro, 2009; Roman *et al.*, 2009). We noted that *F. oxysporum* Msb2 has an arginine-lysine cluster yuxtaposed to the plasma membrane, which is also present in all other fungal orthologues (Figure 13). In mammalian mucins, this positively charged cluster is also conserved in transmembrane mucins and was suggested to serve as a spatially delimiting sequence for the hydrophobic domain, an imperfect or partial nuclear

localisation signal or a potential motif for proteolytic cleavage of the mucin cytoplasmic tail in response to signalling events (Singh and Hollingsworth, 2006).

The yeast, PRD is essential for Msb2 function since mutants lacking this domain are unable to activate neither the FG nor the HOG pathway (Cullen *et al.*, 2004; Tatebayashi *et al.*, 2007; Vadaie *et al.*, 2008). It is worth noting that some human transmembrane mucins such as MUC1, MUC13 and MUC16, contain a so-called sea urchin sperm protein, enterokinase and agrin (SEA) domain of approximately 120 amino acids characteristically located between the O-glycosylated PTS repeats (MHD) and the transmembrane domain (Bork and Patthy, 1995). SEA domains are involved in an autoproteolytic cleavage whereby the mucin form two subunits (Levitin *et al.*, 2005; Ligtenberg *et al.*, 1992; Macao *et al.*, 2006). In the case of MUC1, the N-terminal subunit (MUC1-N) forms a stable, non-covalent complex with the C-terminal transmembrane subunit (MUC1-C) and is thereby anchored to the surface of the cell. Upon stimulation, MUC1-N is released from the cell surface, leaving MUC1-C as a putative receptor that engages in different signalling pathways linked to cellular transformation and tumour progression (Kufe, 2008). Could the fungal PRD domain be functionally related to SEA domains in mammalian mucins? While there is currently no evidence for an autoproteolytic event in *S. cerevisiae* Msb2, there is evidence that the PRD domain is required for Yps1-mediated cleavage and activation of Msb2, and the cleavage site was mapped to residues 1045-1145 of the PRD (Vadaie *et al.*, 2008). SEA domains are also found in secreted mammalian mucins. We have performed a genome wide search for proteins with mucin-related proline, threonine, serine rich (PTS) domains in *F. oxysporum*. Among the 132 retrieved candidate proteins that also contained a putative signal peptide, we found GPI-anchored, secreted and transmembrane proteins. We expect that a more detailed examination of the retrieved sequences will reveal new mucin candidates. In this context, it would be interesting to search other fungal genomes and examine possible conserved domains or evolutionary relationships among mucin-type proteins.

In *S. cerevisiae* Msb2, the MHD contains several exact tandem repeats rich in serine, threonine and proline residues and is heavily glycosylated (Cullen *et al.*, 2004; Yang *et al.*, 2009), two classical hallmarks of mammalian mucins (Hollingsworth and Swanson, 2004). The MHD of *F. oxysporum* Msb2 shares a high content in serine, threonine and proline but lacks exact tandem repeats, similar to most Msb2 orthologues from filamentous ascomycetes identified in this study. The absence of exact repeats in the MHD was previously reported for mucins of the protozoan parasite *Trypanosoma cruzi,* suggesting that exact repeats may not be essential for mucin function, but rather represent an evolutionary mechanism for rapid expansion of serine and threonine residues serving as O-glycosylation sites (Almeida *et al.*, 1994; Di Noia *et al.*, 1996). Serine-threonine rich domains of secreted mucins like Flo11 in *S. cerevisiae* were shown to undergo rapid evolution (Verstrepen *et al.*, 2005). Sequencing of the MHD domain of Msb2 amplified from genomic DNA of different isolates and formae speciales of *F. oxysporum*, including *f.sp. conglutinans* (strain 699), *f.sp. melonis* (strains 1127 and 18M), *f.sp. lycopercisi* (strain 218), *f.sp. gladioli* (strain 2868) and *f.sp. lini* (strain 2159), revealed no nucleotide sequence divergences (data not shown). *F. oxysporum* Msb2 has multiple predicted sites for O-glycosylation and eight N-glycosylation sites, and its apparent molecular weight estimated from western blot analysis (>250 kDa) was more than double than predicted (117.5 Kda). Comparison of the apparent size of full-length Msb2-HA protein before and after EndoH treatment or with Msb2-HA isolated from tunycamicin-treated cells did not reveal a detectable size shift. Prof. Hauro Saito (University of Tokio) suggested that the much larger contribution of O-glycosylation to the protein size may be masking the contribution of N-glycosylation. He pointed out that in *S. cerevisiae* they had to use shorter versions of Msb2 that lack certain regions of the MHD, to visually detect the effect of *pmt* mutations and Endo H treatment on the electrophoretic mobility of the protein (Yang *et al.*, 2009). Consistent with this idea, Msb2*HA, a version of *F. oxysporum* Msb2-HA lacking most of the MHD, migrated at an apparent molecular mass of 52 kDa, very close to the expected size of 48.9 kDa. Collectively, our results strongly suggest that *F. oxysporum* Msb2 is a highly glycosylated transmembrane mucin.

## 2. Evidence for a role of Msb2 in surface-induced MAPK activation

Infection-related development in fungal pathogens is often triggered by contact with the host surface (Kumamoto, 2008). In aerial plant pathogens such as the rice blast fungus *M. oryzae,* contact with the leaf surface induces differentiation of an appressorium that builds up turgor pressure to promote entry into the host plant (Wilson and Talbot, 2009). In the non-appressorium forming pathogen *F. oxysporum*, presence of the host roots induces adhesion and differentiation of infection hyphae that directly penetrate the root surface (Bishop and Cooper, 1983a; Rodriguez-Gálvez and Mendgen, 1995). The MAPK Fmk1 was previously shown to be essential for these early infection processes (Di Pietro *et al*., 2001). However, the mechanism involved in surface sensing upstream of Fmk1 has so far remained elusive.

Here we provide evidence showing that contact of *F. oxysporum* with a solid surface triggers a rapid and transient increase in Fmk1 phosphorylation levels, and that this response requires Msb2. These results place Msb2 upstream of the Fmk1 MAPK. Two additional lines of evidence support a role of Msb2 in MAPK activation. Besides Fmk1 phosphorylation, Msb2 also controls expression of two Fmk1-regulated genes, *fpr1* encoding a secreted PR-1-like protein (Prados-Rosales *et al*. in preparation) and *chsV* encoding a class V chitin synthase with a myosin domain that is essential for plant infection (Madrid *et al*., 2003). More importantly, Δ*msb2* and Δ*fmk1* mutants share characteristic phenotypes such as defects in hyphal growth under nutrient-limited conditions, penetration of cellophane membranes, colonization of fruit tissue, and virulence on tomato plants. However, with the exception of hyphal growth, the defects of the Δ*msb2* strains were less severe than those of the Δ*fmk1* mutant, suggesting the presence of additional upstream components involved in Fmk1 activation, whose function could be partially redundant with Msb2.

The role of Msb2 and Fmk1 in surface response of *F. oxysporum* is further supported by the finding that Δ*msb2* and Δ*fmk1* mutants are specifically affected in hyphal extension on solid media, but not in submerged growth (This work and (Prados Rosales and Di Pietro,

2008). Intriguingly, the hyphal phenotype in Δ*msb2* and Δ*fmk1* mutants was only detected under nutrient-limited but not on nutrient-rich solid media, which suggests that the role of Msb2 and Fmk1 in *F. oxysporum* may be controlled by nutrient status. In *S. cerevisiae*, it has been shown that the nutritional status of the cell regulates the role of Msb2 during FG at the level of YPS1 expression (Vadaie *et al.*, 2008). Although we found no synergistic phenotype with respect to hyphal extension on minimal solid medium in the double Δ*msb2*Δ*fmk1* mutant, we provide evidence for a genetic interaction between Msb2 and Fmk1 with respect to the expression of the *gas1* gene. *gas1* encodes a β-1,3-glucanosyltransferase essential for pathogenicity of *F. oxysporum* and, interestingly, is required for filamentous hyphal growth on solid surfaces but not during submerged culture (Caracuel *et al.*, 2005). Under solid, nutrient-limited conditions, *msb2* and *fmk1* single mutants show similarly reduced levels of *gas1* expression, and these are significantly more reduced in the double mutant. The synergistic effect of Msb2 and Fmk1 in the regulation of *gas1* suggests the participation of different pathways in the Msb2- and Fmk1-mediated regulation of surface and/or nutrient sensing. A possible candidate for such an additional pathway is the cAMP-Protein kinase A pathway. A solid surface–related role in hyphal growth was previously reported for the protein kinase A isoform Tpk1 of *C. albicans* (Bockmuhl *et al.*, 2001). Tpk1 is specifically required for hyphal formation on solid but not on liquid-inducing media, suggesting that contact to a solid surface triggers Tpk1p activation (Bockmuhl *et al.*, 2001). The components mediating this function during the infection process on mammalian hosts are stil unknown, but could include mucin-mediated contact to host cells and to structures such as the extracellular matrix.

How Msb2 senses the surface is unclear. The glycosylated extracellular domain of transmembrane mucins has been proposed to function as a sensor of environmental cues (Cullen, 2007; de Nadal *et al.*, 2007). In support of this idea, deletion of the MHD of Msb2 in *S. cerevisiae* resulted in constitutive activation of the FG pathway (Cullen *et al.*, 2004). Moreover, a combination of O- and N-glycosylation defects induced by tunicamycin treatment and *pmt4* mutation, stimulated FG signalling in a Msb2-dependent manner (Yang *et al.*, 2009). A recent report on *in vivo* measurement of the mechanical

behaviour of the glycosylated transmembrane sensor Wsc1, which functions upstream of the yeast cell wall integrity (CWI) MAPK pathway (Levin, 2005), suggested that it behaves like a linear nanospring in response to cell surface stress (Dupres *et al.*, 2009). Interestingly, underglycosylation of Wsc1 by *pmt4* deletion caused dramatic alterations in protein spring properties (Dupres *et al.*, 2009). Collectively, these results suggest an important role of glycosylation at the extracellular domain of mucin-type transmembrane sensors.

We tried to study the role of the MHD in *F. oxysporum* Msb2 by expressing a *msb2*HA* allele lacking most of this extracellular domain. Unexpectedly, transformants showing Msb2*HA expression displayed an abnormal growth phenotype with reduced hyphal development and absence of microconidia production in liquid culture. We were unable to further investigate this phenotype, since it was not possible to obtain conidia for long-term storage from these transformants, or for reproducing their growth in liquid culture. Replacement of the endogenous *msb2* promoter by two independent inducible promoters, *Pstl35* which is repressed by thiamine (Ruiz-Roldan *et al.*, 2008) and P*pg1* which is induced by pectin and repressed by glucose (Di Pietro and Roncero, 1998) was not efficient so far in overcoming the supposedly deleterious effect of Msb2*HA (EPN and ADP, unpublished data). Protein expression analyses still detected Msb2*HA in the transformants even under repressing conditions, suggesting that repression of these promoters was not sufficiently tight under the experimental conditions used. Thus, the identification of a more efficient system for regulated gene expression will be required to further investigate the effect of the *msb2*HA* allele in *F. oxysporum*. Additionally, we are currently using an alternative approach based on functional complementation of the FG-defective phenotype of *S. cerevisiae msb2* strains with the full length Msb2 protein of *F. oxysporum*. If successful, this system would provide us with an efficient tool to extend the biochemical characterization of the protein without the constraints of the more labor-intensive generation of mutants in *F. oxysporum*, which is often limited by a lack of sufficient antibiotic markers.

Mutations in O-mannosyltransferase (PMT) familiy proteins have been linked to defects in *S. pombe* morphogenesis (Willer *et al.*, 2003), reduced pathogenicity of *C. albicans* (Prill *et al.*, 2005; Timpel *et al.*, 2000), *Cryptoccocus neoformans* (Olson *et al.*, 2007; Willger *et al.*, 2009) and *U. maydis* (Fernandez-Alvarez *et al.*, 2009). Among the Pmt family, Pmt4 is unique because it specifically glycosylates Ser/Thr-rich extracellular segments in membrane-attached proteins (Hutzler *et al.*, 2007). Pmt4-dependent O-glycosylation of the pathogen *C. albicans* was shown to affect hyphal morphology. *C. albicans pmt4* mutans show defective hyphal morphogenesis under aerobic induction conditions, a phenotype that is exacerbated under embedded or hypoxic conditions, suggesting a role of Pmt4-mediated O-glycosylation for environment-specific morphogenetic signalling and pathogenesis (Prill *et al.*, 2005). Interestingly, *C. albicans pmt* mutants were hypersensitive to antifungals and to cell wall-targeting agents (Prill *et al.*, 2005). In *U. maydis*, *pmt4* is essential for pathogenesis but is dispensable for other aspects of the life cyle. Deletion of *pmt4* results in strong reduction in the frequency of appressorium formation, with the few appresporia that form lacking the capacity to penetrate the plant cuticle (Fernandez-Alvarez *et al.*, 2009). Because *F. oxysporum* Msb2 regulates cell wall integrity, hyphal growth on solid limiting nutrient media and pathogenicity, it is tempting to speculate that the *F. oxysporum pmt4* gene (*FOXG_00440*) may also be involved in regulation of the MAPK signalling cascade. Further studies are required to explore the possible link between O-glycosylation defects, status of Msb2 glycosylation and their influence on Fmk1 MAPK activation.

## 3. Msb2 and Fmk1 contribute to cell wall integrity of *F. oxysporum* through separate pathways

In addition to its role in the FG pathway, *S. cerevisiae* Msb2 also functions as an osmosensor upstream of the Sho1 branch of the high-osmolarity glycerol (HOG) MAPK pathway (Tatebayashi *et al.*, 2007). In the present study, *F. oxysporum* Δ*msb2* mutants showed no changes in the osmotic or oxidative stress response. However, deletion of *msb2* in *F. oxysporum* resulted in increased sensitivity to CR and CFW, two compounds

affecting cell wall biosynthesis and composition (Roncero and Duran, 1985). Unexpectedly, the Δ*fmk1*Δ*msb2* double mutant showed significantly higher sensitivity to CR and CFW that either of the single mutants, revealing a genetic interaction between Msb2 and Fmk1. Based on the mutant phenotypes, we consider it likely that Msb2 and Fmk1 promote cell wall integrity of *F. oxysporum* through independent pathways. In support of this hypothesis, expression of the chitin synthase gene *chsV,* which is required for resistance of *F. oxysporum* to CR and CFW (Madrid *et al*., 2003), was reduced in Δ*msb2* mutants, but even more so in the Δ*fmk1*Δ*msb2* double mutant. As mentioned before, a similar trend was observed with respect to expression levels of the *gas1* gene. The increased sensitivity of the *msb2* mutants to cell wall targeting compounds was partially relieved by the osmotic stabilizer sorbitol, suggesting a possible link between the cell wall stress phenotype and the presence of structural alterations in the cell wall. Based on the gene expression analysis, we would expect structural alterations in the cell wall such as reduced glucan and chitin contents, although these and related phenotypes such as resistance to cell wall–degrading enzymes remain to be investigated.

Deletion of *msb2* in the human pathogen *C. albicans* also resulted in increased sensitivity to CR and reduced phosphorylation of the Fmk1 MAPK orthologue Cek1 in response to cell wall stress, although a genetic interaction between the two component was not tested in this system (Roman *et al.*, 2009). In *S. cerevisiae*, the CWI MAPK pathway receptors Wcs2 and Mid2 could stimulate the FG pathway through Msb2 and other components of the Kss1 MAPK cascade (Birkaya *et al.*, 2009). Similar to Msb2, Wsc2 and Mid2 are cell surface sensors with a serine/threonine rich extracellular region, a single transmembrane domain and a cytoplasmic tail. It is possible that these mucin-like fungal transmembrane receptors cooperate in detecting different types of cell surface signals, leading to an orchestrated response that involves both the FG and CWI MAPK pathways. Inriguingly, *F. oxysporum* mutants in *gas1* or *rho1* are dramatically affected by CR and CFW treatment, similar to the Δ*fmk1*Δ*msb2* double mutant (EPN and ADP, unpublished data), suggesting a possible connection with the Mpk1 integrity pathway.

## 4. Sho1 and Msb2 interact to regulate Fmk1-mediated virulence functions and plant infection.

We found that Δ*msb2* strains shared several, but not all phenotypes of the Δ*fmk1* mutant. For example, Msb2 is non-essential for vegetative hyphal fusion, a process that requires Fmk1 (Prados Rosales and Di Pietro, 2008). On the other hand, all known Fmk1-controlled functions related to invasive growth were affected to some extent in the Δ*msb2* mutants, including extracellular pectinolytic activity, penetration of cellophane membranes and colonization of tomato or apple fruit tissue. Interestingly, a similar subset of Fmk1-dependent invasive growth functions was impaired in *F. oxysporum* mutants lacking the homeodomain transcription factor Ste12 (Rispail and Di Pietro, 2009). Moreover, virulence on tomato plants is severely reduced both in Δ*msb2* and Δ*ste12* mutants, albeit not as dramatically as in the Δ*fmk1* mutant. This suggests that Msb2 contributes to invasive growth, the major virulence function of Fmk1 (Rispail and Di Pietro, 2009). However, the more severe phenotype of the Δ*fmk1* mutant points to the presence of additional upstream components involved in Fmk1 activation.

We regarded Sho1 as a likely candidate for an upstream component of the Fmk1 MAPK cascade, since in yeast, Msb2 and Sho1 interact physically (Cullen *et al.*, 2004) and a dominant activated version of Sho1 can partially activate the FG MAPK pathway even in the absence of Msb2 (Vadaie *et al.*, 2008). In *C. albicans*, Msb2 was recently shown to cooperate with Sho1 in the control phosphorylation of the Fmk1 MAPK orthologue Cek1 in response to cell wall stress (Roman *et al.*, 2009).

The Sho1 protein is broadly conserved in filamentous ascomycetes (Ma *et al.*, 2008; Rispail *et al.*, 2009; Roman *et al.*, 2005). *F. oxysporum* Sho1 was identified by its homology to the Sho1 protein from *S. cerevisiae*. In support of our starting hypothesis, *F. oxysporum* deletion mutants in *sho1* were defective in several Msb2- and Fmk1-dependent functions, including hyphal extension on nutrient-poor solid media, response to cell wall stress, extracellular pectinolytic activity, colonization of apple fruit tissue and pathogenicity. Phenotypic comparison of single and double *msb2* and *sho1* mutants with

the wild type and the Δ*fmk1* strain suggest that Sho1 and Msb2 have both redundant and independent roles in the regulation of Fmk1-mediated functions in *F. oxysporum*.

Sho1 and Msb2 contribute to similar extents to hyphal growth on solid nutrient-limiting medium, since we did not observe additive effect in the double mutant. Δ*msb2* and Δ*sho1* mutants showed similar sensitivity to the cell wall targeting compound Congo Red, and more detailed analyses will be required to assess a hypothetical synergistic effect in the double mutant.

Sho1 and Msb2 clearly exert a synergistic effect in activation of *fpr1*, *chsV* and *gas1* gene expression. Interestingly, the synergistic effect of a double mutation with respect to expression of these genes was not significatly different from that of the Δ*fmk1* mutants, except for *chsV,* in which Δ*fmk1*Δ*msb2* and Δ*msb2*Δ*sho1* double mutants showed significantly decreased transcript levels compared to any of the single mutants, suggesting that Msb2 and Sho1 interact to regulate the expression of these virulence genes in *F. oxysporum.* This synergistic effect was also apparent for extracellular pectinolytic activity, but not so clear in colonization of apple fruit tissue.

Most importantly, we show for the first time that virulence of *F. oxysporum* on tomato plants is severely reduced both in Δ*msb2* and Δ*sho1* mutants. However only the Δ*msb2*Δ*sho1* double deletion mutant had a complete defect in virulence which was as dramatic as in the Δ*fmk1* mutant. This suggests that Msb2 and Sho1 have partially redundant roles during infection. Further research will be required to dissect the individual signalling inputs of Msb2 and Sho1 upstream of Fmk1, and to define the exact outputs that control pathogenicity of *F. oxysporum*.

# References

Agrawal, B., Gendler, S.J., and Longenecker, B.M. (1998). The biological role of mucins in cellular interactions and immune regulation: prospects for cancer immunotherapy. Molecular medicine today *4*, 397-403.

Agrios, G.N. (1997). Plant Pathology. San Diego, CA, EEUU, Academic Press Inc.

Alexander, M.R., Tyers, M., Perret, M., Craig, B.M., Fang, K.S., and Gustin, M.C. (2001). Regulation of cell cycle progression by Swe1p and Hog1p following hypertonic stress. Mol Biol Cell *12*, 53-62.

Alonso-Monge, R.A., Roman, E., Nombela, C., and Pla, J. (2006). The MAP kinase signal transduction network in Candida albicans. Microbiology *152*, 905-912.

Armstrong, G.M., and Armstrong, J.K. (1981). Formae speciales and races of Fusarium oxysporum causing wilt diseases (Philadelphia, PA, Pennsylvania State University Press).

Asuncion Garcia-Sanchez, M., Martin-Rodrigues, N., Ramos, B., de Vega-Bartol, J.J., Perlin, M.H., and Diaz-Minguez, J.M. (2009). fost12, the Fusarium oxysporum homolog of the transcription factor Ste12, is upregulated during plant infection and required for virulence. Fungal Genet Biol.

Baker, B., Zambryski, P., Staskawicz, B., and Dinesh-Kumar, S.P. (1997). Signaling in plant-microbe interactions. Science *276*, 726-733.

Barral, Y., Parra, M., Bidlingmaier, S., and Snyder, M. (1999). Nim1-related kinases coordinate cell cycle progression with the organization of the peripheral cytoskeleton in yeast. Genes Dev *13*, 176-187.

Beckman, C.H. (1987). The nature of Wilt Diseases of Plants. St Paul, MN (EEUU) APS Press.

Beckman, C.H., and Halmos, S. (1962). Relation of vascular occluding reactions in banana roots to pathogenicity of root-invading fungi. Phytopathology *52*, 893-897.

Beckman, C.H., Mace, M.E., Halmos, S., and McGahan, M.W. (1961). Physical barriers associated with resistance in Fusarium wilt of bananas. Phytopathology *52*, 134-140.

Bender, A., and Pringle, J.R. (1992). A Ser/Thr-rich multicopy suppressor of a cdc24 bud emergence defect. Yeast (Chichester, England) *8*, 315-323.

Bendtsen, J.D., Nielsen, H., von Heijne, G., and Brunak, S. (2004). Improved prediction of signal peptides: SignalP 3.0. Journal of molecular biology *340*, 783-795.

Bennett, R.J., and Johnson, A.D. (2005). Mating in Candida albicans and the search for a sexual cycle. Annu Rev Microbiol *59*, 233-255.

Bermejo, C., Rodriguez, E., Garcia, R., Rodriguez-Pena, J.M., Rodriguez de la Concepcion, M.L., Rivas, C., Arias, P., Nombela, C., Posas, F., and Arroyo, J. (2008). The sequential activation of the yeast HOG and SLT2 pathways is required for cell survival to cell wall stress. Mol Biol Cell *19*, 1113-1124.

Birkaya, B., Maddi, A., Joshi, J., Free, S.J., and Cullen, P.J. (2009). Role of the cell wall integrity and filamentous growth mitogen-activated protein kinase pathways in cell wall remodeling during filamentous growth. Eukaryot Cell *8*, 1118-1133.

Bishop, C.D., and Cooper, R.M. (1983a). An ultrastructural study of root invasion in three vascular wilt diseases. Physiol Mol Plant Path *22*, 15-27.

Bishop, C.D., and Cooper, R.M. (1983b). An ultrastructural study of root invasion of three vascular wilt diseases. . Physiological Molecular Plant Pathology *22*, 15-27.

Bluhm, B.H., Zhao, X., Flaherty, J.E., Xu, J.R., and Dunkle, L.D. (2007). RAS2 regulates growth and pathogenesis in Fusarium graminearum. Mol Plant Microbe Interact *20*, 627-636.

Bockmuhl, D.P., Krishnamurthy, S., Gerads, M., Sonneborn, A., and Ernst, J.F. (2001). Distinct and redundant roles of the two protein kinase A isoforms Tpk1p and Tpk2p in morphogenesis and growth of Candida albicans. Mol Microbiol *42*, 1243-1257.

Boisnard, S., Ruprich-Robert, G., Florent, M., Da Silva, B., Chapeland-Leclerc, F., and Papon, N. (2008). Role of Sho1p adaptor in the pseudohyphal development, drugs sensitivity, osmotolerance and oxidant stress adaptation in the opportunistic yeast Candida lusitaniae. Yeast (Chichester, England) *25*, 849-859.

Bolker, M. (1998). Sex and crime: heterotrimeric G proteins in fungal mating and pathogenesis. Fungal Genet Biol *25*, 143-156.

Booth, C. (1971). The genus Fusarium. The Eastern Press limited London and Reading.

Bork, P., and Patthy, L. (1995). The SEA module: a new extracellular domain associated with O-glycosylation. Protein Sci *4*, 1421-1425.

Borneman, A.R., Gianoulis, T.A., Zhang, Z.D., Yu, H., Rozowsky, J., Seringhaus, M.R., Wang, L.Y., Gerstein, M., and Snyder, M. (2007). Divergence of transcription factor binding sites across related yeast species. Science *317*, 815-819.

Bouarab, K., Melton, R., Peart, J., Baulcombe, D., and Osbourn, A. (2002). A saponin-detoxifying enzyme mediates suppression of plant defences. Nature *418*, 889-892.

Boutati, E.I., and Anaissie, E.J. (1997). Fusarium, a significant emerging pathogen in patients with hematologic malignancy: ten years' experience at a cancer center and implications for management. Blood *90*, 999-1008.

Brachmann, A., Schirawski, J., Muller, P., and Kahmann, R. (2003). An unusual MAP kinase is required for efficient penetration of the plant surface by Ustilago maydis. Embo J *22*, 2199-2210.

Buehrer, B.M., and Errede, B. (1997). Coordination of the mating and cell integrity mitogen-activated protein kinase pathways in Saccharomyces cerevisiae. Mol Cell Biol *17*, 6517-6525.

Burgess, L.W. (1981). General ecology of the fusaria In Fusarium: diseases, biology, and taxonomy T.A.T. P. E. Nelson, and R. J. Cook ed. (Philadelphia, PA, Pennsylvania State University Press), pp. 225-235.

Bussink, H.J., and Osmani, S.A. (1999). A mitogen-activated protein kinase (MPKA) is involved in polarized growth in the filamentous fungus, Aspergillus nidulans. FEMS Microbiol Lett *173*, 117-125.

Butty, A.C., Pryciak, P.M., Huang, L.S., Herskowitz, I., and Peter, M. (1998). The role of Far1p in linking the heterotrimeric G protein to polarity establishment proteins during yeast mating. Science *282*, 1511-1516.

Calera, J.A., Zhao, X.J., and Calderone, R. (2000). Defective hyphal development and avirulence caused by a deletion of the SSK1 response regulator gene in Candida albicans. Infect Immun *68*, 518-525.

Callow, J.A. (1987). Models for host-pathogen interactions. The applied mycology of Fusarium Ed, Cambridge University Press, 39-69.

Canero, D.C., and Roncero, M.I. (2008). Influence of the chloride channel of Fusarium oxysporum on extracellular laccase activity and virulence on tomato plants. Microbiology *154*, 1474-1481.

Caracuel, Z., Martinez-Rocha, A.L., Di Pietro, A., Madrid, M.P., and Roncero, M.I. (2005). Fusarium oxysporum gas1 encodes a putative beta-1,3-glucanosyltransferase required for virulence on tomato plants. Mol Plant Microbe Interact *18*, 1140-1147.

Caracuel, Z., Roncero, M.I., Espeso, E.A., Gonzalez-Verdejo, C.I., Garcia-Maceira, F.I., and Di Pietro, A. (2003). The pH signalling transcription factor PacC controls virulence in the plant pathogen Fusarium oxysporum. Mol Microbiol *48*, 765-779.

Carraway, K.L., Ramsauer, V.P., Haq, B., and Carothers Carraway, C.A. (2003). Cell signaling through membrane mucins. Bioessays *25*, 66-71.

Carson, D.D., DeSouza, M.M., Kardon, R., Zhou, X., Lagow, E., and Julian, J. (1998). Mucin expression and function in the female reproductive tract. Human reproduction update *4*, 459-464.

Clotet, J., Escote, X., Adrover, M.A., Yaakov, G., Gari, E., Aldea, M., de Nadal, E., and Posas, F. (2006). Phosphorylation of Hsl1 by Hog1 leads to a G2 arrest essential for cell survival at high osmolarity. Embo J *25*, 2338-2346.

Correll, J.C. (1991). The relationship between formae speciales, races and vegetative compatibility groups in *Fusarium oxysporum*. Phytopathology *81*, 1061-1064.

Csank, C., Schroppel, K., Leberer, E., Harcus, D., Mohamed, O., Meloche, S., Thomas, D.Y., and Whiteway, M. (1998). Roles of the Candida albicans mitogen-activated protein kinase homolog, Cek1p, in hyphal development and systemic candidiasis. Infect Immun *66*, 2713-2721.

Cullen, P.J. (2007). Signaling mucins: the new kids on the MAPK block. Crit Rev Eukaryot Gene Expr *17*, 241-257.

Cullen, P.J., Sabbagh, W., Jr., Graham, E., Irick, M.M., van Olden, E.K., Neal, C., Delrow, J., Bardwell, L., and Sprague, G.F., Jr. (2004). A signaling mucin at the head of the Cdc42- and MAPK-dependent filamentous growth pathway in yeast. Genes Dev *18*, 1695-1708.

Cullen, P.J., Schultz, J., Horecka, J., Stevenson, B.J., Jigami, Y., and Sprague, G.F., Jr. (2000). Defects in protein glycosylation cause SHO1-dependent activation of a STE12 signaling pathway in yeast. Genetics *155*, 1005-1018.

Chauhan, N., Inglis, D., Roman, E., Pla, J., Li, D., Calera, J.A., and Calderone, R. (2003). Candida albicans response regulator gene SSK1 regulates a subset of genes whose functions are associated with cell wall biosynthesis and adaptation to oxidative stress. Eukaryot Cell *2*, 1018-1024.

Chen, J., Chen, J., Lane, S., and Liu, H. (2002). A conserved mitogen-activated protein kinase pathway is required for mating in Candida albicans. Mol Microbiol *46*, 1335-1344.

Chen, R.E., and Thorner, J. (2007). Function and regulation in MAPK signaling pathways: lessons learned from the yeast Saccharomyces cerevisiae. Biochimica et biophysica acta *1773*, 1311-1340.

Choi, K.Y., Satterberg, B., Lyons, D.M., and Elion, E.A. (1994). Ste5 tethers multiple protein kinases in the MAP kinase cascade required for mating in S. cerevisiae. Cell *78*, 499-512.

de Groot, M.J., Bundock, P., Hooykaas, P.J., and Beijersbergen, A.G. (1998). Agrobacterium tumefaciens-mediated transformation of filamentous fungi. Nat Biotechnol *16*, 839-842.

de Nadal, E., Alepuz, P.M., and Posas, F. (2002). Dealing with osmostress through MAP kinase activation. EMBO reports *3*, 735-740.

de Nadal, E., Real, F.X., and Posas, F. (2007). Mucins, osmosensors in eukaryotic cells? Trends Cell Biol *17*, 571-574.

De Wit, P.J., Mehrabi, R., Van den Burg, H.A., and Stergiopoulos, I. (2009). Fungal effector proteins: past, present and future. Mol Plant Pathol *10*, 735-747.

Delgado-Jarana, J., Martinez-Rocha, A.L., Roldan-Rodriguez, R., Roncero, M.I., and Di Pietro, A. (2005). Fusarium oxysporum G-protein beta subunit Fgb1 regulates hyphal growth, development, and virulence through multiple signalling pathways. Fungal Genet Biol *42*, 61-72.

Desjardins, A.E., Hohn, T.M., and McCormick, S.P. (1993). Trichothecene biosynthesis in Fusarium species: chemistry, genetics, and significance. Microbiol Rev *57*, 595-604.

Di Pietro, A., Garcia-Maceira, F.I., Meglecz, E., and Roncero, M.I. (2001). A MAP kinase of the vascular wilt fungus *Fusarium oxysporum* is essential for root penetration and pathogenesis. Mol Microbiol *39*, 1140-1152.

Di Pietro, A., Gonzalez Roncero, M.I., Ruiz Roldán, C., and Claus, H. (2009). From tools of survival to weapons of destruction: role of cell wall-degrading enzymes in plant infection. In The Mycota, pp. 181-200.

Di Pietro, A., Madrid, M.P., Caracuel, Z., Delgado-Jarana, J., and Roncero, M.I. (2003). Fusarium oxysporum: exploring the molecular arsenal of a vascular wilt fungus. Mol Plant Pathol *4*, 315-325.

Di Pietro, A., and Roncero, M.I. (1998). Cloning, expression, and role in pathogenicity of pg1 encoding the major extracellular endopolygalacturonase of the vascular wilt pathogen Fusarium oxysporum. Mol Plant Microbe Interact *11*, 91-98.

Diez-Orejas, R., Molero, G., Navarro-Garcia, F., Pla, J., Nombela, C., and Sanchez-Perez, M. (1997). Reduced virulence of Candida albicans MKC1 mutants: a role for mitogen-activated protein kinase in pathogenesis. Infect Immun *65*, 833-837.

Divon, H., Ziv, C., Davydov, O., Yarden, O., and Fluhr, R. (2006). The global nitrogen regulator, FNR1, regulates fungal nutrition-genes and fitness during Fusarium oxysporum pathogenesis. Mol Plant Pathol *7*, 485-497.

Dixon, K.P., Xu, J.R., Smirnoff, N., and Talbot, N.J. (1999). Independent signaling pathways regulate cellular turgor during hyperosmotic stress and appressorium-mediated plant infection by Magnaporthe grisea. Plant Cell *11*, 2045-2058.

Du, C., Sarfati, J., Latge, J.P., and Calderone, R. (2006). The role of the sakA (Hog1) and tcsB (sln1) genes in the oxidant adaptation of Aspergillus fumigatus. Med Mycol *44*, 211-218.

Dupres, V., Alsteens, D., Wilk, S., Hansen, B., Heinisch, J.J., and Dufrene, Y.F. (2009). The yeast Wsc1 cell surface sensor behaves like a nanospring in vivo. Nat Chem Biol *5*, 857-862.

Duyvesteijn, R.G., van Wijk, R., Boer, Y., Rep, M., Cornelissen, B.J., and Haring, M.A. (2005). Frp1 is a Fusarium oxysporum F-box protein required for pathogenicity on tomato. Mol Microbiol *57*, 1051-1063.

Eisman, B., Alonso-Monge, R., Roman, E., Arana, D., Nombela, C., and Pla, J. (2006). The Cek1 and Hog1 mitogen-activated protein kinases play complementary roles in cell wall biogenesis and chlamydospore formation in the fungal pathogen Candida albicans. Eukaryot Cell *5*, 347-358.

Elion, E.A. (1998). Routing MAP kinase cascades. Science *281*, 1625-1626.

Elion, E.A. (2000). Pheromone response, mating and cell biology. Curr Opin Microbiol *3*, 573-581.

Elion, E.A., Satterberg, B., and Kranz, J.E. (1993). FUS3 phosphorylates multiple components of the mating signal transduction cascade: evidence for STE12 and FAR1. Mol Biol Cell *4*, 495-510.

Escote, X., Zapater, M., Clotet, J., and Posas, F. (2004). Hog1 mediates cell-cycle arrest in G1 phase by the dual targeting of Sic1. Nature cell biology *6*, 997-1002.

Esch, R.K., Wang, Y., and Errede, B. (2006). Pheromone-induced degradation of Ste12 contributes to signal attenuation and the specificity of developmental fate. Eukaryot Cell *5*, 2147-2160.

Farman, M.L., Eto, Y., Nakao, T., Tosa, Y., Nakayashiki, H., Mayama, S., and Leong, S.A. (2002). Analysis of the structure of the AVR1-CO39 avirulence locus in virulent rice-infecting isolates of Magnaporthe grisea. Mol Plant Microbe Interact *15*, 6-16.

Fernandez-Alvarez, A., Elias-Villalobos, A., and Ibeas, J.I. (2009). The O-mannosyltransferase PMT4 is essential for normal appressorium formation and penetration in Ustilago maydis. Plant Cell *21*, 3397-3412.

Flor, H.H. (1947). Inheritance of pathogenicity in Melampsora lini. Phytopathology *32*, 653-669.

Flor, H.H. (1971). Current status of the gene for gene concept. Annu Rev Phytopathol *9*, 275-296.

Fravel, D., Olivain, C., and Alabouvette, C. (2003). Fusarium oxysporum and its biocontrol. New Phytologist *157*, 493-502.

Fritig, B., Heitz, T., and Legrand, M. (1998). Antimicrobial proteins in induced plant defense. Current opinion in immunology *10*, 16-22.

Furukawa, K., Hoshi, Y., Maeda, T., Nakajima, T., and Abe, K. (2005). Aspergillus nidulans HOG pathway is activated only by two-component signalling pathway in response to osmotic stress. Molecular microbiology *56*, 1246-1261.

Gancedo, J.M. (2001). Control of pseudohyphae formation in Saccharomyces cerevisiae. FEMS microbiology reviews *25*, 107-123.

Garcia-Pedrajas, M.D., and Roncero, M.I. (1996). A homologous and self-replicating system for efficient transformation of Fusarium oxysporum. Curr Genet *29*, 191-198.

Garcia-Rodriguez, L.J., Valle, R., Duran, A., and Roncero, C. (2005). Cell integrity signaling activation in response to hyperosmotic shock in yeast. FEBS letters *579*, 6186-6190.

Garcia, R., Bermejo, C., Grau, C., Perez, R., Rodriguez-Pena, J.M., Francois, J., Nombela, C., and Arroyo, J. (2004). The global transcriptional response to transient cell wall damage in Saccharomyces cerevisiae and its regulation by the cell integrity signaling pathway. The Journal of biological chemistry *279*, 15183-15195.

Garcia, R., Rodriguez-Pena, J.M., Bermejo, C., Nombela, C., and Arroyo, J. (2009). The high osmotic response and cell wall integrity pathways cooperate to regulate transcriptional responses to zymolyase-induced cell wall stress in Saccharomyces cerevisiae. The Journal of biological chemistry *284*, 10901-10911.

Gordon, T.R., and Martyn, R.D. (1997). The evolutionary biology of Fusarium oxysporum. Annu Rev Phytopathol *35*, 111-128.

Gregori, C., Schuller, C., Roetzer, A., Schwarzmuller, T., Ammerer, G., and Kuchler, K. (2007). The high-osmolarity glycerol response pathway in the human fungal pathogen Candida glabrata strain ATCC 2001 lacks a signaling branch that operates in baker's yeast. Eukaryot Cell *6*, 1635-1645.

Guindon, S., and Gascuel, O. (2003). A simple, fast, and accurate algorithm to estimate large phylogenies by maximum likelihood. Systematic biology *52*, 696-704.

Gustin, M.C., Albertyn, J., Alexander, M., and Davenport, K. (1998). MAP kinase pathways in the yeast Saccharomyces cerevisiae. Microbiol Mol Biol Rev *62*, 1264-1300.

Hahn, M.G. (1996). Microbial elicitors and their receptors in plants. Annu Rev Phytopathol *34*, 387-412.

Hamer, J.E., and Talbot, N.J. (1998). Infection-related development in the rice blast fungus Magnaporthe grisea. Curr Opin Microbiol *1*, 693-697.

Hammond-Kosack, K.E., and Jones, J.D. (1996). Resistance gene-dependent plant defense responses. Plant Cell *8*, 1773-1791.

Hanahan, D. (1985). Techniques for transformation of Escherichia coli. Oxford (G B), Ed D M Glover.

Hao, N., Zeng, Y., Elston, T.C., and Dohlman, H.G. (2008). Control of MAPK specificity by feedback phosphorylation of shared adaptor protein Ste50. The Journal of biological chemistry *283*, 33798-33802.

Hardie, D.G., Carling, D., and Carlson, M. (1998). The AMP-activated/SNF1 protein kinase subfamily: metabolic sensors of the eukaryotic cell? Annual review of biochemistry *67*, 821-855.

Hawksworth, D.L., Kirk, P.M., Sutton, B.C., and Pegler, D.N. (1995). Dictionary of the Fungi 8th 10 edn (CAB International, Wallingford, UK).

Hawle, P., Horst, D., Bebelman, J.P., Yang, X.X., Siderius, M., and van der Vies, S.M. (2007). Cdc37p is required for stress-induced high-osmolarity glycerol and protein kinase C mitogen-activated protein kinase pathway functionality by interaction with Hog1p and Slt2p (Mpk1p). Eukaryot Cell *6*, 521-532.

Ho, S.N., Hunt, H.D., Horton, R.M., Pullen, J.K., and Pease, L.R. (1989). Site-directed mutagenesis by overlap extension using the polymerase chain reaction. Gene *77*, 51-59.

Hollingsworth, M.A., and Swanson, B.J. (2004). Mucins in cancer: protection and control of the cell surface. Nature reviews *4*, 45-60.

Horazdovsky, B.F., and Emr, S.D. (1993). The VPS16 gene product associates with a sedimentable protein complex and is essential for vacuolar protein sorting in yeast. The Journal of biological chemistry *268*, 4953-4962.

Hou, Z., Xue, C., Peng, Y., Katan, T., Kistler, H.C., and Xu, J.R. (2002). A mitogen-activated protein kinase gene (MGV1) in Fusarium graminearum is required for female fertility, heterokaryon formation, and plant infection. Mol Plant Microbe Interact *15*, 1119-1127.

Huertas-González, M.D., Ruiz-Roldán, M.C., Di Pietro, A., and Roncero, M.I. (1999). Cross protection provides evidence for race-specific avirulence factors in Fusarium oxysporum. Physiol Mol Plant Pathol *54*, 63-72.

Hutzler, J., Schmid, M., Bernard, T., Henrissat, B., and Strahl, S. (2007). Membrane association is a determinant for substrate recognition by PMT4 protein O-mannosyltransferases. Proc Natl Acad Sci U S A *104*, 7827-7832.

Imazaki, I., Kurahashi, M., Iida, Y., and Tsuge, T. (2007). Fow2, a Zn(II)2Cys6-type transcription regulator, controls plant infection of the vascular wilt fungus Fusarium oxysporum. Mol Microbiol *63*, 737-753.

Inoue, I., Namiki, F., and Tsuge, T. (2002). Plant colonization by the vascular wilt fungus Fusarium oxysporum requires FOW1, a gene encoding a mitochondrial protein. Plant Cell *14*, 1869-1883.

Isaacson, R.E. (2002). Genomics and the prospects for the discovery of new targets for antibacterial and antifungal agents. Curr Pharm Des *8*, 1091-1098.

Jain, S., Akiyama, K., Kan, T., Ohguchi, T., and Takata, R. (2003). The G protein beta subunit FGB1 regulates development and pathogenicity in Fusarium oxysporum. Curr Genet *43*, 79-86.

Jain, S., Akiyama, K., Mae, K., Ohguchi, T., and Takata, R. (2002). Targeted disruption of a G protein alpha subunit gene results in reduced pathogenicity in Fusarium oxysporum. Curr Genet *41*, 407-413.

Jain, S., Akiyama, K., Takata, R., and Ohguchi, T. (2005). Signaling via the G protein alpha subunit FGA2 is necessary for pathogenesis in Fusarium oxysporum. FEMS Microbiol Lett *243*, 165-172.

Jenczmionka, N.J., Maier, F.J., Losch, A.P., and Schafer, W. (2003). Mating, conidiation and pathogenicity of Fusarium graminearum, the main causal agent of the head-blight disease of wheat, are regulated by the MAP kinase gpmk1. Curr Genet *43*, 87-95.

Jones, J.D., and Dangl, J.L. (2006). The plant immune system. Nature *444*, 323-329.

Jonkers, W., Rodrigues, C.D., and Rep, M. (2009). Impaired colonization and infection of tomato roots by the Deltafrp1 mutant of Fusarium oxysporum correlates with reduced CWDE gene expression. Mol Plant Microbe Interact *22*, 507-518.

Joobeur, T., King, J.J., Nolin, S.J., Thomas, C.E., and Dean, R.A. (2004). The Fusarium wilt resistance locus Fom-2 of melon contains a single resistance gene with complex features. Plant J *39*, 283-297.

Julenius, K., Molgaard, A., Gupta, R., and Brunak, S. (2005). Prediction, conservation analysis, and structural characterization of mammalian mucin-type O-glycosylation sites. Glycobiology *15*, 153-164.

Jung, U.S., Sobering, A.K., Romeo, M.J., and Levin, D.E. (2002). Regulation of the yeast Rlm1 transcription factor by the Mpk1 cell wall integrity MAP kinase. Mol Microbiol *46*, 781-789.

Kawabe, M., Mizutani, K., Yoshida, T., Teraoka, T., Yoneyama, K., Yamaguchi, I., and Arie, T. (2004). Cloning of the pathogenicity-related gene FPD1 in Fusarium oxysporum f. sp. lycopersici. J Gen Plant Pathol *70*, 16-20.

Keyse, S.M. (2008). Dual-specificity MAP kinase phosphatases (MKPs) and cancer. Cancer metastasis reviews *27*, 253-261.

Kistler, H.C. (1997). Genetic Diversity in the Plant-Pathogenic Fungus Fusarium oxysporum. Phytopathology *87*, 474-479.

Klein, S., Reuveni, H., and Levitzki, A. (2000). Signal transduction by a nondissociable heterotrimeric yeast G protein. Proc Natl Acad Sci U S A *97*, 3219-3223.

Knogge, W. (1996). Fungal Infection of Plants. Plant Cell *8*, 1711-1722.

Kojima, K., Kikuchi, T., Takano, Y., Oshiro, E., and Okuno, T. (2002). The mitogen-activated protein kinase gene MAF1 is essential for the early differentiation phase of appressorium formation in Colletotrichum lagenarium. Mol Plant Microbe Interact *15*, 1268-1276.

Kollar, R., Reinhold, B.B., Petrakova, E., Yeh, H.J., Ashwell, G., Drgonova, J., Kapteyn, J.C., Klis, F.M., and Cabib, E. (1997). Architecture of the yeast cell wall. Beta(1-->6)-glucan interconnects mannoprotein, beta(1-->)3-glucan, and chitin. The Journal of biological chemistry *272*, 17762-17775.

Krantz, M., Becit, E., and Hohmann, S. (2006). Comparative genomics of the HOG-signalling system in fungi. Curr Genet *49*, 137-151.

Krogh, A., Larsson, B., von Heijne, G., and Sonnhammer, E.L. (2001). Predicting transmembrane protein topology with a hidden Markov model: application to complete genomes. Journal of molecular biology *305*, 567-580.

Kron, S.J., Styles, C.A., and Fink, G.R. (1994). Symmetric cell division in pseudohyphae of the yeast Saccharomyces cerevisiae. Mol Biol Cell *5*, 1003-1022.

Kufe, D.W. (2008). Targeting the human MUC1 oncoprotein: a tale of two proteins. Cancer biology & therapy *7*, 81-84.

Kultz, D., and Burg, M. (1998). Evolution of osmotic stress signaling via MAP kinase cascades. J Exp Biol *201*, 3015-3021.

Kumamoto, C.A. (2005). A contact-activated kinase signals Candida albicans invasive growth and biofilm development. Proceedings of the National Academy of Sciences of the United States of America *102*, 5576-5581.

Kumamoto, C.A. (2008). Molecular mechanisms of mechanosensing and their roles in fungal contact sensing. Nat Rev Microbiol *6*, 667-673.

Kurjan, J. (1993). The pheromone response pathway in Saccharomyces cerevisiae. Annu Rev Genet *27*, 147-179.

Laemmli, U.K. (1970). Cleavage of structural proteins during the assembly of the head of bacteriophage T4. Nature *227*, 680-685.

Lamson, R.E., Winters, M.J., and Pryciak, P.M. (2002). Cdc42 regulation of kinase activity and signaling by the yeast p21-activated kinase Ste20. Mol Cell Biol *22*, 2939-2951.

Lang, T., Alexandersson, M., Hansson, G.C., and Samuelsson, T. (2004). Bioinformatic identification of polymerizing and transmembrane mucins in the puffer fish Fugu rubripes. Glycobiology *14*, 521-527.

Leberer, E., Harcus, D., Dignard, D., Johnson, L., Ushinsky, S., Thomas, D.Y., and Schroppel, K. (2001). Ras links cellular morphogenesis to virulence by regulation of the MAP kinase and cAMP signalling pathways in the pathogenic fungus Candida albicans. Mol Microbiol *42*, 673-687.

Lee, B.N., and Elion, E.A. (1999). The MAPKKK Ste11 regulates vegetative growth through a kinase cascade of shared signaling components. Proc Natl Acad Sci U S A *96*, 12679-12684.

Lee, N., and Kronstad, J.W. (2002). ras2 Controls morphogenesis, pheromone response, and pathogenicity in the fungal pathogen Ustilago maydis. Eukaryot Cell *1*, 954-966.

Lee, Y.H., and Dean, R.A. (1993). cAMP Regulates Infection Structure Formation in the Plant Pathogenic Fungus Magnaporthe grisea. Plant Cell *5*, 693-700.

Lemaire, K., Van de Velde, S., Van Dijck, P., and Thevelein, J.M. (2004). Glucose and sucrose act as agonist and mannose as antagonist ligands of the G protein-coupled receptor Gpr1 in the yeast Saccharomyces cerevisiae. Mol Cell *16*, 293-299.

Lesage, G., and Bussey, H. (2006). Cell wall assembly in Saccharomyces cerevisiae. Microbiol Mol Biol Rev *70*, 317-343.

Lev, S., and Horwitz, B.A. (2003). A mitogen-activated protein kinase pathway modulates the expression of two cellulase genes in Cochliobolus heterostrophus during plant infection. Plant Cell *15*, 835-844.

Lev, S., Sharon, A., Hadar, R., Ma, H., and Horwitz, B.A. (1999). A mitogen-activated protein kinase of the corn leaf pathogen Cochliobolus heterostrophus is involved in conidiation, appressorium formation, and pathogenicity: diverse roles for mitogen-activated protein kinase homologs in foliar pathogens. Proc Natl Acad Sci U S A *96*, 13542-13547.

Levin, D.E. (2005). Cell wall integrity signaling in Saccharomyces cerevisiae. Microbiol Mol Biol Rev *69*, 262-291.

Levitin, F., Stern, O., Weiss, M., Gil-Henn, C., Ziv, R., Prokocimer, Z., Smorodinsky, N.I., Rubinstein, D.B., and Wreschner, D.H. (2005). The MUC1 SEA module is a self-cleaving domain. The Journal of biological chemistry *280*, 33374-33386.

Li Destri Nicosia, M.G., Brocard-Masson, C., Demais, S., Hua Van, A., Daboussi, M.J., and Scazzocchio, C. (2001). Heterologous transposition in Aspergillus nidulans. Mol Microbiol *39*, 1330-1344.

Ligtenberg, M.J., Kruijshaar, L., Buijs, F., van Meijer, M., Litvinov, S.V., and Hilkens, J. (1992). Cell-associated episialin is a complex containing two proteins derived from a common precursor. The Journal of biological chemistry *267*, 6171-6177.

Livak, K.J., and Schmittgen, T.D. (2001). Analysis of relative gene expression data using real-time quantitative PCR and the 2(-Delta Delta C(T)) Method. Methods *25*, 402-408.

Lopez-Berges, M.S., Di Pietro, A., Daboussi, M.J., Wahab, H.A., Vasnier, C., Roncero, M.I., Dufresne, M., and Hera, C. (2009). Identification of virulence genes in Fusarium oxysporum f. sp. lycopersici by large-scale transposon tagging. Mol Plant Pathol *10*, 95-107.

Lorenz, M.C., and Heitman, J. (1998). The MEP2 ammonium permease regulates pseudohyphal differentiation in Saccharomyces cerevisiae. The EMBO journal *17*, 1236-1247.

Lorenz, M.C., Pan, X., Harashima, T., Cardenas, M.E., Xue, Y., Hirsch, J.P., and Heitman, J. (2000). The G protein-coupled receptor gpr1 is a nutrient sensor that regulates pseudohyphal differentiation in Saccharomyces cerevisiae. Genetics *154*, 609-622.

Lucas, J.A. (1998). Plant Pathology and Plant Pathogens. In, B. Science, ed., p. 274.

Ma, L.J., Van der Does, H.C., Borkovich, K.A., Coleman, J.J., Daboussi, M.J., Di Pietro, A., Dufresne, M., Freitag, M., Grabherr, M., Henrissat, B., Houterman, P.M., Kang, S., Shim, W.B., Woloshuk, C., Xie, X., Xu, J.R., Antoniw, J., Baker, S.E., Bluhm, B.H., Breakspear, A., Brown, D.W., Butchko, R.A.E., Chapman, S., Coulson, R., Coutinho, P.M., Danchin, E.G.J., Diener, A., Gale, L.R., Gardiner, D.M., Goff, S., Hammond-Kosack, K.E., Hilburn, K., Hua-Van, A., Jonkers, W., Kazan, K., Kodira, C.D., Koehrsen, M., Kumar, L., Lee, Y.H., Li, L., Manners, J.M., Miranda-Saavedra, D., Mukherjee, M., Park, G., Park, J., Park, S.Y., Proctor, R.H., Regev, A., Ruiz-Roldan, M.C., Sain, D., Sakthikumar, S., Sykes, S., Schwartz, D.C., Turgeon, B.G., Wapinski, I., Yoder, O., Young, S., Zeng, Q., Zhou, S., Galagan, J., Cuomo, C.A., Kistler, H.C., and Rep, M. (2010). Comparative genomics reveals mobile pathogenicity chromosomes in Fusarium oxysporum. Nature *464 (in press)*.

Ma, Y., Qiao, J., Liu, W., Wan, Z., Wang, X., Calderone, R., and Li, R. (2008). The sho1 sensor regulates growth, morphology, and oxidant adaptation in Aspergillus fumigatus but is not essential for development of invasive pulmonary aspergillosis. Infect Immun *76*, 1695-1701.

Macao, B., Johansson, D.G., Hansson, G.C., and Hard, T. (2006). Autoproteolysis coupled to protein folding in the SEA domain of the membrane-bound MUC1 mucin. Nature structural & molecular biology *13*, 71-76.

Madhani, H.D., and Fink, G.R. (1997). Combinatorial control required for the specificity of yeast MAPK signaling. Science *275*, 1314-1317.

Madhani, H.D., Styles, C.A., and Fink, G.R. (1997). MAP kinases with distinct inhibitory functions impart signaling specificity during yeast differentiation. Cell *91*, 673-684.

Madrid, M.P., Di Pietro, A., and Roncero, M.I. (2003). Class V chitin synthase determines pathogenesis in the vascular wilt fungus Fusarium oxysporum and mediates resistance to plant defence compounds. Mol Microbiol *47*, 257-266.

Maeda, T., Takekawa, M., and Saito, H. (1995). Activation of yeast PBS2 MAPKK by MAPKKKs or by binding of an SH3-containing osmosensor. Science *269*, 554-558.

Maiti, I.B., and Kolattukudy, P.E. (1979). Prevention of Fungal Infection of Plants by Specific Inhibition of Cutinase. Science *205*, 507-508.

Malardier, L., Daboussi, M.J., Julien, J., Roussel, F., Scazzocchio, C., and Brygoo, Y. (1989). Cloning of the nitrate reductase gene (niaD) of Aspergillus nidulans and its use for transformation of Fusarium oxysporum. Gene *78*, 147-156.

Malevich, K. (1926). The Non-Objective World: The Manifesto of Suprematism, trans. Howard Dearstyne.

Marcus, S., Polverino, A., Barr, M., and Wigler, M. (1994). Complexes between STE5 and components of the pheromone-responsive mitogen-activated protein kinase module. Proceedings of the National Academy of Sciences of the United States of America *91*, 7762-7766.

Marles, J.A., Dahesh, S., Haynes, J., Andrews, B.J., and Davidson, A.R. (2004). Protein-protein interaction affinity plays a crucial role in controlling the Sho1p-mediated signal transduction pathway in yeast. Mol Cell *14*, 813-823.

Martin-Urdiroz, M., Roncero, M.I., Gonzalez-Reyes, J.A., and Ruiz-Roldan, C. (2008). ChsVb, a class VII chitin synthase involved in septation, is critical for pathogenicity in Fusarium oxysporum. Eukaryot Cell *7*, 112-121.

Martin, H., Flandez, M., Nombela, C., and Molina, M. (2005). Protein phosphatases in MAPK signalling: we keep learning from yeast. Mol Microbiol *58*, 6-16.

Martinez-Rocha, A.L., Roncero, M.I., Lopez-Ramirez, A., Marine, M., Guarro, J., Martinez-Cadena, G., and Di Pietro, A. (2008). Rho1 has distinct functions in morphogenesis, cell wall biosynthesis and virulence of Fusarium oxysporum. Cell Microbiol *10*, 1339-1351.

Mattern, I.E., Punt, P.J., and van den Hondel, D.A. (1988). A vector of Aspergillus transformation conferring phleomycin resistance. Fungal Genet News *35*, 25.

Mayorga, M.E., and Gold, S.E. (2001). The ubc2 gene of Ustilago maydis encodes a putative novel adaptor protein required for filamentous growth, pheromone response and virulence. Mol Microbiol *41*, 1365-1379.

McMillan, J.N., Longtine, M.S., Sia, R.A., Theesfeld, C.L., Bardes, E.S., Pringle, J.R., and Lew, D.J. (1999). The morphogenesis checkpoint in Saccharomyces cerevisiae: cell cycle control of Swe1p degradation by Hsl1p and Hsl7p. Mol Cell Biol *19*, 6929-6939.

Mendgen, K., Hahn, M., and Deising, H. (1996). Morphogenesis and mechanisms of penetration by plant pathogenic fungi. Annu Rev Phytopathol *34*, 367-386.

Mey, G., Held, K., Scheffer, J., Tenberge, K.B., and Tudzynski, P. (2002). CPMK2, an SLT2-homologous mitogen-activated protein (MAP) kinase, is essential for pathogenesis of Claviceps purpurea on rye: evidence for a second conserved pathogenesis-related MAP kinase cascade in phytopathogenic fungi. Mol Microbiol *46*, 305-318.

Michielse, C.B., and Rep, M. (2009). Pathogen profile update: Fusarium oxysporum. Mol Plant Pathol *10*, 311-324.

Michielse, C.B., van Wijk, R., Reijnen, L., Cornelissen, B.J., and Rep, M. (2009a). Insight into the molecular requirements for pathogenicity of Fusarium oxysporum f. sp. lycopersici through large-scale insertional mutagenesis. Genome Biol *10*, R4.

Michielse, C.B., van Wijk, R., Reijnen, L., Manders, E.M., Boas, S., Olivain, C., Alabouvette, C., and Rep, M. (2009b). The nuclear protein Sge1 of Fusarium oxysporum is required for parasitic growth. PLoS Pathog *5*, e1000637.

Mitchell, T.K., and Dean, R.A. (1995). The cAMP-dependent protein kinase catalytic subunit is required for appressorium formation and pathogenesis by the rice blast pathogen Magnaporthe grisea. Plant Cell *7*, 1869-1878.

Mosch, H.U., Kubler, E., Krappmann, S., Fink, G.R., and Braus, G.H. (1999). Crosstalk between the Ras2p-controlled mitogen-activated protein kinase and cAMP pathways during invasive growth of Saccharomyces cerevisiae. Mol Biol Cell *10*, 1325-1335.

Mosch, H.U., Roberts, R.L., and Fink, G.R. (1996). Ras2 signals via the Cdc42/Ste20/mitogen-activated protein kinase module to induce filamentous growth in Saccharomyces cerevisiae. Proceedings of the National Academy of Sciences of the United States of America *93*, 5352-5356.

Mott, R. (2000). Accurate formula for P-values of gapped local sequence and profile alignments. Journal of molecular biology *300*, 649-659.

Muller, P., Weinzierl, G., Brachmann, A., Feldbrugge, M., and Kahmann, R. (2003). Mating and pathogenic development of the Smut fungus Ustilago maydis are regulated by one mitogen-activated protein kinase cascade. Eukaryot Cell *2*, 1187-1199.

Namiki, F., Matsunaga, M., Okuda, M., Inoue, I., Nishi, K., Fujita, Y., and Tsuge, T. (2001). Mutation of an arginine biosynthesis gene causes reduced pathogenicity in Fusarium oxysporum f. sp. melonis. Mol Plant Microbe Interact *14*, 580-584.

Nasmyth, K., and Dirick, L. (1991). The role of SWI4 and SWI6 in the activity of G1 cyclins in yeast. Cell *66*, 995-1013.

Nelson, B., Parsons, A.B., Evangelista, M., Schaefer, K., Kennedy, K., Ritchie, S., Petryshen, T.L., and Boone, C. (2004). Fus1p interacts with components of the Hog1p mitogen-activated protein kinase and Cdc42p morphogenesis signaling pathways to control cell fusion during yeast mating. Genetics *166*, 67-77.

Nern, A., and Arkowitz, R.A. (1999). A Cdc24p-Far1p-Gbetagamma protein complex required for yeast orientation during mating. The Journal of cell biology *144*, 1187-1202.

Nucci, M., and Anaissie, E. (2002). Cutaneous infection by Fusarium species in healthy and immunocompromised hosts: implications for diagnosis and management. Clin Infect Dis *35*, 909-920.

O'Donnell, K., Sutton, D.A., Rinaldi, M.G., Magnon, K.C., Cox, P.A., Revankar, S.G., Sanche, S., Geiser, D.M., Juba, J.H., van Burik, J.A., Padhye, A., Anaissie, E.J., Francesconi, A., Walsh, T.J., and Robinson, J.S. (2004). Genetic diversity of human pathogenic members of the Fusarium oxysporum complex inferred from multilocus DNA sequence data and amplified fragment length polymorphism analyses: evidence for the recent dispersion of a geographically widespread clonal lineage and nosocomial origin. J Clin Microbiol *42*, 5109-5120.

O'Rourke, S.M., and Herskowitz, I. (1998). The Hog1 MAPK prevents cross talk between the HOG and pheromone response MAPK pathways in Saccharomyces cerevisiae. Genes Dev *12*, 2874-2886.

O'Rourke, S.M., and Herskowitz, I. (2002). A third osmosensing branch in Saccharomyces cerevisiae requires the Msb2 protein and functions in parallel with the Sho1 branch. Mol Cell Biol *22*, 4739-4749.

Ochiai, N., Tokai, T., Nishiuchi, T., Takahashi-Ando, N., Fujimura, M., and Kimura, M. (2007). Involvement of the osmosensor histidine kinase and osmotic stress-activated protein kinases in the regulation of secondary metabolism in Fusarium graminearum. Biochem Biophys Res Commun *363*, 639-644.

Olson, G.M., Fox, D.S., Wang, P., Alspaugh, J.A., and Buchanan, K.L. (2007). Role of protein O-mannosyltransferase Pmt4 in the morphogenesis and virulence of Cryptococcus neoformans. Eukaryot Cell *6*, 222-234.

Ori, N., Eshed, Y., Paran, I., Presting, G., Aviv, D., Tanksley, S., Zamir, D., and Fluhr, R. (1997). The I2C family from the wilt disease resistance locus I2 belongs to the nucleotide binding, leucine-rich repeat superfamily of plant resistance genes. Plant Cell *9*, 521-532.

Orlova, M., Kanter, E., Krakovich, D., and Kuchin, S. (2006). Nitrogen availability and TOR regulate the Snf1 protein kinase in Saccharomyces cerevisiae. Eukaryotic cell *5*, 1831-1837.

Ortoneda, M., Guarro, J., Madrid, M.P., Caracuel, Z., Roncero, M.I., Mayayo, E., and Di Pietro, A. (2004). Fusarium oxysporum as a multihost model for the genetic dissection of fungal virulence in plants and mammals. Infect Immun *72*, 1760-1766.

Ospina-Giraldo, M.D., Mullins, E., and Kang, S. (2003). Loss of function of the Fusarium oxysporum SNF1 gene reduces virulence on cabbage and Arabidopsis. Curr Genet *44*, 49-57.

Ozaki, K., Tanaka, K., Imamura, H., Hihara, T., Kameyama, T., Nonaka, H., Hirano, H., Matsuura, Y., and Takai, Y. (1996). Rom1p and Rom2p are GDP/GTP exchange proteins (GEPs) for the Rho1p small GTP binding protein in Saccharomyces cerevisiae. Embo J *15*, 2196-2207.

Pareja-Jaime, Y., Roncero, M.I., and Ruiz-Roldan, M.C. (2008). Tomatinase from Fusarium oxysporum f. sp. lycopersici is required for full virulence on tomato plants. Mol Plant Microbe Interact *21*, 728-736.

Park, G., Xue, C., Zhao, X., Kim, Y., Orbach, M., and Xu, J.R. (2006). Multiple upstream signals converge on the adaptor protein Mst50 in Magnaporthe grisea. Plant Cell *18*, 2822-2835.

Peter, M., Gartner, A., Horecka, J., Ammerer, G., and Herskowitz, I. (1993). FAR1 links the signal transduction pathway to the cell cycle machinery in yeast. Cell *73*, 747-760.

Pfaffl, M.W. (2001). A new mathematical model for relative quantification in real-time RT-PCR. Nucleic acids research *29*, e45.

Philip, B., and Levin, D.E. (2001). Wsc1 and Mid2 are cell surface sensors for cell wall integrity signaling that act through Rom2, a guanine nucleotide exchange factor for Rho1. Mol Cell Biol *21*, 271-280.

Pierleoni, A., Martelli, P.L., and Casadio, R. (2008). PredGPI: a GPI-anchor predictor. BMC bioinformatics *9*, 392.

Pitoniak, A., Birkaya, B., Dionne, H.M., Vadaie, N., and Cullen, P.J. (2009). The signaling mucins Msb2 and Hkr1 differentially regulate the filamentation mitogen-activated protein kinase pathway and contribute to a multimodal response. Mol Biol Cell *20*, 3101-3114.

Posas, F., and Saito, H. (1997). Osmotic activation of the HOG MAPK pathway via Ste11p MAPKKK: scaffold role of Pbs2p MAPKK. Science *276*, 1702-1705.

Posas, F., Wurgler-Murphy, S.M., Maeda, T., Witten, E.A., Thai, T.C., and Saito, H. (1996). Yeast HOG1 MAP kinase cascade is regulated by a multistep phosphorelay mechanism in the SLN1-YPD1-SSK1 "two-component" osmosensor. Cell *86*, 865-875.

Powell, W.A., and Kistler, H.C. (1990). In vivo rearrangement of foreign DNA by Fusarium oxysporum produces linear self-replicating plasmids. J Bacteriol *172*, 3163-3171.

Prados-Rosales, R., Luque-Garcia, J.L., Martinez-Lopez, R., Gil, C., and Di Pietro, A. (2009). The Fusarium oxysporum cell wall proteome under adhesion-inducing conditions. Proteomics *9*, 4755-4769.

Prados-Rosales, R.C., Serena, C., Delgado-Jarana, J., Guarro, J., and Di Pietro, A. (2006). Distinct signalling pathways coordinately contribute to virulence of Fusarium oxysporum on mammalian hosts. Microbes Infect *8*, 2825-2831.

Prados Rosales, R.C., and Di Pietro, A. (2008). Vegetative hyphal fusion is not essential for plant infection by Fusarium oxysporum. Eukaryot Cell *7*, 162-171.

Prill, S.K., Klinkert, B., Timpel, C., Gale, C.A., Schroppel, K., and Ernst, J.F. (2005). PMT family of Candida albicans: five protein mannosyltransferase isoforms affect growth, morphogenesis and antifungal resistance. Mol Microbiol *55*, 546-560.

Printen, J.A., and Sprague, G.F., Jr. (1994). Protein-protein interactions in the yeast pheromone response pathway: Ste5p interacts with all members of the MAP kinase cascade. Genetics *138*, 609-619.

Puhalla, J.E. (1968). Compatibility reactions on solid medium and interstrain inhibition in Ustilago maydis. Genetics *60*, 461-474.

Puhalla, J.E. (1985). Classification of strains of Fusarium oxysporum on the basis of vegetative incompatibility. Can J Bot *63*, 183.

Punt, P.J., Oliver, R.P., Dingemanse, M.A., Pouwels, P.H., and van den Hondel, C.A. (1987). Transformation of Aspergillus based on the hygromycin B resistance marker from Escherichia coli. Gene *56*, 117-124.

Punt, P.J., Schuren, F.H., Lehmbeck, J., Christensen, T., Hjort, C., and van den Hondel, C.A. (2008). Characterization of the Aspergillus niger prtT, a unique regulator of extracellular protease encoding genes. Fungal Genet Biol *45*, 1591-1599.

Qi, M., and Elion, E.A. (2005). MAP kinase pathways. J Cell Sci *118*, 3569-3572.

Raitt, D.C., Posas, F., and Saito, H. (2000). Yeast Cdc42 GTPase and Ste20 PAK-like kinase regulate Sho1-dependent activation of the Hog1 MAPK pathway. Embo J *19*, 4623-4631.

Ram, A.F., and Klis, F.M. (2006). Identification of fungal cell wall mutants using susceptibility assays based on Calcofluor white and Congo red. Nature protocols *1*, 2253-2256.

Ramos, B., Alves-Santos, F.M., Garcia-Sanchez, M.A., Martin-Rodrigues, N., Eslava, A.P., and Diaz-Minguez, J.M. (2007). The gene coding for a new transcription factor (ftf1) of Fusarium oxysporum is only expressed during infection of common bean. Fungal Genet Biol *44*, 864-876.

Reiser, V., Salah, S.M., and Ammerer, G. (2000). Polarized localization of yeast Pbs2 depends on osmostress, the membrane protein Sho1 and Cdc42. Nature cell biology *2*, 620-627.

Rep, M., Meijer, M., Houterman, P.M., van der Does, H.C., and Cornelissen, B.J. (2005). Fusarium oxysporum evades I-3-mediated resistance without altering the matching avirulence gene. Mol Plant Microbe Interact *18*, 15-23.

Rep, M., van der Does, H.C., Meijer, M., van Wijk, R., Houterman, P.M., Dekker, H.L., de Koster, C.G., and Cornelissen, B.J. (2004). A small, cysteine-rich protein secreted by Fusarium oxysporum during colonization of xylem vessels is required for I-3-mediated resistance in tomato. Mol Microbiol *53*, 1373-1383.

Reyes, G., Romans, A., Nguyen, C.K., and May, G.S. (2006). Novel mitogen-activated protein kinase MpkC of Aspergillus fumigatus is required for utilization of polyalcohol sugars. Eukaryot Cell *5*, 1934-1940.

Rispail, N., and Di Pietro, A. (2009). *Fusarium oxysporum* Ste12 controls invasive growth and virulence downstream of the Fmk1 MAPK cascade. Mol Plant Microbe Interact *22*, 830-839.

Rispail, N., Soanes, D.M., Ant, C., Czajkowski, R., Grunler, A., Huguet, R., Perez-Nadales, E., Poli, A., Sartorel, E., Valiante, V., Yang, M., Beffa, R., Brakhage, A.A., Gow, N.A., Kahmann, R., Lebrun, M.H., Lenasi, H., Perez-Martin, J., Talbot, N.J., Wendland, J., and Di Pietro, A. (2009). Comparative genomics of MAP kinase and calcium-calcineurin signalling components in plant and human pathogenic fungi. Fungal Genet Biol *46*, 287-298.

Roberts, R.L., and Fink, G.R. (1994). Elements of a single MAP kinase cascade in Saccharomyces cerevisiae mediate two developmental programs in the same cell type: mating and invasive growth. Genes Dev *8*, 2974-2985.

Rodriguez-Galvez, E., and Mendgen, K. (1995). Cell wall synthesis in cotton roots after infection with Fusarium oxysporum. The deposition of callose, arabinogalactans, xyloglucans, and pectic components into walls, wall appositions, cell plates and plasmodesmata. Planta *197*, 535-545.

Rodriguez-Gálvez, E., and Mendgen, K. (1995). The infection process of *Fusarium oxysporum* in cotton root tips. Protoplasma *189*, 61-72.

Rohde, J.R., and Cardenas, M.E. (2004). Nutrient signaling through TOR kinases controls gene expression and cellular differentiation in fungi. Current topics in microbiology and immunology *279*, 53-72.

Roldan-Arjona, T., Perez-Espinosa, A., and Ruiz-Rubio, M. (1999). Tomatinase from Fusarium oxysporum f. sp. lycopersici defines a new class of saponinases. Mol Plant Microbe Interact *12*, 852-861.

Roman, E., Cottier, F., Ernst, J.F., and Pla, J. (2009). Msb2 signaling mucin controls activation of Cek1 mitogen-activated protein kinase in Candida albicans. Eukaryot Cell *8*, 1235-1249.

Roman, E., Nombela, C., and Pla, J. (2005). The Sho1 adaptor protein links oxidative stress to morphogenesis and cell wall biosynthesis in the fungal pathogen Candida albicans. Mol Cell Biol *25*, 10611-10627.

Roncero, C., and Duran, A. (1985). Effect of Calcofluor white and Congo red on fungal cell wall morphogenesis: in vivo activation of chitin polymerization. J Bacteriol *163*, 1180-1185.

Rua, D., Tobe, B.T., and Kron, S.J. (2001). Cell cycle control of yeast filamentous growth. Curr Opin Microbiol *4*, 720-727.

Ruiz-Roldan, C., Puerto-Galan, L., Roa, J., Castro, A., Di Pietro, A., Roncero, M.I., and Hera, C. (2008). The Fusarium oxysporum sti35 gene functions in thiamine biosynthesis and oxidative stress response. Fungal Genet Biol *45*, 6-16.

Ruiz-Roldan, M.C., Maier, F.J., and Schafer, W. (2001). PTK1, a mitogen-activated-protein kinase gene, is required for conidiation, appressorium formation, and pathogenicity of Pyrenophora teres on barley. Mol Plant Microbe Interact *14*, 116-125.

Ryals, J.A., Neuenschwander, U.H., Willits, M.G., Molina, A., Steiner, H.Y., and Hunt, M.D. (1996). Systemic Acquired Resistance. Plant Cell *8*, 1809-1819.

Sabbagh, W., Jr., Flatauer, L.J., Bardwell, A.J., and Bardwell, L. (2001). Specificity of MAP kinase signaling in yeast differentiation involves transient versus sustained MAPK activation. Mol Cell *8*, 683-691.

Sambrook, J., Fritsch, E.F., and Maniatis, T. (1989). "Molecular cloning: A laboratory manual" (2nd ed.). New York, NY (EEUU), Cold Spring Harbour Laboratory Press.

Sánchez López-Berges, M., Di Pietro, A., Daboussi, M.J., abdel Wahab, H., Vasnier, C., Roncero, M.I.G., Dufresne, M., and Hera, C. (2009). Identification of virulence genes in *Fusarium oxysporum* f. sp. *lycopersici* by large-scale transposon tagging. Mol Plant Pathol *(in press)*.

Sanz, P. (2003). Snf1 protein kinase: a key player in the response to cellular stress in yeast. Biochemical Society transactions *31*, 178-181.

Sato, N., Kawahara, H., Toh-e, A., and Maeda, T. (2003). Phosphorelay-regulated degradation of the yeast Ssk1p response regulator by the ubiquitin-proteasome system. Mol Cell Biol *23*, 6662-6671.

Scheel, D. (1998). Resistance response physiology and signal transduction. Curr Opin Plant Biol *1*, 305-310.

Schippers, B., and Van Eck, W.H. (1981). Formation and survival of chlamydospores in

Fusarium. In Fusarium: Diseases, Biology and Taxonomy, T.A.T. P.E. Nelson, R.J. Cook, eds, ed. (University Park and London., The Pennysylvania State University Press), pp. 250-260.

Sheu, Y.J., Santos, B., Fortin, N., Costigan, C., and Snyder, M. (1998). Spa2p interacts with cell polarity proteins and signaling components involved in yeast cell morphogenesis. Molecular and cellular biology *18*, 4053-4069.

Shulewitz, M.J., Inouye, C.J., and Thorner, J. (1999). Hsl7 localizes to a septin ring and serves as an adapter in a regulatory pathway that relieves tyrosine phosphorylation of Cdc28 protein kinase in Saccharomyces cerevisiae. Mol Cell Biol *19*, 7123-7137.

Siderius, M., Kolen, C.P., van Heerikhuizen, H., and Mager, W.H. (2000). Candidate osmosensors from Candida utilis and Kluyveromyces lactis: structural and functional homology to the Sho1p putative osmosensor from Saccharomyces cerevisiae. Biochimica et biophysica acta *1517*, 143-147.

Silverman, H.S., Parry, S., Sutton-Smith, M., Burdick, M.D., McDermott, K., Reid, C.J., Batra, S.K., Morris, H.R., Hollingsworth, M.A., Dell, A., and Harris, A. (2001). In vivo glycosylation of mucin tandem repeats. Glycobiology *11*, 459-471.

Singh, K.K. (2000). The Saccharomyces cerevisiae Sln1p-Ssk1p two-component system mediates response to oxidative stress and in an oxidant-specific fashion. Free radical biology & medicine *29*, 1043-1050.

Singh, P.K., and Hollingsworth, M.A. (2006). Cell surface-associated mucins in signal transduction. Trends Cell Biol *16*, 467-476.

Smith, D.G., Garcia-Pedrajas, M.D., Hong, W., Yu, Z., Gold, S.E., and Perlin, M.H. (2004). An ste20 homologue in Ustilago maydis plays a role in mating and pathogenicity. Eukaryot Cell *3*, 180-189.

Smith, S.E., Csank, C., Reyes, G., Ghannoum, M.A., and Berlin, V. (2002). Candida albicans RHO1 is required for cell viability in vitro and in vivo. FEMS Yeast Res *2*, 103-111.

Snyder, W.C., and Hansen, H.N. (1940). The species concept in Fusarium. Am J Bot *27*, 64-67.

Somssich, I.E., and Hahlbrock, K. (1998). Pathogen defense in plants - a paradigm of biological complexity. Trends Plant Sci *3*, 86-90.

Soupene, E., Ramirez, R.M., and Kustu, S. (2001). Evidence that fungal MEP proteins mediate diffusion of the uncharged species NH(3) across the cytoplasmic membrane. Molecular and cellular biology *21*, 5733-5741.

Sticher, L., Mauch-Mani, B., and Metraux, J.P. (1997). Systemic acquired resistance. Annu Rev Phytopathol *35*, 235-270.

Sweigard, J.A., Chumley, F.G., and Valent, B. (1992). Disruption of a Magnaporthe grisea cutinase gene. Mol Gen Genet *232*, 183-190.

Takano, Y., Kikuchi, T., Kubo, Y., Hamer, J.E., Mise, K., and Furusawa, I. (2000). The Colletotrichum lagenarium MAP kinase gene CMK1 regulates diverse aspects of fungal pathogenesis. Mol Plant Microbe Interact *13*, 374-383.

Takken, F.L.W., and Rep, M. (2010). The arms race between tomato and Fusarium oxysporum. Molecular Plant Pathology *11*, 309-314.

Tamaki, H., Miwa, T., Shinozaki, M., Saito, M., Yun, C.W., Yamamoto, K., and Kumagai, H. (2000). GPR1 regulates filamentous growth through FLO11 in yeast Saccharomyces cerevisiae. Biochemical and biophysical research communications *267*, 164-168.

Tatebayashi, K., Tanaka, K., Yang, H.Y., Yamamoto, K., Matsushita, Y., Tomida, T., Imai, M., and Saito, H. (2007). Transmembrane mucins Hkr1 and Msb2 are putative osmosensors in the SHO1 branch of yeast HOG pathway. Embo J.

Tatebayashi, K., Yamamoto, K., Tanaka, K., Tomida, T., Maruoka, T., Kasukawa, E., and Saito, H. (2006). Adaptor functions of Cdc42, Ste50, and Sho1 in the yeast osmoregulatory HOG MAPK pathway. Embo J *25*, 3033-3044.

Thompson, J.D., Higgins, D.G., and Gibson, T.J. (1994). CLUSTAL W: improving the sensitivity of progressive multiple sequence alignment through sequence weighting, position-specific gap penalties and weight matrix choice. Nucleic Acids Res *22*, 4673-4680.

Timpel, C., Zink, S., Strahl-Bolsinger, S., Schroppel, K., and Ernst, J. (2000). Morphogenesis, adhesive properties, and antifungal resistance depend on the Pmt6 protein mannosyltransferase in the fungal pathogen candida albicans. J Bacteriol *182*, 3063-3071.

Torres, A.M., Weeden, N.F., and Martín, A. (1993). Linkage among isozyme, RFLP and RAPD markers in Vicia faba. Theor Appl Genet *85*, 937-945.

Torres, L., Martin, H., Garcia-Saez, M.I., Arroyo, J., Molina, M., Sanchez, M., and Nombela, C. (1991). A protein kinase gene complements the lytic phenotype of Saccharomyces cerevisiae lyt2 mutants. Mol Microbiol *5*, 2845-2854.

Truckses, D.M., Garrenton, L.S., and Thorner, J. (2004). Jekyll and Hyde in the microbial world. Science (New York, NY *306*, 1509-1511.

Tsuji, G., Fujii, S., Tsuge, S., Shiraishi, T., and Kubo, Y. (2003). The Colletotrichum lagenariu Ste12-like gene CST1 is essential for appressorium penetration. Mol Plant Microbe Interact *16*, 315-325.

Vadaie, N., Dionne, H., Akajagbor, D.S., Nickerson, S.R., Krysan, D.J., and Cullen, P.J. (2008). Cleavage of the signaling mucin Msb2 by the aspartyl protease Yps1 is required for MAPK activation in yeast. J Cell Biol *181*, 1073-1081.

Valiante, V., Heinekamp, T., Jain, R., Hartl, A., and Brakhage, A.A. (2008). The mitogen-activated protein kinase MpkA of Aspergillus fumigatus regulates cell wall signaling and oxidative stress response. Fungal Genet Biol *45*, 618-627.

van Drogen, F., and Peter, M. (2002). Spa2p functions as a scaffold-like protein to recruit the Mpk1p MAP kinase module to sites of polarized growth. Curr Biol *12*, 1698-1703.

Van Loon, L.C. (1997). Induced resistance in plants and role of pathogenesis-related proteins. Eur J Plant Pathol *103*, 753-765.

Van Nuland, A., Vandormael, P., Donaton, M., Alenquer, M., Lourenco, A., Quintino, E., Versele, M., and Thevelein, J.M. (2006). Ammonium permease-based sensing mechanism for rapid ammonium activation of the protein kinase A pathway in yeast. Molecular microbiology *59*, 1485-1505.

Verstrepen, K.J., Jansen, A., Lewitter, F., and Fink, G.R. (2005). Intragenic tandem repeats generate functional variability. Nat Genet *37*, 986-990.

Verstrepen, K.J., and Klis, F.M. (2006). Flocculation, adhesion and biofilm formation in yeasts. Mol Microbiol *60*, 5-15.

Vinod, P.K., Sengupta, N., Bhat, P.J., and Venkatesh, K.V. (2008). Integration of global signaling pathways, cAMP-PKA, MAPK and TOR in the regulation of FLO11. PLoS One *3*, e1663.

Wang, C., Duan, Z., and St Leger, R.J. (2008). MOS1 osmosensor of Metarhizium anisopliae is required for adaptation to insect host hemolymph. Eukaryot Cell *7*, 302-309.

Wang, Y., and Dohlman, H.G. (2002). Pheromone-dependent ubiquitination of the mitogen-activated protein kinase kinase Ste7. The Journal of biological chemistry *277*, 15766-15772.

Wang, Y., and Dohlman, H.G. (2004). Pheromone signaling mechanisms in yeast: a prototypical sex machine. Science *306*, 1508-1509.

Wang, Y., Ge, Q., Houston, D., Thorner, J., Errede, B., and Dohlman, H.G. (2003). Regulation of Ste7 ubiquitination by Ste11 phosphorylation and the Skp1-Cullin-F-box complex. The Journal of biological chemistry *278*, 22284-22289.

Westfall, P.J., and Thorner, J. (2006). Analysis of mitogen-activated protein kinase signaling specificity in response to hyperosmotic stress: use of an analog-sensitive HOG1 allele. Eukaryot Cell *5*, 1215-1228.

Widmann, C., Gibson, S., Jarpe, M.B., and Johnson, G.L. (1999). Mitogen-activated protein kinase: conservation of a three-kinase module from yeast to human. Physiol Rev *79*, 143-180.

Wiebe, M.G. (2002). Myco-protein from Fusarium venenatum: a well-established product for human consumption. Appl Microbiol Biotechnol *58*, 421-427.

Wiget, P., Shimada, Y., Butty, A.C., Bi, E., and Peter, M. (2004). Site-specific regulation of the GEF Cdc24p by the scaffold protein Far1p during yeast mating. The EMBO journal *23*, 1063-1074.

Wilson, R.A., and Talbot, N.J. (2009). Under pressure: investigating the biology of plant infection by Magnaporthe oryzae. Nat Rev Microbiol *7*, 185-195.

Willer, T., Valero, M.C., Tanner, W., Cruces, J., and Strahl, S. (2003). O-mannosyl glycans: from yeast to novel associations with human disease. Current opinion in structural biology *13*, 621-630.

Willger, S.D., Ernst, J.F., Alspaugh, J.A., and Lengeler, K.B. (2009). Characterization of the PMT gene family in Cryptococcus neoformans. PLoS One *4*, e6321.

Wollenweber, H.W., and Reinking, O.A. (1935). Die fusarien, ihre eschreibung, schadwirkung und bekämpfung. Berlin, Alemania, Ed Parey, P.

Wreschner, D.H., Zrihan-Licht, S., Baruch, A., Sagiv, D., Hartman, M.L., Smorodinsky, N., and Keydar, I. (1994). Does a novel form of the breast cancer marker protein, MUC1, act as a receptor molecule that modulates signal transduction? Adv Exp Med Biol *353*, 17-26.

Wu, C., Jansen, G., Zhang, J., Thomas, D.Y., and Whiteway, M. (2006). Adaptor protein Ste50p links the Ste11p MEKK to the HOG pathway through plasma membrane association. Genes & development *20*, 734-746.

Xu, F., Palmer, A.E., Yaver, D.S., Berka, R.M., Gambetta, G.A., Brown, S.H., and Solomon, E.I. (1999). Targeted mutations in a Trametes villosa laccase. Axial perturbations of the T1 copper. The Journal of biological chemistry *274*, 12372-12375.

Xu, J.R., and Hamer, J.E. (1996). MAP kinase and cAMP signaling regulate infection structure formation and pathogenic growth in the rice blast fungus Magnaporthe grisea. Genes Dev *10*, 2696-2706.

Xu, J.R., Staiger, C.J., and Hamer, J.E. (1998). Inactivation of the mitogen-activated protein kinase Mps1 from the rice blast fungus prevents penetration of host cells but allows activation of plant defense responses. Proc Natl Acad Sci U S A *95*, 12713-12718.

Xue, T., Nguyen, C.K., Romans, A., and May, G.S. (2004). A mitogen-activated protein kinase that senses nitrogen regulates conidial germination and growth in Aspergillus fumigatus. Eukaryot Cell *3*, 557-560.

Xue, Y., Batlle, M., and Hirsch, J.P. (1998). GPR1 encodes a putative G protein-coupled receptor that associates with the Gpa2p Galpha subunit and functions in a Ras-independent pathway. Embo J *17*, 1996-2007.

Yang, H.Y., Tatebayashi, K., Yamamoto, K., and Saito, H. (2009). Glycosylation defects activate filamentous growth Kss1 MAPK and inhibit osmoregulatory Hog1 MAPK. Embo J *28*, 1380-1391.

Yang, L., Ukil, L., Osmani, A., Nahm, F., Davies, J., De Souza, C.P., Dou, X., Perez-Balaguer, A., and Osmani, S.A. (2004). Rapid production of gene replacement constructs and generation of a green fluorescent protein-tagged centromeric marker in Aspergillus nidulans. Eukaryot Cell *3*, 1359-1362.

Zapater, M., Clotet, J., Escote, X., and Posas, F. (2005). Control of cell cycle progression by the stress-activated Hog1 MAPK. Cell cycle (Georgetown, Tex *4*, 6-7.

Zarrinpar, A., Bhattacharyya, R.P., Nittler, M.P., and Lim, W.A. (2004). Sho1 and Pbs2 act as coscaffolds linking components in the yeast high osmolarity MAP kinase pathway. Mol Cell *14*, 825-832.

Zarrinpar, A., Park, S.H., and Lim, W.A. (2003). Optimization of specificity in a cellular protein interaction network by negative selection. Nature *426*, 676-680.

Zarzov, P., Mazzoni, C., and Mann, C. (1996). The SLT2(MPK1) MAP kinase is activated during periods of polarized cell growth in yeast. Embo J *15*, 83-91.

Zhang, N., O'Donnell, K., Sutton, D.A., Nalim, F.A., Summerbell, R.C., Padhye, A.A., and Geiser, D.M. (2006). Members of the Fusarium solani species complex that cause infections in both humans and plants are common in the environment. J Clin Microbiol *44*, 2186-2190.

Zhao, X., Mehrabi, R., and Xu, J.R. (2007). Mitogen-activated protein kinase pathways and fungal pathogenesis. Eukaryot Cell *6*, 1701-1714.

Zheng, L., Campbell, M., Murphy, J., Lam, S., and Xu, J.R. (2000). The BMP1 gene is essential for pathogenicity in the gray mold fungus Botrytis cinerea. Mol Plant Microbe Interact *13*, 724-732.

Zheng, W., Zhao, Z., Chen, J., Liu, W., Ke, H., Zhou, J., Lu, G., Darvill, A.G., Albersheim, P., Wu, S., and Wang, Z. (2009). A Cdc42 ortholog is required for penetration and virulence of Magnaporthe grisea. Fungal Genet Biol *46*, 450-460.

# Supplementary data

**Table 16. F. oxysporum mucins**
See Section 9.3 of Materials and Methods for a detailed explanation of mucinpredictor (PTSpred algorithm) and output. Results are summarised in Table 14. N/Y, No/Yes

| mucinpredictor | | BlastP | SignalP | | PSORT | TMHMM | | | | PredGPI |
|---|---|---|---|---|---|---|---|---|---|---|
| positives | output | | N/Y | site | S=secretory pathway | N/Y | TMHs | N-terminus | Protein lenght | Specificity |
| 1 >FOXT_00212 | 131 180 153 | N | Y | 18 | S | N | | | len=202 | 100% |
| 2 >FOXT_00406 | 276 330 300 | N | Y | 21 | S | N | | | len=349 | |
| 3 >FOXT_00651 | 86 140 401 | N | Y | 17 | | N | | | len=450 | |
| 4 >FOXT_00727 | 176 225 810 | N | Y | 25 | | N | | | len=859 | |
| 5 >FOXT_00987 | 591 640 662 | N | Y | 20 | | N | | | len=711 | |
| 6 >FOXT_01333 | 21 135 397/ 241 315 397 | N | Y | 22 | S | N | | | len=446 | |
| 7 >FOXT_01457 | 96 215 232 | N | Y | 22 | S | N | | | len=281 | |
| 8 >FOXT_01836 | 56 140 739 | N | Y | 30 | | N | | | len=788 | |
| 9 >FOXT_01864 | 286 350 373 | N | Y | 39 | | Y | 1 | inside 1 27 | len=422 | Lowly probable 99,1% |
| 10 >FOXT_02131 | 76 145 842 | N | Y | 25 | | N | | | len=891 | |
| 11 >FOXT_02179 | 281 400 624 | N | Y | 22 | S | N | | | len=673 | |
| 12 >FOXT_02477 | 251 310 657 | N | Y | 18 | S | N | | | len=706 | 100% |
| 13 >FOXT_02535 | 16 65 349 | N | Y | 19 | S | N | | | len=398 | |
| 14 >FOXT_02549 | 236 305 396/ 316 380 396 | N | Y | 22 | S | N | | | len=445 | |
| 15 >FOXT_02684 | 21 70 930 | N | Y | 23 | S | N | | | len=979 | |
| 16 >FOXT_02708 | 16 70 253 | N | Y | 23 | S | N | | | len=302 | |
| 17 >FOXT_02748 | 226 500 516 | FOXG_09254.2 | Y | 22 | S | N | | | len=565 | |
| 18 >FOXT_02757 | 226 290 738/316 395 738/ 601 660 738 | N | Y | 22 | S | N | | | len=787 | |
| 19 >FOXT_02830 | 21 75 579/ 396 450 579 | FOXG_09254.2 | Y | 20 | S | N | | | len=628 | |
| 20 >FOXT_03079 | 41 90 2254 | N | Y | 22 | | N | | | len=2303 | |
| 21 >FOXT_03295 | 546 600 800 | N | Y | 28 | S | N | | | len=849 | |
| 22 >FOXT_03318 | 6 55 536 | N | Y | 19 | S | N | | | len=585 | |
| 23 >FOXT_03627 | 1 60 97 | N | Y | 20 | S | Y | 1 | outside 1 59 | len=146 | |
| 24 >FOXT_03689 | 76 140 636 | N | Y | 21 | | N | | | len=685 | |
| 25 >FOXT_03736 | 551 600 1263/1051 1100 1263 | N | Y | 22 | S | N | | | len=1312 | |
| 26 >FOXT_03771 | 241 340 323 | N | Y | 22 | S | N | | | len=372 | |
| 27 >FOXT_03977 | 6 65 262 | N | Y | 17 | S | N | | | len=311 | |
| 28 >FOXT_04235 | 191 245 1277 | N | Y | 25 | | N | | | len=1326 | |
| 29 >FOXT_04380 | 96 145 573 | N | Y | 25 | | N | | | len=622 | |

| mucinpredictor | | BlastP | SignalP | | PSORT | | TMHMM | | | PredGPI |
|---|---|---|---|---|---|---|---|---|---|---|
| positives | output | | N/Y | site | S=secretory pathway | N/Y | TMHs | N-terminus | Protein lenght | Specificity |
| 30 >FOXT_04390 | 56 145 493/ 206 255 493 | N | Y | 20 | S | N | | | len=542 | |
| 31 >FOXT_04429 | 151 290 409 | N | Y | 23 | S | N | | | len=458 | 100% |
| 32 >FOXT_04531 | 11 90 128 | N | Y | 20 | S | N | | | len=177 | |
| 33 >FOXT_04553 | 16 70 279/ 81 140 279/ 201 250 279 | N | Y | 20 | S | N | | | len=210 | |
| 34 >FOXT_04554 | 16 70 240 | N | Y | 22 | S | N | | | len=289 | |
| 35 >FOXT_04562 | 26 100 270 | N | Y | 20 | S | N | | | len=319 | |
| 36 >FOXT_04584 | 16 70 276 | N | Y | 20 | S | N | | | len=325 | |
| 37 >FOXT_04672 | 431 495 1130 | FOXG_09254.2 | Y | 18 | S | N | | | len=1179 | |
| 38 >FOXT_04871 | 471 525 795/ 546 650 795 | N | Y | 20 | S | N | | | len=844 | |
| 39 >FOXT_04945 | 116 175 218 | N | Y | 21 | S | Y | 1 | outside 1 178 | len=268 | |
| 40 >FOXT_05153 | 406 475 854 | N | Y | 20 | S | Y | 1 | outside 1 467 | len=903 | |
| 41 >FOXT_05232 | 221 300 380 | N | Y | 22 | S | N | | | len=429 | 99,90% |
| 42 >FOXT_05237 | 46 125 395 | N | Y | 21 | S | N | | | len=444 | 99,90% |
| 43 >FOXT_05751 | 141 190 268 | N | Y | 24 | S | N | | | len=317 | |
| 44 >FOXT_05799 | 66 130 209 | N | Y | 20 | S | N | | | len=258 | |
| 45 >FOXT_05951 | 16 90 593/286 335 593/ 391 555 593 | YGR014W/FOXG_09254.2 | Y | 22 | S | N | | | len=642 | |
| 46 >FOXT_06133 | 41 90 80 | N | Y | 18 | S | N | | | len=129 | 100% |
| 47 >FOXT_07786 | 191 245 219 | N | Y | 23 | S | N | | | len=268 | 100% |
| 48 >FOXT_07817 | 186 245 335 | N | Y | 30 | S | Y | 2 | inside 1 11 | len=384 | |
| 49 >FOXT_08027 | 476 555 588 | N | Y | 21 | S | N | | | len=637 | |
| 50 >FOXT_08348 | 131 245 212 | N | Y | 21 | S | N | | | len=261 | 100% |
| 51 >FOXT_08449 | 161 225 424 | N | Y | 26 | S | Y | 1 | outside 1 292 | len=473 | |
| 52 >FOXT_08464 | 396 690 671 | N | Y | 20 | S | N | | | len=720 | |
| 53 >FOXT_08601 | 326 450 448 | N | Y | 23 | S | N | | | len=497 | 99,90% |
| 54 >FOXT_08719 | 71 165 145 | N | Y | 21 | S | N | | | len=194 | 100% |
| 55 >FOXT_08834 | 456 525 522 | N | Y | 22 | | N | | | len=516 | |
| 56 >FOXT_09508 | 81 140 485 | N | Y | 19 | | N | | | len=534 | |
| 57 >FOXT_09610 | 301 350 334 | N | Y | 18 | S | N | | | len=383 | |
| 58 >FOXT_09662 | 11 75 270 | N | Y | 17 | S | N | | | len=319 | |
| 59 >FOXT_09715 | 86 240 305 | N | Y | 22 | S | N | | | len=354 | |
| 60 >FOXT_09839 | 126 185 235 | N | Y | 17 | | N | | | | |
| 61 >FOXT_09982 | 121 170 316 | N | Y | 17 | S | Y | 1 | outside 1 171 | len=365 | |

| mucinpredictor | | BlastP | SignalP | | PSORT | TMHMM | | | | PredGPI |
|---|---|---|---|---|---|---|---|---|---|---|
| positives | output | | N/Y | site | S=secretory pathway | N/Y | TMHs | N-terminus | Protein lenght | Specificity |
| 62 >FOXT_10069 | 456 505 647 | FOXG_09254.2 | Y | 18 | S | N | | | len=696 | |
| 63 >FOXT_10325 | 396 455 430 | N | Y | 19 | S | N | | | len=479 | 100% |
| 64 >FOXT_10371 | 126 180 228 | N | Y | 21 | S | Y | 1 | outside 1 187 | len=277 | |
| 65 >FOXT_10582 | 51 110 796/ 466 585 796 | N | Y | 24 | S | N | | | len=845 | |
| 66 >FOXT_10761 | 626 680 842 | FOXG_09254.2 | Y | 24 | S | N | | | len=891 | |
| 67 >FOXT_11116 | 151 280 653/ 321 385 653 | FOXG_09254.2 | Y | 17 | S | N | | | len=702 | |
| 68 >FOXT_11136 | 111 170 307 | N | Y | 17 | S | N | | | len=356 | |
| 69 >FOXT_11183 | 281 335 786 | N | Y | 17 | | N | | | len=835 | |
| 70 >FOXT_11586 | 41 125 437 | N | Y | 22 | S | Y | 1 | inside 1 4 | len=486 | |
| 71 >FOXT_11705 | 386 515 694 | N | Y | 18 | S | N | | | len=743 | 100% |
| 72 >FOXT_11738 | 16 70 212 | N | Y | 20 | S | N | | | len=261 | |
| 73 >FOXT_11839 | 86 145 357 | N | Y | 21 | S | N | | | len=406 | |
| 74 >FOXT_12168 | 186 235 215 | N | Y | 19 | S | N | | | len=264 | 100% |
| 75 >FOXT_12393 | 156 235 201 | N | Y | 19 | S | N | | | len=250 | |
| 76 >FOXT_12408 | 96 205 417 | N | Y | 24 | S | N | | | len=466 | 100% |
| 77 >FOXT_12567 | 296 350 1299 | N | Y | 27 | | N | | | len=1348 | |
| 78 >FOXT_12618 | 296 350 1299 | N | Y | 27 | | N | | | len=1348 | |
| 79 >FOXT_12739 | 36 90 171 | N | Y | 18 | S | Y | 1 | outside 1 166 | len=220 | |
| 80 >FOXT_12855 | 61 150 259 | N | Y | 17 | S | N | | | len=308 | |
| 81 >FOXT_12886 | 91 515 1099/ 616 685 1099 | N | Y | 37 | S | N | | | len=1148 | |
| 82 >FOXT_12956 | 16 65 236 | N | Y | 19 | S | N | | | len=285 | |
| 83 >FOXT_13040 | 16 100 149 | N | Y | 18 | S | N | | | len=198 | |
| 84 >FOXT_13111 | 391 440 407 | N | Y | 19 | S | N | | | len=456 | |
| 85 >FOXT_13131 | 21 105 212 | N | Y | 22 | S | N | | | len=261 | |
| 86 >FOXT_13141 | 11 75 114/ 81 140 114 | N | Y | 23 | S | N | | | len=163 | |
| 87 >FOXT_13158 | 591 640 707 | N | Y | 19 | S | Y | 7 | outside 1 158 | len=756 | |
| 88 >FOXT_13293 | 306 405 387 | N | Y | 20 | S | N | | | len=436 | |
| 89 >FOXT_13529 | 11 70 197 | N | Y | 20 | S | N | | | len=246 | 99,60% |
| 90 >FOXT_13532 | 336 385 609 | N | Y | 20 | S | N | | | len=658 | |
| 91 >FOXT_13555 | 291 350 328 | N | Y | 20 | S | N | | | len=377 | |
| 92 >FOXT_13562 | 11 105 137 | N | Y | 19 | S | N | | | len=186 | |
| 93 >FOXT_13582 | 71 125 271 | N | Y | 20 | S | N | | | len=320 | |
| 94 >FOXT_13656 | 371 425 1603 | N | Y | 23 | | N | | | len=1653 | |
| 95 >FOXT_13674 | 106 155 334 | N | Y | 19 | S | N | | | len=383 | |

| mucinpredictor | | BlastP | SignalP | | PSORT | TMHMM | | | | PredGPI |
|---|---|---|---|---|---|---|---|---|---|---|
| positives | output | | N/Y | site | S=secretory pathway | N/Y | TMHs | N-terminus | Protein lenght | Specificity |
| 96 >FOXT_13794 | 331 395 1348/ 736 805 1348 | N | Y | 20 | S | N | | | len=1397 | |
| 97 >FOXT_13800 | 236 320 801/ 536 600 801/ 696 760 801 | N | Y | 22 | S | N | | | len=850 | |
| 98 >FOXT_13973 | 296 350 1299 | N | Y | 27 | | N | | | len=1348 | |
| 99 >FOXT_14129 | 121 205 417 | N | Y | 24 | S | N | | | len=466 | 99,90% |
| 100 >FOXT_14221 | 396 450 1399 | N | Y | 24 | | N | | | len=1448 | |
| 101 >FOXT_14372 | 176 235 191 | N | Y | 22 | S | N | | | len=240 | |
| 102 >FOXT_14577 | 196 250 342 | N | Y | 20 | S | Y | 1 | outside 1 247 | len=391 | |
| 103 >FOXT_14758 | 121 210 215 | N | Y | 20 | S | Y | 1 | inside 1 6 | len=264 | |
| 104 >FOXT_14817 | 221 315 374 | N | Y | 16 | S | N | | | len=423 | |
| 105 >FOXT_14996 | 526 575 1181/ 956 1005 1181 | N | Y | 18 | S | N | | | len=1230 | |
| 106 >FOXT_15109 | 176 235 191 | N | Y | 22 | S | N | | | len=240 | |
| 107 >FOXT_15304 | 131 180 220 | N | Y | 23 | S | Y | 1 | outside 1 192 | len=269 | |
| 108 >FOXT_15436 | 181 240 321 | N | Y | 17 | S | Y | 1 | outside 1 233 | len=370 | |
| 109 >FOXT_15439 | 11 75 797/246 305 797/ 421 475 797/ 591 655 797 | N | Y | 20 | S | N | | | len=846 | |
| 110 >FOXT_15778 | 21 75 635/ 241 315 635 | N | Y | 19 | S | N | | | len=684 | |
| 111 >FOXT_16792 | 66 145 228 | N | Y | 19 | S | N | | | len=277 | 99,90% |
| 112 >FOXT_16838 | 231 295 304 | N | Y | 20 | S | N | | | len=353 | |
| 113 >FOXT_17058 | 296 350 1299 | N | Y | 27 | | N | | | len=1348 | |
| 114 >FOXT_17095 | 101 170 379/ 276 340 379 | N | Y | 38 | | N | | | len=428 | |
| 115 >FOXT_17167 | 136 200 642 | N | Y | 29 | S | N | | | len=691 | |
| 116 >FOXT_17323 | 101 170 379/ 276 340 379 | N | Y | 38 | | N | | | len=428 | |